JOURNAL OF APPLIED PHYSICS

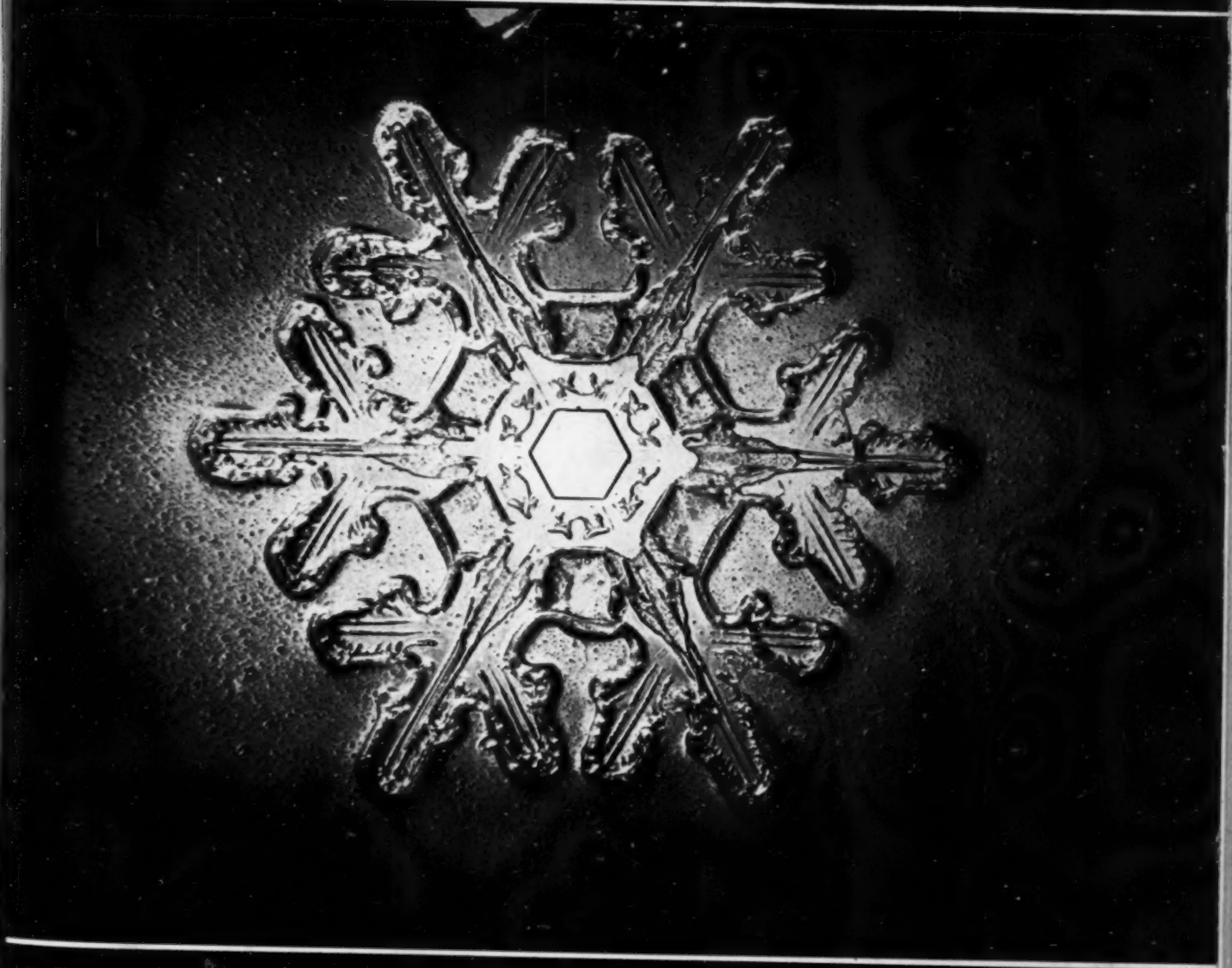

JOURNAL
OF
APPLIED PHYSICS

JULY, 1942 Vol. 13, No. 7

In This Issue

Page

Professional Manpower for the War HENRY A. BARTON 415

Resonance CARL A. LUDEKE 418

Résumés of Recent Research 424

Contributed Original Research

Surface Replicas for Use in the Electron Microscope VINCENT J. SCHAEFER AND DAVID HARKER 427

Matrix Theory of Torsional Oscillations LOUIS A. PIPES 434

Mechanism of the Electric Spark JOHN ZELENY 444

Photographic Action of Electrons in the Range Between 40 and 212 Kilovolts R. F. BAKER, E. G. RAMBERG, AND J. HILLIER 450

Torsion of a Prism with Cross Section the Inverse of an Ellipse THOMAS JAMES HIGGINS 457

Human Trajectories RUFUS OLDENBURGER 460

In Every Issue

Calendar of Meetings 423

Here and There 425

New Instrument Booklets 469

Innovations in Instruments 470

Index to Advertisers viii

BOARD OF EDITORS

ELMER HUTCHISSON, *Editor*

Associate Editors

FRANCIS BITTER
W. F. BUSSE
S. H. CALDWELL
ROBLEY D. EVANS
MORRIS MUSKAT
FREDERICK SEITZ
B. E. WARREN
J. B. WHITEHEAD

Publication of the American Institute of Physics

ADMINISTRATIVE STAFF

HENRY A. BARTON, *Director*

MADELINE M. MITCHELL, *Publications Manager*

JOHN T. TATE, *Adviser on Publications*

GOVERNING BOARD

PAUL E. KLOPSTEG, *Chairman*
GEORGE B. PEGRAM, *Secretary*
R. B. DOW
L. A. DUBRIDGE
FLOYD A. FIRESTONE
HARVEY FLETCHER
R. C. GIBBS
K. S. GIBSON
ARTHUR C. HARDY
GEORGE R. HARRISON
HERMANN MARK
A. G. WORTHING
JOHN T. TATE
N. W. TAYLOR
WALLACE WATERFALL

The JOURNAL OF APPLIED PHYSICS, published monthly at Prince and Lemon Sts., Lancaster, Pa., is devoted to physics in its role as the science basic to other natural sciences and to the arts and industries. Previous to 1937 this publication was known as PHYSICS. It aims to be of service not only in physical laboratories, but also in the laboratories of industrial, chemical, geological, geophysical, meteorological, radio, and similar concerns. The JOURNAL OF APPLIED PHYSICS publishes editorials, news of physicists and reviews, as well as technical papers of applied physics.

Manuscripts should be submitted to Elmer Hutchisson, Editor, American Institute of Physics, 175 Fifth Avenue, New York, New York.

Subscriptions and orders for back numbers should be addressed to Prince and Lemon Streets, Lancaster, Pa. or to the American Institute of Physics, 175 Fifth Avenue, New York, N. Y.

SUBSCRIPTION PRICE

	U. S. AND CANADA	ELSEWHERE
To members of scientific societies	$5.00	$5.70
To all others	7.00	7.70

Single copies are $.70 each.

Changes of address and proofs should be addressed to the Publications Manager.

Advertising rates supplied on request. Orders, advertising copy and cuts should be sent to the American Institute of Physics.

Entered as second class matter at the Post Office at Lancaster, Pennsylvania, under the Act of March 3, 1897. Accepted for mailing at the special rate of postage provided for in the Act of February 28, 1925, authorized May 2, 1932.

Copyright 1942, by the American Institute of Physics.

Journal
of
Applied Physics

Volume 13 July, 1942 Number 7

Professional Manpower for the War

BY HENRY A. BARTON

Director, American Institute of Physics

THE following outline is a study of the job a national manpower administration faces in a highly technical profession. It is idealistic—at least it probably goes beyond the hope of practical realization. Nevertheless it was prepared as a contribution to the work of the branch of the new National Manpower Commission which is charged with administration of professions.

I. ADMINISTRATION OF MANPOWER

Nothing so important is so scarce as manpower of high professional caliber in certain fields whose utilization is essential to the winning of the war. A national administration is imperatively needed to insure that available manpower in these fields is fully used and most effectively used. It is needed further to take all possible steps to augment the supply. Since positive measures in so complex a structure as a nation cannot be 100 percent effective, the administration must also provide safeguards *against* known forces tending to waste the supply or use it at less than full efficiency.

II. UNDERSTANDING THE PROBLEM

Such a manpower administration can be successful only to the extent that it has an intimate, competent, and comprehensive *understanding* of the manpower situation in all of its aspects in those fields which are important. This implies more than statistics, however valid, complete and comparable. It is difficult to delimit what is implied. Included must be a real knowledge of the subject matter of the field, the pedagogical experience in the field, the points of view and habits of thought of members of the profession, their organizations, the experience of industrial management in applying the field, the nature of services the field renders to offensive and defensive combat operations, etc.

III. HOW TO OBTAIN THE UNDERSTANDING —EXAMPLE: PHYSICS

Such an understanding can be pictured best by an example. It is proposed to outline below what is needed to obtain an understanding of a particularly compact, unified, and strategic field —namely, physics—with the thought that the new Manpower Commission should attempt to obtain this understanding, and, in so doing, establish a pattern of procedure, obtain experience in fact-finding, and set up standards for the critical examination of information gathered—all as a valuable guide to the process of obtaining a similar understanding of other strategic fields.

IV. QUANTITY, QUALITY, AND LOCATION OF SUPPLY OF PHYSICISTS

This function has been developed by the National Roster and needs little discussion. A manpower administration may need more frequent reports as to location than have been available. One secretary, full time, could keep a list current if several other sources of information

(American Institute of Physics lists, government rolls, etc.) were coordinated with the Roster. This job can be done better and with less annoyance in the manner of a secretary keeping track of members than of a government agency using extensive questionnaire procedures. It is pertinent to enquire what records of physicists in uniform the Army and Navy maintain.

V. PRESENT USE OF PHYSICISTS

With little or no national coordination and insufficient understanding of the national supply and demand, the work of physicists is at present administered by various agencies. These include:

A. The Army, Navy, and other armed services.
B. Special government agencies coordinating research and development on war devices and methods (O.S.R.D., N.A.C.A., N.R.C., etc.).
C. Other government agencies supporting the war effort (National Bureau of Standards, Public Health Service, etc.)
D. Industries engaged in development and production of war devices and supplies.
E. Industries making instruments and equipment necessary to research and testing work of A, B, C, and D.
F. Universities, colleges, and high schools.
G. Miscellaneous organizations including endowed research laboratories, national societies, independent consulting laboratories.
H. Individuals working as consultants, writers, etc.

VI. EFFICIENCY OF USE

The efficient use of a physicist requires the use by him of his intellect and energy in work which by its nature demands for its successful accomplishment the knowledge, habits of thought, resourcefulness, and other qualities which are specifically developed by training and experience in physics. Such work is usually teaching, research, development, or operations but it may be administrative. Insofar as it is possible or desirable to distinguish the capacities of a physicist from those of an engineer, chemist, geophysicist, biophysicist, meteorologist, etc., a physicist has relatively more readily available for his use a knowledge and understanding of other branches of physics than the one most used by him and an understanding of his own specialty which goes deep into the pertinent fundamental principles and facts and the mathematical relationships between them.

A manpower administration would be obliged to assure itself that the organizations of Section V were using physicists efficiently. This involves knowing, among other things:

A. That every physicist in the organization is working as a physicist (at least any other use would require defense on the ground that it is either intrinsically more important work or is in a field in which the individual is at least equally competent, and in which there is at least as serious a shortage of supply).
B. That provision is made of adequate equipment.
C. That where any portion of the work on which physicists are engaged can be done by others less trained in physics, such helpers are provided (laboratory assistants, set wirers, mechanics, glass blowers, data takers, purchasing clerks, laboratory managers, etc.).
D. That there is a wise administrative choice of what shall be taught, developed, and operated or in what directions research carried out—i.e., that physicists be set to the most useful tasks. Here again some coordination on a national scale is essential. Examples: (a) A physicist teaching a course in a branch of physics not important to the war may be needed to operate a device to detect submarines. (b) A physicist who is "putting-together" radio-locaters may be more useful training hundreds of men to operate them.
E. That physicists will be disturbed as little as possible (as long as their work is in a valuable direction) by transfers or threats of impending transfers. (Short period deferments are disturbing; uncoordinated competition for one's services is disturbing.)

A valuable contribution to physicists' morale and efficiency will be made if a manpower administration can bring about a situation in which every physicist can feel he is playing his proper role in the war effort, and it is generally recognized that his work is patriotic and important.

VII. ALLOCATION

The most obvious and a very difficult problem of manpower administration is the distribution of emphasis between major functions, i.e., the determination of priorities and the allocation of quotas. In physics the problem is well illustrated. What percentage of the national resource of physicists should be allocated to Army operations, Navy operations, research and development, or methods and devices of war, industrial production of war equipment and supplies, college, or high school level teaching?

An intimate knowledge of the situation as a whole is essential in finding the answer. Tomorrow's answer will be different from today's.

For example, last year in physics it was desirable to continue education to the most advanced levels and to initiate researches for new war devices. We are entering a stage in which more emphasis should be placed on the operation of devices which are now nearing completion and hence on the training of large numbers of men in the first principles of physics required for such operations.

To follow such comprehensive developments and trends with intelligent allocations of quotas, broadly informed policy committees in the strategic fields will be necessary. Physics has a War Policy Committee in the American Institute of Physics available for consultation and this Committee is already concerning itself with such problems.

VIII. TRAINING

The supply of physicists being insufficient, a manpower administration would coordinate facilities for training men. Experience with functions already discussed would indicate what aspects of physics should be taught (other than fundamentals and prerequisite mathematics) and how far training should be carried. The number needed at various levels would have to be determined. The administration must see that teachers are used effectively in classes neither too small nor too large and that proper equipment for teaching and laboratory experience is available (involving recommendations to the War Production Board regarding priorities). Above all the number of physicists needed for the teaching work must be determined and the conditions for their efficient use (see Section VI) satisfied (especially freedom from transfers—VI-E).

Parenthetically there is a distinction between "a man who has had a basic course in physics" and a "physicist." By the latter we mean a holder of the bachelor's degree with major emphasis on physics plus one year or more experience or further education. The former may be trained for many operations, relieving some physicists. It is to be noted that short intensive educational procedures do not create a physicist except out of a man who is already "almost" a physicist.

The administration would require current figures on enrolments of students and would probably need to assemble and distribute vocational information which schools, colleges, and universities could use to stimulate enrolments up to quotas desired.

It is possible that an efficient national program would require the concentration of students, teachers, and equipment in a suitable number of selected institutions. Data enabling a wise selection would have to be obtained.

IX. INFORMATION AND GUIDANCE

In addition to directions, the administration would have to issue information and guidance to organizations and individuals. Only from this source could the latter get information which is based on a national viewpoint. The morale of individuals can be improved by proper attention to their inquiries as to the best direction of their efforts. Information assembled by the administration for its other functions might suffice for this one.

X. TECHNIQUE OF GATHERING INFORMATION

Theoretically the manpower administration would need intimate information about the work of organizations, prying (e.g.) into the assignment of physicists to certain types of service in the army or into the respective merits of two projects of the National Defense Research Committee. Practically this would amount to an absurd usurpation and centralization of the management function. It should be possible to establish, short of this, an understanding relationship with operating agencies in which any seeming interference with the latter would be more than counterbalanced by the benefits arising from the existence of a manpower administration. Such a degree of cooperation with these agencies can only be obtained if they are themselves really represented in making the judgments, decisions, allocations, and the like on the basis of the information assembled. The administration's contact men should be competent and acceptable to all agencies. It is suggested that policy committees by fields should be called upon for the initial contacts as well as subsequent consultation.

Resonance

CARL A. LUDEKE

Department of Mathematics and Mechanics, University of Cincinnati, Cincinnati, Ohio

RESONANCE is perhaps the most interesting and practical phenomenon in the theory of forced vibrations. The physicist and engineer are vitally concerned over the conditions under which resonance may occur, either for the purpose of eliminating it or encouraging it. For systems having one degree of freedom, three types of resonance are possible, namely: harmonic, multiple harmonic, and sub-harmonic. These derive their names from the relationship between the frequencies of the applied force and the system; the frequency of the system being, respectively,

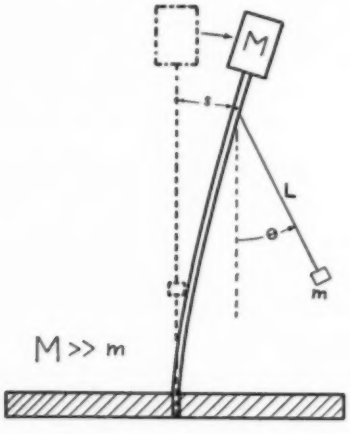

FIG. 1. A pendulum with a horizontally moving (harmonic) point of support.

equal to, an integral multiple of, a sub-multiple of, the frequency of the applied force. It is the purpose of this paper to discuss the mathematical and physical conditions under which each of these types of resonance may occur, and to illustrate each type with photographs of actual models.

I. THEORY

The equation of motion of a vibrating system having one degree of freedom can be written in the form,

$$md^2x/dt^2 = F_s + F_d + F_e, \qquad (1)$$

in which m is the mass, x is the displacement, F_s is the spring or elastic force, F_d is the damping force, and F_e is the external or applied force. An investigation of resonance involves a study of the response of the system described by the equation

$$md^2x/dt^2 = F_s + F_d,$$

to the external force F_e.

Harmonic Resonance[1]

Consider Eq. (1) in the form,

$$md^2x/dt^2 + \beta dx/dt + kx = F_0 \sin \omega t. \qquad (2)$$

This is a linear equation and its solution for large values of t is easily found to be:

$$x = A \sin (\omega t - \varphi),$$

in which the phase angle, φ, equals $\tan^{-1} \beta\omega/(k - m\omega^2)$ and the amplitude A equals $F_0/[(k - m\omega^2)^2 + \beta^2\omega^2]^{\frac{1}{2}}$. If $\beta^2 < 2km$, A is a maximum when

$$\omega^2 = \omega_0^2 - \beta^2/2m^2, \quad \text{where} \quad \omega_0^2 = k/m. \qquad (3)$$

When this condition is satisfied the external force, $F_0 \sin \omega t$, causes our system to have its maximum amplitude, and we have the phenomenon of harmonic resonance. If β is small we see that harmonic resonance occurs when the frequency of vibration of the external force is approximately the frequency of the free vibration of the system.

Multiple Harmonic Resonance[1]

Consider next Eq. (1) in the form,

$$md^2x/dt^2 + \beta dx/dt + kx = \sum A_n \sin n\omega t + \sum B_n \cos n\omega t. \qquad (4)$$

This linear equation has, for large values of t, the solution:

$$x = \sum \frac{A_n \sin (n\omega t - \varphi_n)}{[(k - mn^2\omega^2)^2 + \beta^2 n^2 \omega^2]^{\frac{1}{2}}} + \sum \frac{B_n \cos (n\omega t - \alpha_n)}{[(k - mn^2\omega^2)^2 + \beta^2 n^2 \omega^2]^{\frac{1}{2}}},$$

from which we see, provided β is small, that the

nth term in the sine and cosine series will have a very large amplitude if,

$$n^2\omega^2=\omega_0^2-\beta^2/2m^2. \quad (5)$$

Thus if our external force F_e has in its expansion a term whose frequency, $n\omega/2\pi$, is related to the free vibration frequency by the above expression, resonance will occur. Therefore an "impure" applied force of frequency f can be in resonance with a system whose frequency is an integral multiple of f. This is the case of multiple resonance, or resonance at the higher harmonics.

Sub-Harmonic Resonance

The two previous cases were represented by linear* differential equations of motion in which the spring force was proportional to the displacement. This is no longer true for the case of sub-harmonic resonance. The special case of half-harmonic resonance is often observed in a system whose spring force is an explicit function of time; sub-harmonic resonance involving the sub-multiples $\frac{1}{3}$, $\frac{1}{4}$, $\frac{1}{5}$, $\cdots$ is observed in systems whose equations of motion are non-linear.

Consider Eq. (1) in the linear form,[2]

$$md^2x/dt^2+\beta dx/dt+(k-2A_0\sin 2\omega t)x=0, \quad (6)$$

in which m, β, k, and A_0 are constants. Knowing from experiments (von Melde's, etc.) that a steady state solution exists, we can assume, if β and A_0 are very small, that the solution, to a first approximation, is in the form:

$$x=A\sin\omega t+B\cos\omega t.$$

Putting this value of x in Eq. (6) it becomes,

$$D_1\sin\omega t-A_0B\sin 3\omega t+D_2\cos\omega t+A_0A\cos 3\omega t=0,$$

in which $D_1=kA-m\omega^2A-\beta\omega B-A_0B$, and $D_2=kB-m\omega^2B+\beta\omega A-A_0A$; and must be true for all values of t. Letting ωt have the values 0 and $\pi/2$, we get the following equations:

$$\begin{aligned}\beta\omega A+(k-m\omega^2)B&=0,\\(k-m\omega^2)A-\beta\omega B&=0.\end{aligned} \quad (7)$$

The existence of our assumed solution depends on the existence of A and B, and therefore on the vanishing of the determinant of Eqs. (7). We find the condition for the existence of our solution to be:

$$\omega^2=\beta^2/2m^2+[(\beta^2/2m^2)^2+k^2/m^2]^{\frac{1}{2}}. \quad (8)$$

For small values of β this reduces to the equation $\omega^2\cong\omega_0^2$. Thus the applied force, $(2A_0\sin 2\omega t)x$, can keep the system in a steady state of motion if the frequency (ω/π) of the applied force is twice the frequency $(\omega_0/2\pi)$ of the system. We have, therefore, an example of half-harmonic resonance in a linear system.

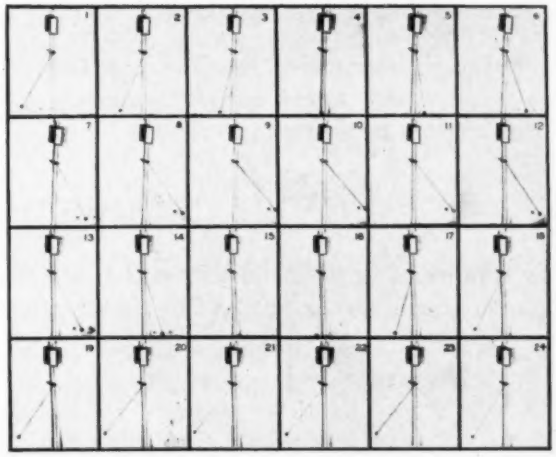

FIG. 2. Harmonic resonance.

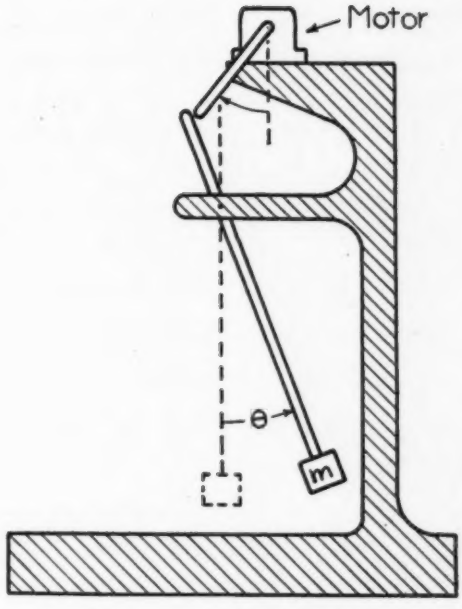

FIG. 3. A pendulum maintained in motion by impulses from a revolving crank arm.

* An equation in the form $d^2x/dt^2+Pdx/dt+Qx=R$ is said to be linear provided P, Q, and R are functions of t or constants.

Consider next Eq. (1) in the form,[3]

$$md^2x/dt^2+kx=F_e(t)+\epsilon f_1(x, dx/dt), \qquad (9)$$

in which $|\epsilon|<1$, $-kx+\epsilon f_1(x, dx/dt)=F_s+F_d$, and k and ϵ are constants. This equation is in general not linear, but it can be solved approximately by the perturbation method. To this end, we expand $F_e(t)$ in a Fourier series,

$$F_e(t)=\sum A_n \sin n\omega t+\sum B_n \cos n\omega t;$$

and assume that the solution of Eq. (9) is,

$$x=x^{(0)}+\epsilon x^{(1)}+\epsilon^2x^{(2)}+\epsilon^3x^{(3)}+\cdots.$$

Putting this value of x in Eq. (9) and equating like powers of ϵ, we have:

$$\begin{aligned} md^2x^{(0)}/dt^2+kx^{(0)}&=\sum A_n \sin n\omega t+\sum B_n \cos n\omega t \\ md^2x^{(1)}/dt^2+kx^{(1)}&\equiv f_1(x^{(0)}, dx^{(0)}/dt) \\ &\vdots \qquad\qquad \vdots \end{aligned}$$

The first of these equations has as its solution,

$$x^{(0)}=C^{(0)} \sin (\omega_0 t-\alpha^{(0)}) +\sum\frac{A_n \sin n\omega t}{m(\omega_0^2-n^2\omega^2)}+\sum\frac{B_n \cos n\omega t}{m(\omega_0^2-n^2\omega^2)},$$

in which $\omega_0^2=k/m$, and $C^{(0)}$ and $\alpha^{(0)}$ are constants yet to be determined. We now have $x^{(0)}$ and hence $dx^{(0)}/dt$ as a function of t, and thus our second equation can be written,

$$md^2x^{(1)}/dt^2+kx^{(1)}\equiv\sum a_n \sin n\omega t+\sum b_n \cos n\omega t,$$

which has as its solution,

$$x^{(1)}=C^{(1)} \sin (\omega^0 t-\alpha^{(1)}) +\sum\frac{a_n \sin n\omega t}{m(\omega_0^2-n^2\omega^2)}+\sum\frac{b_n \cos n\omega t}{m(\omega_0^2-n^2\omega^2)}.$$

The constants $C^{(1)}$ and $\alpha^{(1)}$ are chosen so that at any time $t=0$, the system is unperturbed; i.e.,

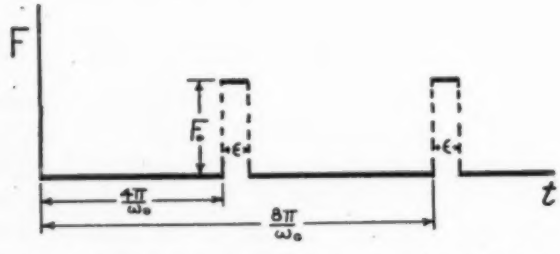

FIG. 4. The discontinuous force F supplied by the motor in Fig. 3, as a function of time t.

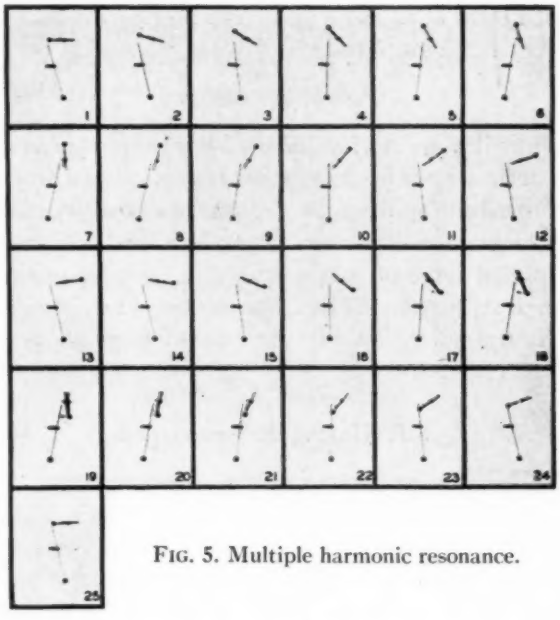

FIG. 5. Multiple harmonic resonance.

$x^{(1)}=dx^{(1)}/dt=0$ when $t=0$. Thus to the first approximation, the solution of Eq. (9) is,

$$x=x^{(0)}(C^{(0)}, \alpha^{(0)})+\epsilon x^{(1)},$$

in which $C^{(0)}$ and $\alpha^{(0)}$ are determined by the initial conditions on x and dx/dt. By continuing the above perturbation process, Eq. (9) can be solved to any degree of accuracy, the method being applicable provided $\epsilon f_1(x, dx/dt)$ can be considered as a term which "perturbs" the equation,

$$md^2x/dt^2+kx=F_e(t).$$

To insure resonance in the first approximation, we must require $x^{(1)}$ to have a frequency $\omega/2\pi$. Since $x^{(1)}$ can be written in the form,

$$x^{(1)}=(1/m\omega_0)\int_0^t f_1(x^{(0)}, dx^{(0)}/dt) \sin \omega_0(t-\tau)d\tau;$$

the conditions on $C^{(0)}$ and $\alpha^{(0)}$ so that $x^{(1)}$ does have a frequency $\omega/2\pi$ are given by the equations:

$$\begin{aligned} x^{(1)}(2\pi/\omega_0)&=-\int_0^{2\pi/\omega_0} f_1\{x^{(0)}(\tau), \\ &\qquad d[x^{(0)}(\tau)]/dt\} \sin \omega_0\tau d\tau=0, \\ d[x^{(1)}(2\pi/\omega_0)]/dt&=\int_0^{2\pi/\omega_0} f_1\{x^{(0)}(\tau), \\ &\qquad d[x^{(0)}(\tau)]/dt\} \cos \omega_0\tau d\tau=0. \end{aligned} \qquad (10)$$

The solution of Eq. (9) to a first approximation is now,

$$x = x^{(0)} + \epsilon x^{(1)}(C^{(1)}, \alpha^{(1)}),$$

in which $x^{(1)}$ has a frequency $\omega_0/2\pi$ and $C^{(1)}$ and $\alpha^{(1)}$ are to be determined by the initial conditions.

If $F_e(t)$ is a force of small amplitude but frequency $n\omega_0/2\pi$, then approximately, $x^{(0)}$ has a frequency $\omega_0/2\pi$; but we made $x^{(1)}$ (by Eqs. (10)) have a frequency $\omega_0/2\pi$, and therefore our solution x has a frequency $\omega_0/2\pi$. Thus the terms introduced by the damping and non-linear part of our equation, i.e., by $\epsilon \neq 0$, provided real

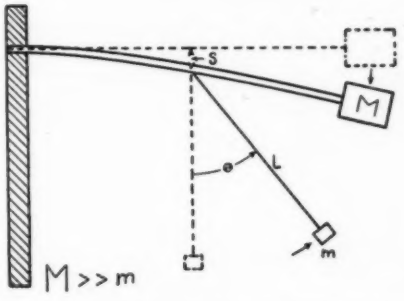

FIG. 6. A pendulum with a vertically moving (harmonic) point of support.

values of $C^{(0)}$ and $\alpha^{(0)}$ can be found to satisfy Eqs. (10), do not cause the natural vibration, of frequency $\omega_0/2\pi$ to vanish and be replaced by the forced frequency $n\omega_0/2\pi$ as would be the case if the system were linear. Therefore a non-linear system of frequency f is kept in motion by an external force of frequency nf.

II. EXPERIMENTAL EXAMPLES

As an experimental example of harmonic resonance consider the system shown in Fig. 1, whose equation of motion is:

$$d^2\theta/dt^2 + (1/L)d^2s/dt^2 \cos\theta + (mg/2L)\sin\theta = 0.$$

The massive vertical cantilever supplies approximately simple harmonic motion $s = A\sin\omega t$ to the supporting end of the pendulum, so that the equation of motion can be written,

$$d^2\theta/dt^2 + K_1 \sin\theta = K_2 \cos\theta \sin\omega t,$$

in which $K_1 = mg/2L$ and $K_2 = A\omega^2/L$. For small values of θ this becomes,

$$d^2\theta/dt^2 + K_1\theta = K_2 \sin\omega t,$$

and is the same as Eq. (2) with $\theta = x$, and $\beta = 0$. Thus resonance will occur if the frequency of the pendulum is the same as the frequency of the cantilever. These results are shown in Fig. 2, which is made up of rapid sequence photographs[4] of system 1 in motion.

The pendulum can be seen oscillating with considerable amplitude due to the small horizontal motion of its pivoted end. From pictures 1, 13, 24, it is quite obvious that the pendulum and the cantilever have the same frequency.

As an example of multiple resonance, consider the system (shown in Fig. 3) in which a pendulum is supplied with impulses having a frequency one-half the frequency of the pendulum. The equation of motion for small values of θ is,

$$d^2\theta/dt^2 + \omega_0^2\theta = \sum b_n \sin(n\pi t/T) \quad 0 < t < T,$$

in which the right-hand term represents the periodically applied force $f(t)$ which is shown graphically in Fig. 4. After m (1, 2, 3, $\cdots$) cycles of this applied force the equation of motion becomes,

$$d^2\theta/dt^2 + \omega_0^2\theta = \sum b_n \sin(n/4m)\omega_0 t;$$

in which the Fourier coefficients are given by the equation,

$$b_n = (\omega_0/2m\pi)\int_0^{4m\pi/\omega_0} f(t)\sin\omega_0 t dt.$$

From our theoretical discussion of multiple resonance we know that it will occur if there is a term in $f(t)$ which has the same frequency $(\omega_0/2\pi)$ as has the pendulum. This is so when $n = 4m$; and

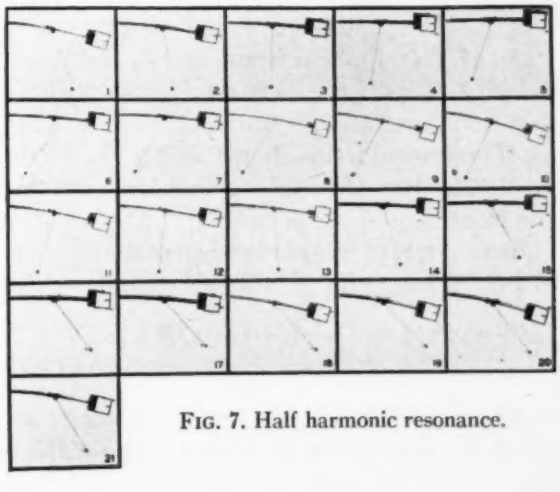

FIG. 7. Half harmonic resonance.

to guarantee resonance we must show that $b_{4m} \neq 0$. Putting the values of $f(t)$ in the equation for b_n we find:

$$b_n = F_0 \sum_{j=1}^{m} \int_{4\pi j/\omega_0}^{(4\pi j/\omega_0)+\epsilon} \sin \omega_0 t \, dt = (F_0/2\pi)(1-\cos \epsilon\omega_0).$$

Thus $b_{4m} \neq 0$, and therefore we have an example of multiple harmonic resonance, the results of

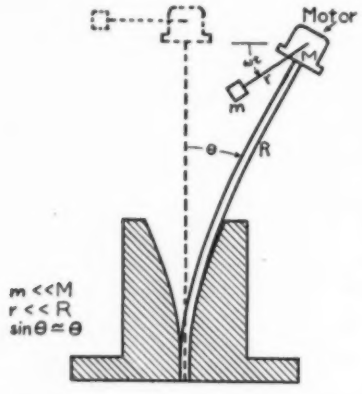

FIG. 8. A cantilever spring of gradually increasing stiffness maintained in motion by an unbalanced motor mounted on its free end.

which are shown in Fig. 5. From pictures 1, 13, 25, it is quite obvious that the applied force has a frequency one half that of the pendulum.

A system exhibiting half harmonic resonance is shown in Fig. 6. Its equation of motion, for small values of θ, and a massive pendulum, is

$$d^2\theta/dt^2 + (\omega_0^2 - K \sin \omega t)\theta = 0,$$

in which $\omega_0^2 = g/L$ and $K = -A_0\omega^2/L$, L being the length of the pendulum, A_0 the maximum amplitude of the applied force, and ω its angular velocity. This is the same as Eq. (6) with $x = \theta$ and $\beta = 0$, and we expect resonance if ω is twice ω_0. These results are shown in Fig. 7. Pictures 1, 11, 21, show that the applied force has twice the frequency of the pendulum.

An example of sub-harmonic resonance,[5] shown in Fig. 8, has as its equation of motion,

$$(M+m)d^2z/dt^2 + [\alpha - (M+m)g/R]z = -mr\omega^2 \cos \omega t - Kz^3,$$

in which $z = R\theta$, ω is the angular velocity with which m is rotated about M, and $-\alpha z - Kz^3$ is the non-linear spring force resolved into a straight line and a cubical parabola. The actual spring force is shown by curve I, Fig. 9; the linear and non-linear components are shown by curves II and III. For this model, $\alpha = 33{,}300$ dynes/cm and $K = 1700$ dynes/cm^3. The above equation of motion can be written in the form,

$$d^2z/dt^2 + (\omega_0')^2 = B \cos \omega t - \epsilon z^3,$$

in which $\omega_0' = [\alpha/(M+m) - g/R]^{\frac{1}{2}}$, $B = -mr\omega^2/(M+m)$ and $\epsilon = K/\alpha$. This is the same as Eq. (9) and has as its *zero*th order solution,

$$z^{(0)} = C^{(0)} \sin (\omega_0' t - \alpha^{(0)}) + [B/[(\omega_0')^2 - \omega^2]] \cos \omega t,$$

in which $C^{(0)}$ and $\alpha^{(0)}$ must be determined so that z has a frequency $\omega_0'/2\pi$. If we consider the case of $\omega = 3\omega_0'$, the equations determining $C^{(0)}$ and $\alpha^{(0)}$ are:

$$\int_0^{2\pi/\omega_0'} [C^{(0)} \sin (\omega_0' t - \alpha^{(0)}) + B' \cos 3\omega_0' t]^3 \sin \omega_0' t \, dt = 0,$$

$$\int_0^{2\pi/\omega_0'} [C^{(0)} \sin (\omega_0' t - \alpha^{(0)}) + B' \cos 3\omega_0' t]^3 \cos \omega_0' t \, dt = 0,$$

in which $B' = B/[(\omega_0')^2 - \omega^2]$. From these integrals we determine that real values of $C^{(0)}$ and $a^{(0)}$ exist. Thus we have an experimental example

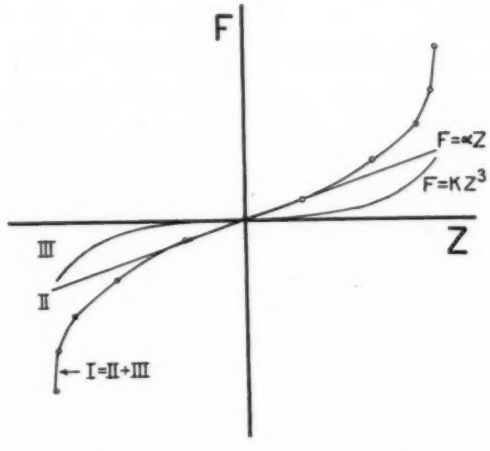

FIG. 9. Curve I. The non-linear spring force F, of the cantilever of Fig. 5, as a function of displacement z. This is resolved into a linear curve (II) plus a non-linear curve (III).

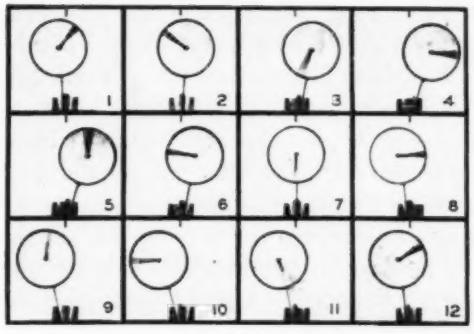

FIG. 10a. Sub-harmonic resonance, one to three.

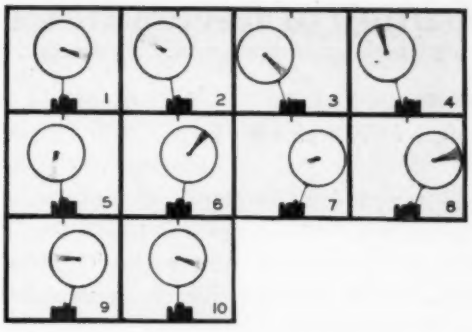

FIG. 10b. Sub-harmonic resonance, one to four.

of one-third harmonic resonance. The experimental results are shown in Fig. 10a. Pictures 1, 4, 8, 12 show that m makes three revolutions while M completes one cycle.

The experimental results for $(\frac{1}{4})$ sub-harmonic resonance are shown in Fig. 10b. Pictures 1, 3, 6, 8, 10 show that the applied force has four times the frequency of the cantilever.

REFERENCES

(1) Th. von Kármán and M. A. Biot, *Mathematical Methods in Engineering* (McGraw-Hill, 1940).
(2) Lord Rayleigh, "On maintained vibrations," Phil. Mag. **15**, No. 94 (April, 1883).
(3) Th. von Kármán, "The engineer grapples with nonlinear problems," Bull. Am. Math. Soc. **46**, No. 8 (August, 1940).
(4) The experimental and photographic procedure is similar to that stated in a previous paper. See C. A. Ludeke, "Experimental examples in dynamics," Am. J. Phys. **9**, 162 (June, 1941).
(5) J. P. Den Hartog, *Mechanical Vibrations* (McGraw-Hill, 1940).

Calendar of Meetings

July

11 American Physical Society, Pacific Coast Section, Berkeley, California
21–22 Optical Society of America, Cambridge, Massachusetts
22–24 American Society of Civil Engineers, Spokane, Washington

September

7– 9 Mathematical Association of America, Ithaca, New York
7–11 American Chemical Society, Buffalo, New York
8–11 American Mathematical Society, Ithaca, New York
9–11 American Institute of Electrical Engineers, Vancouver, B. C.
29–Oct. 1 Technical Association of Pulp and Paper Industry, Boston, Massachusetts

October

5– 9 National Safety Council, Chicago, Illinois
12–14 American Society of Mechanical Engineers, Rochester, New York
12–16 American Welding Society, Detroit, Michigan
12–16 American Society for Metals, Detroit, Michigan
19–24 American Society for Metals, Chicago, Illinois
19–24 American Society for Metals, Cleveland, Ohio
30–31 Optical Society of America, New York, New York
31 American Mathematical Society, New York, New York

November

7 American Physical Society, New York State Section, Albany, New York
16–18 American Institute of Chemical Engineers, Cincinnati, Ohio
27–28 American Mathematical Society, Notre Dame, Indiana
30–Dec. 4 American Society of Mechanical Engineers, New York, New York

December

27–Jan. 1 American Society of Naturalists, New York, New York
28–Jan. 2 American Association for the Advancement of Science, New York, New York
28–Jan. 2 American Standards Association, New York, New York
28–Jan. 2 American Mathematical Society, New York, New York
28–Jan. 2 American Society of Refrigerating Engineers, New York, New York
29–31 Geological Society of America, Ottawa, Canada

Résumés of Recent Research

New Studies on the Clusters of Nebulae Investigations on the large scale distribution of matter in the universe were concerned until recently with the *geometrical* or geographical aspects of this distribution, which, chiefly through the work of Hubble[1] and others, can now be considered as established in general to distances of some hundred millions of light years. The problem of current interest is the analysis of the *physical* principles governing the distribution of nebulae. For example, the question may be raised if Newton's law of gravitational attraction still holds good when the interacting masses are separated by distances of millions of light years rather than by distances not exceeding a small fraction of one light year such as are encountered among the members of the solar system and the components of those double stars for which the validity of the law has been checked.

Observations on the clusters of nebulae promise to furnish proof for a true universality of Newton's law to an excellent degree of approximation. These observations refer to clusters which have reached statistically stationary states; i.e., clusters satisfying the following conditions:

(a) The clusters must possess spherical symmetry subject only to fluctuations derivable from the limited number of nebulae involved.

(b) The velocity dispersion throughout the cluster must be independent of the distance from the center out to distances where the mean free paths of the nebulae exceed a certain critical length (Smoluchowski limit).

(c) The radial distribution curves of the numbers of nebulae per unit volume for different clusters must be reducible to the same standard Emden curve which represents the distribution of matter in a bounded isothermal gravitational gas sphere. The reduction factors involved must be derivable from the velocity dispersion and the central density of the clusters.

(d) A segregation of nebulae of different mass must occur.

Available data on the clusters in Coma, Hydra, Perseus, Cancer, Fornax, and Pegasus indicate that these clusters satisfy the mentioned requirements and that they are stationary assemblies of nebulae whose interactions are governed by the inverse square law of gravitation.

Analysis of the observations on clusters of nebulae also indicates that the time scale necessary for a rational understanding, on the basis of fundamental principles of physics, of the observed large scale distribution of matter is much longer than the hypothesis of the expanding universe would have it.[2]

[1] E. Hubble, *The Realm of the Nebulae* (Yale University Press, 1936).

[2] F. Zwicky, Phys. Rev. **61**, 489 (1942); Astrophys. J. **86**, 217 (1937), and May issue, 1942. Proc. Nat. Acad. Sci. **25**, 604 (1939); **26**, 332 (1940); **27**, 264 (1941); **27**, 366 (1941); see also April issue, 1942. Publ. Astr. Soc. Pacific **50**, 218 (1938).

New Microphotometer The introduction into industrial service of procedures developed in the laboratory usually entails extensive modification

FIG. 1. A production-type microphotometer.

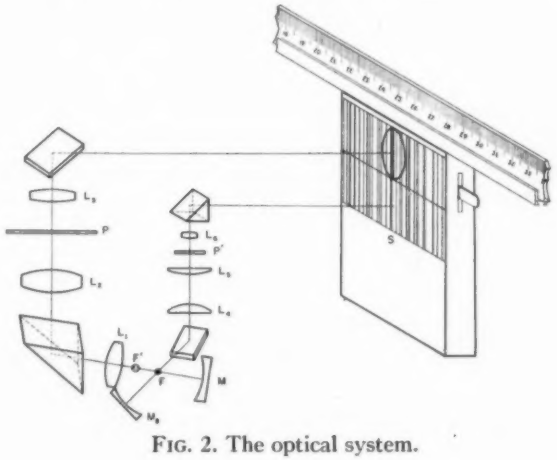

FIG. 2. The optical system.

of apparatus design to provide the ruggedness and stability required for shop use. In these respects, spectrochemistry has proved no exception; current improvements in instrumentation for specific applications are numerous. The new microphotometer described[1] by Vincent and Sawyer is adapted especially to installations where durability and continuous reliability are of more importance than initial cost. Specifically, it is an attempt to provide an instrument adequate for routine ferrous laboratories which may be called upon to make a million readings per year at the highest attainable precision.

The instrument comprises a two hundred pound cast base carrying rails which support a stage adapted for motion along the spectrum. The stage, in turn, carries on a vee way and steel ball a cross-slide on which is mounted a spring-loaded clamp for the spectrum plate. The linearity of the longitudinal motion is provided by a pyramidal rail and two grooved rollers in front; the rear support is a single cylindrical roller and flat-topped rail. Rapid positioning of a spectral line for measurement is made possible through the use of two frictionally loaded work wheels attached to the stage and engaging a worm rotably mounted between two supports attached to the base. The worm may be rotated by either of two coaxial hand wheels, shown in Fig. 1, connected to it by gear trains of different ratios, providing, in all, three speeds of longitudinal motion. Gears are spiral, quarter-inch face, hardened and polished; shafts and rollers are carried on ball bearings.

Excessive error from emulsion grain is avoided by photometering a line length of five millimeters at as great a width as is consistent with resolution requirements. Actual operating widths vary from 35 to 50 microns. The optical system, deriving its illumination from a thirty-watt lamp, is shown in Fig. 2, which details also the provision made for the projection of a reference spectrum carried on the stage. The indicating instrument is a galvanometer of short period located at two meters from its scale to reduce obliquity errors. Close grouping of projected images and scale are designed to minimize fatigue.

A test on the reproducibility of reading of a line pair indicates a relative error of less than 0.05 percent in the average ferrous analysis.

[1] H. B. Vincent and R. A. Sawyer, "A new microphotometer," J. Opt. Soc. Am. **31**, 639–643 (1941).

Here and There

Honor Roll

Five scientists were lost in a collision of two blimps in an accident off Manasquan, New Jersey, Monday night, June 8. The men were: L. S. MOYER, Assistant Professor of Botany, University of Minnesota; C. R. HOOVER, Professor of Chemistry, Wesleyan University; F. C. GILBERT, New London, Connecticut; A. B. WYSE, San Diego, California; I. H. TILLES, San Diego, California. In commenting upon the tragedy, the Office of Scientific Research and Development has issued the following statement: "These men lost their lives in an accident encountered in an experimental flight in connection with important scientific war research and gave their lives for their country as truly as any soldier or sailor killed in battle."

★

Honors and Awards

Among those recently elected to membership at the annual meeting of the National Academy of Sciences were the following: LYMAN J. BRIGGS, Director, National Bureau of Standards; ALBERT EINSTEIN, Professor of Mathematics, Institute for Advanced Study, Princeton; PAUL DYER MERICA, Vice President, International Nickel Company; JOHN TORRENCE TATE, Dean of the College of Science, Literature, and Arts, University of Minnesota.

The American Academy of Arts and Sciences has elected as fellows in the mathematical and physical sciences: WILMER LANIER BARROW, the Massachusetts Institute of Technology; FRANCIS BIRCH, Harvard University; SAMUEL CORNETTE COLLINS, the Massachusetts Institute of Technology; OTTO STRUVE, Director, Yerkes Observatory.

At the annual meeting of the American Philosophical Society members elected in the mathematical and physical sciences were: OLIVER ELLSWORTH BUCKLEY, President, Bell Telephone Laboratories, Inc.; LEE ALVIN DUBRIDGE, Professor of Physics and Dean of the Faculty of Arts and Science, University of Rochester; DUNCAN ARTHUR MACINNES, Rockefeller Institute for Medical Research; ROBERT RAYNOLDS MCMATH, Director, the McMath-Hulbert Observatory, University of Michigan; FRANCIS DOMINIC MURNAGHAN, Professor of Applied Mathematics, Johns Hopkins University; HAROLD MALCOLM WESTERGAARD, Gordon McKay Professor of Civil Engineering and Dean of the Graduate School of Engineering, Harvard University; ROBERT RUNNELS WILLIAMS, Chemical Director, Bell Telephone Laboratories, Inc.

Honorary members elected to the Academy of Sciences of the U.S.S.R. on May 8 included the following: ERNEST O. LAWRENCE, Director of the Radiation Laboratory, University of California and GILBERT N. LEWIS, Professor of Chemistry and Dean of the College of Chemistry, University of California.

The Optical Society of America has announced the award of the Adolph Lomb Medal for 1942 to JAMES G. BAKER of the Harvard College Observatory. This medal, which is awarded biennially for noteworthy contributions to optics, will be presented at the time of the annual meeting of the Society next October. The recipient has made important contributions to the improvement of instruments by which astronomical observations are made. He has originated new methods of procedure in the fields of geometrical optics and lens design.

Three young scientists have been awarded fellowships to carry on their investigations at the Westinghouse Research Laboratories, according to Dr. E. U. Condon, Associate Director of the Laboratories.

The appointees are DR. RUSSELL E. FOX, who will carry on research on the dynamics of high speed machinery which he began at the University of Virginia under Professor J. W. Beams; DR GERSON S. SCHAFFEL, Carnegie Institute of Technology, who will engage in fundamental research on the chemistry of polymers; and DR. ROBERT S. WEISZ, Cornell University, who will work in the field of ceramics, attempting to improve the properties of electric porcelain.

This is the fifth group to be selected under the Westinghouse Research Fellowship plan which was inaugurated in 1938. Appointments under the Fellowship plan are for one year with reappointment for a second year if mutually desirable. Although in the past these men have devoted their entire time to investigations in the realm of pure science, this year they have been asked to indicate the fields in which they feel qualified to contribute to war research if their assistance should be required. Three of last year's appointees are now engaged in war research.

Of last year's fellowship winners, DR. THOMAS W. DAKIN Harvard University, has been reappointed for a second year's study. DR. JAMES S. KOEHLER of the University of Pennsylvania has been granted a year's leave of absence to act as instructor of physics at Carnegie Institute of Technology. The three other 1941 appointees have joined the Westinghouse Research staff. They are DR. DANIEL ALPERT, Stanford University; DR. JOHN W. COLTMAN, University of Illinois; and DR. THEODORE HOLSTEIN, New York University.

★

Conference on Problems of Modern Physics

To celebrate the public opening of the Charles Benedict Stuart Laboratory of Applied Physics, a Conference on Problems of Modern Physics was held at Purdue University on June 19th and 20th. The program was as follows:

JUNE 19

Opening address—**Physics in Industry,** DR. E. U. CONDON, *Associate Director, Westinghouse Research Laboratories.*

JUNE 20

Theories of Nuclear Forces, DR. J. SCHWINGER, *Purdue University.*

Problems of Modern Field Theories, DR. W. PAULI, *The Institute for Advanced Study.*

Design and Construction of the Twenty-Million-Volt Induction Accelerator, DR. D. W. KERST, *University of Illinois.*

The Physics of Statistical Noise, DR. W. W. HANSEN, *Stanford University and the Sperry Gyroscope Company.*

The Electron Microscope and Its Applications, DR. J. A. BECKER, *Bell Telephone Laboratories.*

★

Summer Courses in Physics

To help meet the present urgent need for people with advanced training in physics, the Graduate School of New York University, for the first time in a number of years, is offering courses in physics and mathematics during the summer.

These courses will be given in two short terms from June 29 to August 7 and from August 10 to September 18. They are planned as part of a one-year curriculum designed to cover the basic subjects of physics, including dynamics, electricity and magnetism, thermodynamics, physical optics, atomic structure, advanced laboratory, and methods of mathematical physics. The course in thermodynamics will be given in the first summer term and that in advanced laboratory in the second. The course in methods of mathematical physics will continue through both terms.

★

From College Machine Shop to War Factory

Purdue University's student machine shops at Lafayette, Indiana, customarily used only for routine practice work, recently have been converted into a war production factory under the terms of a Westinghouse subcontract.

More than 275 engineering students enrolled in the shop course are working part-time on the subcontract. Together their production is the equivalent of a 75-man machine shop working full time on war materials. Special stock material required for some parts being made by the students has been supplied by Westinghouse, and the university has received a priority rating from the War Production Board for the purchase of other materials.

★

Necrology

DR. MILLARD F. MANNING, Assistant Professor of Physics at the University of Pittsburgh, died June 1st of a ruptured appendix at the age of 36. For the past few years Dr. Manning had been interested in theoretical calculations concerning the properties of metals and other solids. Recently he and Dr. M. E. Bell completed an extended study of the properties of semi-conductors which was published in the *Reviews of Modern Physics.* Dr. Manning was a member of the American Physical Society.

Contributed Original Research

Surface Replicas for Use in the Electron Microscope

VINCENT J. SCHAEFER AND DAVID HARKER
Research Laboratory, General Electric Company, Schenectady, New York
(Received April 9, 1942)

A simple method is described for making replicas of surfaces for study in the electron microscope. The surface to be studied is cleaned and then coated with a very thin slightly wedge-shaped film of polyvinyl formal having a range in thickness from about 500 to 750A in 2.5 cm. This film is formed by dipping the prepared surface into a 0.5-percent solution of the resin dissolved in dioxane or ethylene dichloride and permitting the solvent to evaporate while the surface is held in a vertical position. The replica film is removed by placing the coated surface under water and peeling the film from it. A description of this technique is given in detail. A graph is presented which shows the thickness of resin films obtainable from various concentrations of resin in dioxane, and a table gives the interference effects which may be used for determining approximate thicknesses of thin resin films. Several easy procedures are described for checking the thickness of such films. A technique is described for preparing strong films having a thickness of 100A and an area of 3 cm² when mounted in air. Such films are very useful when working with the electron microscope and several methods are described for mounting specimens on them, including a conditioning treatment—useful in mounting water suspensions—which makes one surface very hydrophilic. Five micrographs show the results obtainable with the techniques described.

IN a recent paper[1] Zworykin and Ramberg described a method for studying the surfaces of solid materials, such as the etched surfaces of metals. The authors pointed out that the methods described by H. Mahl[2,3] in a series of papers in 1940 had the disadvantage that the specimen was destroyed in obtaining the replica. Zworykin and Ramberg described several techniques which could be used without spoiling the specimen and illustrated by micrographs the results obtained. Of the three methods described in some detail in their paper they indicated a decided preference to the silver-collodion process. This method involves the evaporation in a vacuum chamber of a metal film onto the surface of the specimen to be studied, which is then, if necessary, reinforced by electroplating, to such a thickness that the metal film can be stripped mechanically from the surface. A thin collodion film is then flowed over the metal replica, after which the latter is removed from the plastic by dissolving it in nitric acid. The collodion film is then mounted for study in the microscope.

Several other methods were tried by them, including one in which a resin material termed "vinylite lacquer" was applied directly to the specimen and removed mechanically. This latter method was evaluated in their paper[1] by the following statement: "While extremely simple it is relatively uncertain and yields far poorer resolution than the first method (silver-collodion) discussed."

This paper will attempt to point out possible reasons why this direct method can be "relatively uncertain" and possible ways in which this uncertainty can be nearly, if not completely, eliminated. It is obvious that maximum possible contrast can be obtained from a replica made directly from the original sample if a good replica is produced. Such a replica must be free of imperfections due to surface tension effects, thin enough to avoid electron absorption, thick enough to be removed without undue trouble, and strong enough to be removed from an etched surface without showing strains.

We have found a material which seems to fit these requirements quite well, and Figs. 1–3 illustrate the type of results which can be obtained. The method of forming such replicas is simple and the equipment needed can be assembled in a few hours. The resin used is polyvinyl formal known by the trade name of Formvar 15–95[4] and is dissolved in dioxane or ethylene

[1] V. K. Zworykin and E. G. Ramberg, J. App. Phys. **12**, 692 (1941).
[2] H. Mahl, Zeits. f. tech. Physik **21**, 17 (1940).
[3] H. Mahl, Metallwirtshaft **19**, 1082 (1940).
[4] Shawinigan Products Corporation, Empire State Building, New York City.

FIG. 1. Replica of etched surface of 0.4 percent C steel oil quenched.

dichloride. This material has been used previously[5, 6] where very thin strong films were needed, and occupies an eminent place in certain industrial applications because of its outstanding resistance to abrasion and other mechanical stresses and strains.

In preparing replicas of solid surfaces for observation in the electron microscope certain limitations are imposed by the physical properties of the electron beam impinging on the specimen as well as other related factors. We have found that a film having a thickness of 1500A begins to deteriorate within a few minutes when used in an RCA type B electron microscope at 50–60 kv. With a film of this thickness, observation shows that the degree of contrast is quite poor. A study was made of the effect of thickness on contrast and the results obtained indicate that a thickness between 500 and 750A produced the best image formation with the power supply indicated above. Films whose average thickness was less than 300A showed contrast as poor as those whose thickness exceeded 1000A. To understand this anomaly it would be best to consider the factors involved in preparing good replicas.

A surface carefully polished with MgO is relatively free of scratches. Those which remain are wide and shallow; the difference in height between the deepest groove and the highest elevation is probably not greater than 200A. From such a surface it is easy to obtain a stripping having a thickness of 250A. Under the electron beam little, if any, surface detail can be observed. With a light etch (2–5 sec. with a saturated solution of picric acid in alcohol) on an oil-quenched steel sample containing 1.1 percent C, a stripping having a thickness of 300–350A can be obtained without difficulty. In the electron microscope such a stripping shows a certain amount of "background" indicative of the crystalline structure of the metal, but the contrast is insufficient to be of any use to the observer. When the etching process is carried to the point where it is possible to get a fair photomicrograph at 1000X with the light microscope (15–25 sec. etch) it has been found that the replicas which can be obtained have a minimum thickness of about 550A. When an effort is made to secure replicas thinner than this latter dimension, the results are not successful. An increase of film thickness up to about 750A was found to be permissible without serious loss in contrast. These thicker films are also easier to remove from the metal surface, the main disadvantage being the loss in illumination on the fluorescent screen. It was found to be inadvisable to work with films thicker than 1000A because of this latter difficulty as well as the deterioration which occurs due to electron absorption. Our results indicate that nothing is gained by working with replicas having a thickness greater than that necessary for obtaining a coherent film. The advantage in additional strength which is gained by having the replica thicker by 50–100A than the distance between the high and low points of the etched surface is probably a real one, but anything greater than this can only result in a loss of contrast.

In order to have sufficient contrast to form a good image of an etched surface it is very important that the upper surface of the resin film is flat while that in contact with the metal surface follows it in intimate detail. That surface tension forces actually produce such conditions can be

[5] L. H. Germer, Phys. Rev. **56**, 58 (1939).
[6] V. J. Schaefer, J. Phys. Chem. **45**, 681 (1941).

shown by preparing a relatively thick replica of a heavily etched surface of pure copper. A 3-percent solution of polyvinyl formal was used, the replica made in the usual manner, removed from the copper block, mounted on a frame and viewed in the light microscope at about 200X magnification with vertical illumination which produced interference colors in the replica film. This film had an average thickness of about 3000A and under the microscope appeared identical to the original etched copper surface except that each grain exhibited certain interference colors. The important fact noted was that the interference colors were quite uniform for a given crystal grain right up to the grain boundary. The adjoining grain showed another color, also quite uniform over its entire area and was itself adjacent to other colored patches representing still other grains. A comparison of the observed interference colors with a thickness gauge made it an easy matter to ascertain the relative position in elevation of each grain but more important for present considerations demonstrated that the upper surface of the replica was quite level and did not follow the "hills and valleys"

FIG. 2. Replica of etched surface of 1.1 percent C steel furnace cooled.

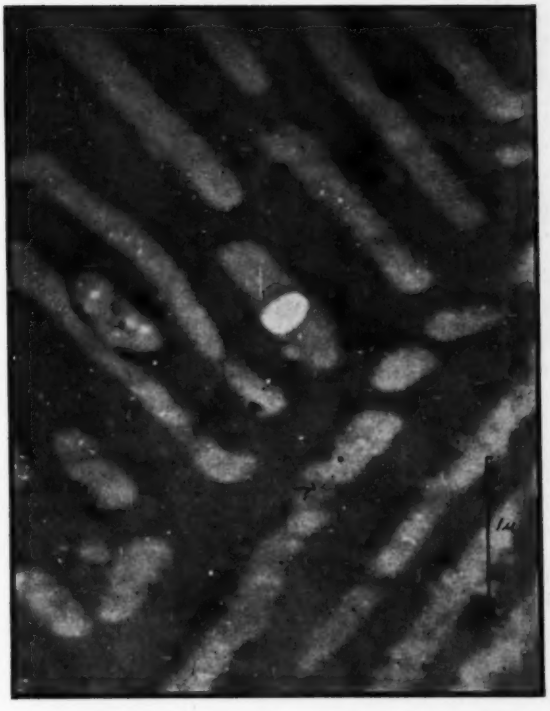

FIG. 3. Replica of etched surface of 0.4 percent C steel furnace cooled.

of the metal surface. If this latter condition were obtained, the interference color for a given grain area would be considerably different in the center from that at the grain boundary. A change in thickness of less than 25A would be readily detectable under the conditions described.

It is desirable from time to time to have a reasonably accurate and simple method for determining the thickness of the replicas which are being prepared from a stock solution so that its strength can be adjusted as the solvent disappears due to evaporation. The film thickness which our experience has shown produces replicas having the best contrast is made from a solution containing 500 mg of polyvinyl formal dissolved in 100 cc of dioxane. As shown in Fig. 4, the mid-thickness of a wedge-shaped film 2.5 cm wide made from a solution of this concentration, in a manner to be described later in this paper, is of the order of 650A. The strength of the stock solution used may be checked occasionally by dipping a cleaned (with wet MgO on a cotton swab) and dried (with filtered air) 1″×3″ ×0.060″ chromium plated slide[7] into the solution

[7] Appollo Metal Works, 66th Place and South Oak Park Avenue, Chicago, Illinois.

and letting the solvent evaporate with the plane of the slide vertical and the long axis horizontal. If, when viewed in white light at nearly grazing incidence ($i=80°$) the thicker edge of the film coating the chromium plated slide appears as a yellow interference color, the solution has the proper concentration for producing good replicas. Table I represents the relation of observed color to actual thickness of a resin film flowed on a polished chromium surface. These colors are best observed by polarized light, although this refinement is not essential. From this table and Fig. 4 it is apparent that the solution should not be allowed to become more concentrated than 0.75 percent which would produce a film having a color range in a distance of 2.5 cm of yellow to purple when viewed at nearly grazing incidence $i=80°$.

The treatment of the surface of a solid preliminary to forming its replica governs to a considerable degree the ease with which the replica may be removed. The replica of the surface of polished glass is probably about the easiest to obtain if the glass is reasonably clean. From such a surface it is a simple process to obtain a stripping having a thickness of 100A. A single layer of molecules of a hydrophobic substance, such as grease or oil, will completely prevent carrying out this normal stripping process and it is necessary to increase the film thickness at least tenfold in order to add sufficient tensile strength to the film to enable its mechanical removal.

Metal surfaces, particularly those etched after polishing, present a much more difficult problem in preparing satisfactory replicas unless certain important factors are recognized. It was found, for example, that a delay of no more than five minutes between the drying of a steel specimen after etching and the formation of the resin film on its surface was sufficient to prevent the removal of the film from the metal. When this film was subsequently removed by a solvent and the surface of the metal cleaned by rubbing lightly with MgO on a cotton swab followed by washing with distilled water and quick drying with a stream of filtered air, a similar film applied without delay was removed easily and showed exceptionally fine detail. Great care must be exercised in the final cleaning of the metallographic specimen so that as the specimen is dried it is quite free of even a portion of a deposited

TABLE I. Actual thickness of thin films on a polished chromium plated surface having a refractive index range of $n=$Ca 1.49.

Actual thickness	Color at $i=80°$
600A	Pale yellow
700A	Yellow
800A	Yellow orange
850A	Orange
900A	Orange red
950A	Red
1000A	Purple
1050A	Deep blue
1100A	Blue
1150A	Light blue
1200A	Pale blue
1300A	Faint blue

monolayer of hydrophobic types of molecules. It is very difficult to obtain this condition with the usual types of thermoplastic mounts often used for holding the specimen during the polishing process since the bond between the metal and the mounting medium often pulls away to leave a tiny crack which harbors surface active molecules. As the specimen is dried these molecules tend to spread over the metal to form metallic soaps and other types of adsorbed monolayers which later are responsible for lack of success in obtaining good replicas. These layers often will form in less than a second. A good test for the presence of a contaminating or hydrophobic layer on the metal surface is to place a drop of distilled water from a carefully cleaned pipette on the surface. If it flashes out and covers the surface without a contact angle, the surface treatment may be considered adequate. If, however, the drop remains as such and shows a definite contact angle with the metal, the cleaning method must be improved upon if good replicas are to be obtained.

For preparing good replicas the following technique has been found to be very successful:

After the specimen has been given a good metallographic polish (we use MgO on polishing cloth known as kitten's-ear for the final polishing of steel specimens), the surface is given an etch of such a depth that a fairly good photomicrograph can be obtained at 1000X in the light microscope. The etching solution is then removed and the surface quickly dried with a jet of clean filtered air. The specimen is then immediately lowered face down into a petri dish containing a small amount of a 0.5-percent solution of polyvinyl formal dissolved in dioxane. The specimen is

removed with a smooth motion and swung into a position such that the plane of the surface is vertical with respect to the surface of the resin solution. The solvent is allowed to evaporate to completion while held in the vertical position. This procedure forms a wedge-shaped film on the metal surface thickest at the lower edge and thinnest at the top. With a specimen having a diameter of 2.5 cm the range in thickness will be from 500 to 750A, although at the very bottom there will be a small area much thicker than this where the draining liquid accumulates. The specimen bearing the resin film is then placed under water in a shallow tray at such a depth that the metal surface is about 3 cm under the water surface.

A good pair of sharp pointed tweezers with both "anvils" in good register is then brought into contact with the edge of the metallographic specimen at the thick end of the resin wedge and the film is carefully "teased" until it is seen to pile up in a small roll. After this has proceeded for a millimeter or so toward the center of the specimen, a purchase is obtained on the edge of the film and the tweezers are slowly drawn toward the thin end of the wedge.

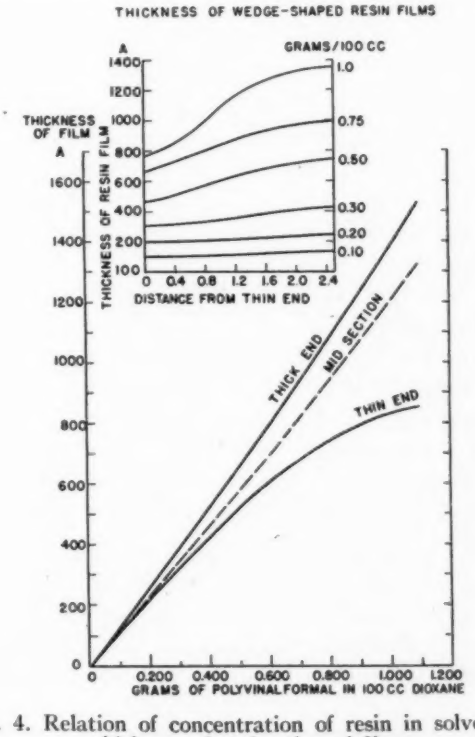

FIG. 4. Relation of concentration of resin in solvent to thickness of wedge-shaped film.

If the surface was free of hydrophobic material, the etch of the right depth, and the metal relatively free of porous inclusions such as oxides, a considerable piece of replica film will easily peel from the surface. Sometimes the complete film may be removed, although as a rule the best replicas tear before reaching the opposite side. While still under water, the peeled film is swung around so that the upper surface will reach the water surface first in an extended condition. Just before bringing the film to the surface, the latter should be swept clean of any contaminating surface film. As the film arrives at the surface it will shed water completely and should be entirely free of wrinkles or folds. While still on the water surface, the nickel mesh screens for mounting the replica in the microscope may be positioned in selected positions on the floating film, after which the film is removed from the water surface. In doing this, we prefer to place a bit of adhesive material, such as rubber cement, on the rim of a metal frame which is then brought down onto the upper surface of the replica. The frame bearing the film and screens is then removed from the cleaned water surface with a smooth tipping motion which finds the plane of the resin film at right angles with the water surface at the end of the movement. This procedure removes the film from the water without subjecting it to undue strain and in a dry condition. With certain metals, such as duralumin, where one constituent is removed preferentially by a special etching technique,[8] the residue will be removed with the replica film and consequently the under surface of the film will be wet when removed from the water bath. A convenient set-up for carrying out these steps is a 6″ petri dish $2\frac{1}{4}$″ deep painted black on the outside and illuminated by the reflection of white light from a sheet of white paper or cloth. The edge of the dish should be made hydrophobic by rubbing with molten wax, and two narrow strips of brass $\frac{1}{8}$″×$\frac{1}{4}$″×8″ similarly treated will be useful for cleaning the water surface of surface contamination.

In the course of making replicas of metal surfaces with polyvinyl formal dissolved in ethylene dichloride, a peculiar spotted structure was often observed. At first it was thought that the ob-

[8] F. Keller and R. A. Bossert, Metal Progress **41**, 63 (1942).

served structure was characteristic of the metal. This idea was discarded, however, when similar detail was found on various unrelated metals including pure nickel and copper. Other reasons were suggested to explain the occurrence of the spots which sometimes varied in size and density, but each was in turn successively discarded. Finally, a theory was proposed that the spots might be due to an oleophobic property of the surface which by a mechanism previously studied[6] would cause the liquid solution of resin to start peeling back from the metal at many nuclei. Before the film could thin sufficiently to form actual holes, as occurred in the work cited, the solvent evaporated.

In order to test out the validity of this proposed explanation of the spotted structure, a chromium plated slide well polished was selected and given various surface treatments. When cleaned very carefully with MgO, taking every precaution to prevent the deposition of a monolayer, a replica from the surface was nearly free of spots and those present were very small. A monolayer consisting of melted ferric stearate well rubbed was then tried and this time the replica showed the type of spotted structure which was typical of many previous strippings. A very oleophobic[6] surface was then prepared of two monolayers of acid barium copper stearate. The replica from this surface showed unusually large spots again spaced quite at random.

FIG. 5. Particle of stearic acid smoke mounted between two thin films of polyvinyl formal.

Although the presence of spots proved to be undesirable in the present instance, it should be mentioned at this point that it will be worthwhile to study this effect more carefully since it is quite possible that the presence of the holes, especially when they show a definite alignment, might be showing the location of oxide or other types of inclusions so small as to be beyond the resolving power of the present electron microscope.

By using dioxane instead of ethylene dichloride as a solvent for polyvinyl formal resin, the trouble due to spotting was entirely eliminated even though the surface of the metal was given only an ordinary cleaning. Because of the difficulty of removing replicas from slightly hydrophobic surfaces, however, it is recommended that the cleaning process described previously be carried out when making replicas with dioxane and polyvinyl formal resin.

Several methods[5, 6, 9] have been described for preparing thin films for holding various types of specimens for study in the electron microscope or electron diffraction camera.

The following procedure has been developed in this laboratory and will be described since it permits a somewhat better control of thickness and conditioning treatment than the other techniques known to us:

A glass plate, such as a microscope slide, is cleaned by rubbing with MgO powder or with a standard glass cleaning solution such as $K_2Cr_2O_7-H_2SO_4$. After drying, the slide is dipped into a 0.1-percent solution of polyvinyl formal in ethylene dichloride or dioxane, and withdrawn and the solvent evaporated. After the solvent evaporates (a matter of less than a minute), the film is scored with a needle or similar sharp pointed tool around the edges of the plate and at the same time the main part of the film may be subdivided into as many smaller areas as may be desired. The plate is then held vertically

[9] L. Harris and E. A. Johnson, Rev. Sci. Inst. **4**, 454 (1933).

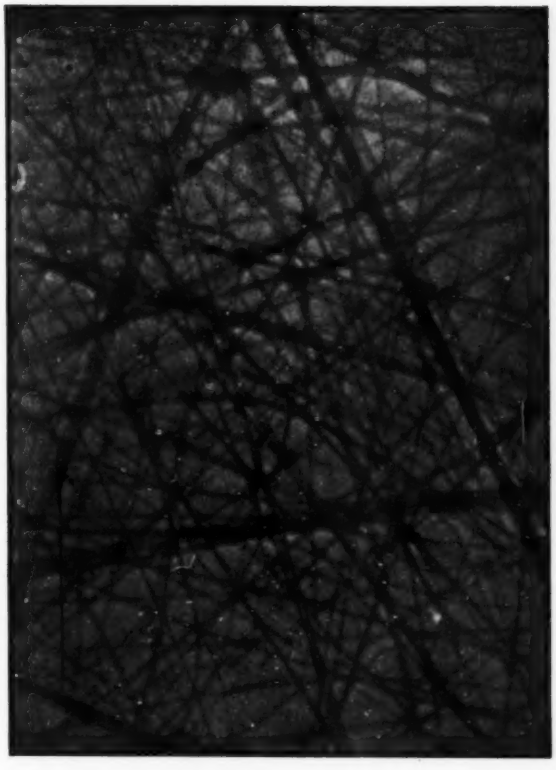

FIG. 6. Sample of colloidal V_2O_5 mounted on conditioned surface of polyvinyl formal film.

over a tray containing water whose surface is clean and with a quick motion plunged under water. The plate is then withdrawn with a slow motion to permit the water to peel from the surface and again lowered, this time at a somewhat slower rate. The film will peel off the plate and float on the water surface.

We have found that freshly split mica, preferably muscovite, as a base for forming thin films has certain advantages over glass slides since such a surface does not require cleaning and is very smooth. A fresh splitting should be used each time.

For mounting the film an ordinary $\frac{3}{8}''$ or $\frac{1}{2}''$ steel washer is given a thin coat of adhesive such as rubber cement, held in a horizontal position with a small magnet, and lowered into contact with the floating film. The mounted film is then removed from the water by raising the frame at one edge and progressively tipping it upward and away from the water. As this is done, the water peels off the under surface of the film and it is removed completely dry and free of any contaminating residue or internal strains. In this manner, using polyvinyl formal, a film only 100A in thickness and an area of 3 cm^2 is easily obtained. Such a film reflects little light and is similar in appearance to a "black" soap bubble. A number of these thin films can be prepared at one time and kept for future use.

By placing specimens which tend to fly off when subjected to the electron beam between two films in contact with each other, they are securely anchored and remain in place in the field. The smoke particle illustrated in Fig. 5 is an example of a specimen which is difficult to observe unless held in place between two films. When specimens in water solution are to be mounted, it is sometimes advantageous to have the film hydrophilic. This is easily accomplished by forming a monolayer[10] of a protein, such as insulin or egg albumin, on a water surface, putting it under a pressure of a few dynes cm^{-1}, lowering a mounted film into contact with it, and then removing the film again from the water surface. This process produces a surface which is completely wet with water with an increased thickness due to the deposited film of not more than 30A. A few drops of the liquid containing the specimens to be examined are placed in contact with the wet surface and then the excess water is drained and the film dried. Figure 6 illustrates a sample of colloidal V_2O_5 prepared in this manner.

Replicas may be stored under ordinary atmospheric conditions for a long time. In our collection, we have polyvinyl formal films 100A in thickness which are now nearly a year old and others less than 1000A which show no sign of deterioration after more than three years. Some of our steel surface replicas used for demonstration purposes have been in and out of the electron microscope more than a score of times over a period of several months without showing any ill effects.

In conclusion, it might be pointed out that we find it possible with the equipment and technique described in this paper to have a good image of the surface of a metallographic specimen on the fluorescent screen of the electron microscope within five minutes after the sample has been received from the polishing room.

[10] I. Langmuir and V. J. Schaefer, Chem. Rev. **24**, 181 (1939).

The Matrix Theory of Torsional Oscillations

LOUIS A. PIPES
Graduate School of Engineering, Harvard University, Cambridge, Massachusetts
(Received March 5, 1942)

The general case of vibration of a shaft with several rotating masses is discussed. The analysis is reduced to a simple matrix multiplication of second-order matrices and the natural frequencies of symmetrical systems are discussed. The connection of the matrix method and the well-known Holzer method of computing the natural frequencies of torsional oscillations is considered. The analysis of geared systems and continuous shafts is discussed.

INTRODUCTION

THE analysis of problems on torsional vibrations in electrical machinery, Diesel engines, and propeller shafts can be reduced to a system of several rotating masses on a shaft.[1,2] In the usual analysis of the torsional oscillations of the crankshaft of an internal combustion engine, the actual system is replaced by an equivalent system consisting of a uniform shaft carrying equidistant identical disks. The regularity of the system leads naturally to an analysis using the calculus of finite differences.[3–5] In this

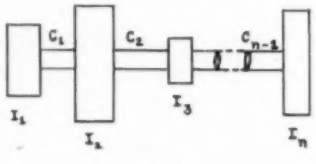

FIG. 1.

discussion the problem will be analyzed by the use of simple matrix multiplication. The matrix analysis emphasizes the physical significance of the mathematical procedure and appears most direct, since the problem of the evaluation of troublesome arbitrary constants is not encountered. Geared and continuous systems may be most effectively analyzed by the matrix method. The connection between the well-known Holzer method of analysis[1] and the matrix method is established.

[1] J. P. Den Hartog, *Mechanical Vibrations* (McGraw-Hill, 1940), Chapter 5.
[2] F. M. Lewis, "Torsional vibration in the Diesel engine," Trans. Soc. Nav. Arch. Marine Eng. **33**, 109 (1925).
[3] M. A. Biot, "Equations of finite differences applied to torsional oscillations of crankshaft," J. App. Phys. **11**, 530–537 (1940).
[4] M. A. Biot, "Vibrations of crankshaft-propeller systems, new method of calculation," J. Ae. Sci. **8**, 107–112 (1940).
[5] Th. von Kármán and M. A. Biot, *Mathematical Methods in Engineering* (McGraw-Hill, 1940).

I. STATEMENT OF THE PROBLEM

The problem under consideration in this discussion is the determination of the natural frequencies and modes of oscillation of a set of disks on a shaft, as shown in Fig. 1, when the torsional elasticity of the shafting c_r and the moment of inertia I_r of the disks are specified.

The assumption will be made that the disks are rigid members and that the connecting sections of shafts are devoid of inertia. The terminal disks will be assumed to be either free or fastened to fixed supports through elastic shafting in a specified manner. The case of geared systems and systems where the inertia of the shafting must be taken into account will be considered also.

II. THE ASSOCIATED MATRICES OF DISKS AND SHAFTS

a. Associated Matrices of a Disk

Consider a disk of moment of inertia I about its central axis AB as shown in Fig. 2. Let M_1 be a couple applied to the left side of the disk tending to cause the disk to rotate in a clockwise sense about the axis AB. Let M_2 be a couple applied to the right side of the disk tending to cause the disk to rotate about AB in the counterclockwise sense. Let ϕ_1 be the angular displacement of a point on the left side of the disk with respect to some fixed point in space and let ϕ_2 be the angular displacement of a corresponding

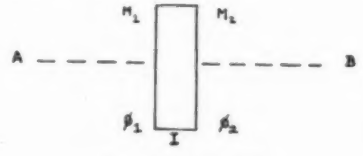

FIG. 2. Stiff disk.

point of the right-hand side of the disk. By Newton's law for a rotating body, we have:

$$M_1 - M_2 = I(d^2\phi_2/dt^2). \tag{1}$$

Since the disk is assumed devoid of elasticity, we have:

$$\phi_1 = \phi_2. \tag{2}$$

Now let it be assumed that the couples applied to the disk are of an oscillatory nature of angular frequency. We then have

$$M_1 = T_1 \sin \omega t, \tag{3}$$

$$M_2 = T_2 \sin \omega t. \tag{4}$$

Let us assume also that these oscillatory couples give rise to an angular deflection of an oscillatory nature. Hence:

$$\phi_1 = \theta_1 \sin \omega t, \tag{5}$$

$$\phi_2 = \theta_2 \sin \omega t. \tag{6}$$

Substituting these relations into Eqs. (1) and (2) and dividing out the common factor sin ωt, we obtain

$$T_1 = T_2 - I\omega^2\theta_2, \tag{7}$$

$$\theta_1 = \theta_2. \tag{8}$$

Equations (7) and (8) may be written in the convenient matrix form:

$$\begin{Bmatrix} T_1 \\ \theta_1 \end{Bmatrix} = \begin{bmatrix} 1 - \omega^2 I \\ 0 \quad 1 \end{bmatrix} \begin{Bmatrix} T_2 \\ \theta_2 \end{Bmatrix}. \tag{9}$$

The associated matrix

$$[\mu]_d = \begin{bmatrix} 1 - \omega^2 I \\ 0 \quad 1 \end{bmatrix} \tag{10}$$

will be called the associated matrix of the disk.

b. The Associated Matrix of a Shaft

Consider a section of shaft as shown in Fig. 3.

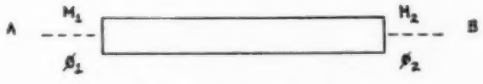

FIG. 3. Massless shaft.

Let the torsional stiffness of the shaft be c. Assume that the inertia of the shaft may be neglected. Let M_1 be a couple applied to the shaft tending to turn the left end of the shaft in a clockwise sense about the central axis of the shaft A–B. Let M_2 be a couple applied to the right end tending to turn the right end of the shaft in a counter-clockwise manner about its central axis A–B. Let ϕ_1 be the angular displacement of a point on the left end of the shaft with respect to a fixed reference point in space, and

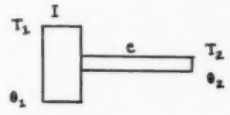

FIG. 4. Combination of disk and shaft.

let ϕ_2 be the angular displacement of a corresponding point on the right end of the shaft with respect to the fixed reference point. Let $\phi_1 = \phi_2$ when the shaft is not undergoing torsional stress. We then have by Newton's third law:

$$M_1 = M_2. \tag{11}$$

By the definition of torsional stiffness, we have:

$$c(\phi_1 - \phi_2) = M_2. \tag{12}$$

Now, as before, assume that the couples that are applied to the shaft are of an oscillatory nature and are given by (3) and (4). Let the angular displacements be given by (5) and (6). Substituting these equations into (11) and (12) and dividing out the common factor sin (ωt) we obtain:

$$T_1 = T_2, \tag{13}$$

$$\theta_1 = (T_2/c) + \theta_2 \tag{14}$$

These equations may be written in the convenient matrix form:

$$\begin{Bmatrix} T_1 \\ \theta_1 \end{Bmatrix} = \begin{bmatrix} 1 \quad 0 \\ 1/c \quad 1 \end{bmatrix} \begin{Bmatrix} T_2 \\ \theta_2 \end{Bmatrix}. \tag{15}$$

The matrix

$$[\mu]_s = \begin{bmatrix} 1 \quad 0 \\ 1/c \quad 1 \end{bmatrix} \tag{16}$$

will be called the associated matrix of the shaft.

c. Associated Matrix of a Disk Attached to a Shaft

Consider the system of Fig. 4 which consists of a stiff disk of moment of inertia I attached to a massless shaft of torsional stiffness c. Let T_1 be

the oscillating torque applied to the left side of the disk in the clockwise sense and T_2 the oscillating torque applied to the right end of the shaft in the counter-clockwise sense. θ_1 and θ_2 are the reference angles of the left side of the mass and the right end of the shaft, respectively. In view of (9) and (15) we have:

$$\begin{Bmatrix} T_1 \\ \theta_1 \end{Bmatrix} = \begin{bmatrix} 1-\omega^2 I & 0 \\ 0 & 1 \end{bmatrix} \begin{bmatrix} 1 & 0 \\ 1/c & 1 \end{bmatrix} \begin{Bmatrix} T_2 \\ \theta_2 \end{Bmatrix}. \quad (17)$$

This relation follows from the fact that the torque transmitted through the right side of the disk is equal to that impressed on the left end of the shaft and the angular displacement of the right side of the disk is equal to that of the left end of the shaft.

Multiplying the two square matrices of (17) together we obtain:

$$\begin{Bmatrix} T_1 \\ \theta_1 \end{Bmatrix} = \begin{bmatrix} (1-\omega^2 I/c)-\omega^2 I & \\ 1/c & 1 \end{bmatrix} \begin{Bmatrix} T_2 \\ \theta_2 \end{Bmatrix}. \quad (18)$$

III. FREQUENCY EQUATIONS OF SIMPLE SYSTEMS

a. Disk and Shaft Attached to Fixed Support

The associated matrices of simple systems are of great value in determining the frequency equations of these systems. Let us consider first the simplest system of Fig. 5. The frequency

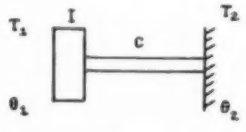

FIG. 5.

equation giving the free oscillations of this simple system may be obtained from (18) by noting that at the fixed support $\theta_2=0$, and that for free oscillations $T_1=0$. In this case we have directly from (18)

$$T_1 = T_2(1-\omega^2 I/c) = 0. \quad (19)$$

Hence

$$(1-\omega^2 I/c) = 0, \quad (20)$$

or

$$\omega = (c/I)^{\frac{1}{2}}. \quad (21)$$

A slightly more complicated system is that of Fig. 6. This system consists of two disks of

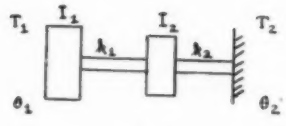

FIG. 6.

moments of inertia I_1 and I_2 coupled by means of two elastic shafts (as shown) to a rigid support. The equations have a somewhat simpler form if we write the associated matrices of the system in terms of the torsional flexibility constant $k=1/c$ rather than the torsional stiffness c. In this case, we have $\theta_2=0$ since the shaft is fixed at the right end. Consequently we have:

$$\begin{Bmatrix} T_1 \\ \theta_1 \end{Bmatrix} = \begin{bmatrix} (1-\omega^2 I_1 k_1)-\omega^2 I_1 & \\ k_1 & 1 \end{bmatrix} \times \begin{bmatrix} (1-\omega^2 I_2 k_2)-\omega^2 I_2 & \\ k_2 & 1 \end{bmatrix} \begin{Bmatrix} T_2 \\ 0 \end{Bmatrix}. \quad (22)$$

Performing the matrix multiplication, we obtain:

$$T_1 = T_2\{(1-\omega^2 I_1 k_1)(1-\omega^2 I_2 k_2)-\omega^2 I_1 k_2\} = 0. \quad (23)$$

Since the left end is oscillating freely, $T_1=0$ and hence the expression in brackets must vanish. This leads directly to the frequency equation:

$$\omega^4 I_1 I_2 k_1 k_2 - \omega^2(I_1 k_1 + I_2 k_2 + I_1 k_2) + 1 = 0. \quad (24)$$

As another example of this method of obtaining the frequency equation of the system, let us consider the system of Fig. 7. In this case k_1, k_2, k_3 are the torsional flexibilities of the shafts as shown and I_1 and I_2 are the moments of inertia of the disks about the axis of rotation.

In this case $\theta_2=0$ since the system is fixed at the right end. Therefore we may write the relation

$$\begin{Bmatrix} T_1 \\ \theta_1 \end{Bmatrix} = \begin{bmatrix} 1 & 0 \\ k_1 & 1 \end{bmatrix} \begin{bmatrix} (1-\omega^2 I_1 k_2)-\omega^2 I_1 & \\ k_2 & 1 \end{bmatrix} \times \begin{bmatrix} (1-\omega^2 I_2 k_3)-\omega^2 I_2 & \\ k_3 & 1 \end{bmatrix} \begin{Bmatrix} T_2 \\ 0 \end{Bmatrix}. \quad (25)$$

Performing the matrix multiplication, we obtain:

$$\theta_1 = T_2[k_1(1-\omega^2 I_1 k_2)(1-\omega^2 I_2 k_3) - \omega^2 I_1 k_1 k_3 + k_2(1-\omega^2 I_2 k_3) + k_3] = 0. \quad (26)$$

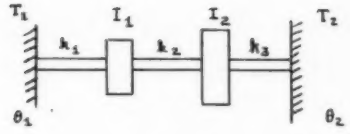

FIG. 7.

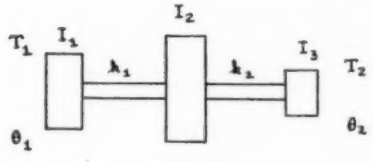

FIG. 8.

Since the left end of the system is rigidly fastened, $\theta_1=0$. It follows that the term in brackets must vanish. This leads to the frequency equation:

$$\omega^4 I_1 I_2 k_1 k_2 k_3 - \omega^2 I_1(k_1 k_2 + k_1 k_3) + I_2(k_1 k_3 + k_2 k_3) + (k_1 + k_2 + k_3) = 0 \quad (27)$$

for the frequency equation of the system of Fig. 7.

As a final example of this method of determining the frequency equation of torsional vibrating systems, let us consider the system of Fig. 8. In this case both ends of the system consisting of three disks and two shafts are free. Consequently we have $T_2=0$. We may, therefore, write the relation:

$$\begin{Bmatrix} T_1 \\ \theta_1 \end{Bmatrix} = \begin{bmatrix} (1-\omega^2 I_1 k_1) & -\omega^2 I_1 \\ k_1 & 1 \end{bmatrix} \times \begin{bmatrix} (1-\omega^2 I_2 k_2) & -\omega^2 I_2 \\ k_2 & 1 \end{bmatrix} \begin{bmatrix} 1-\omega^2 I_3 & \\ 0 & 1 \end{bmatrix} \begin{Bmatrix} 0 \\ \theta_2 \end{Bmatrix}. \quad (28)$$

Performing the matrix multiplication, we obtain:

$$T_1/\theta_2 = -\omega^2 I_3[(1-\omega^2 I_1 k_1)(1-\omega^2 I_2 k_2) - \omega^2 I_1 k_2] - \omega^2 I_2(1-\omega^2 I_1 k_1) - \omega^2 I_1. \quad (29)$$

Since the left end of the system is free, $T_1=0$, so the right member of (29) must vanish. This leads to the conditions:

$$\omega^2 = 0, \quad (30)$$

or

$$\omega^4 I_1 I_2 I_3 k_1 k_2 - \omega^2[I_1 I_2 k_1 + I_1 I_3 k_1 + I_1 I_3 k_2 + I_2 I_3 k_2] + (I_1 + I_2 + I_3) = 0. \quad (31)$$

More complicated systems having a greater number of disks may be analyzed in a similar manner.

IV. FREQUENCY EQUATION OF EQUIDISTANT IDENTICAL DISKS

In the analysis of the torsional oscillations of internal combustion engines, the vibrating system is reduced to one of a uniform shaft carrying equidistant identical disks. The analysis of systems of this type has been carried out by Biot[3-5] using the calculus of finite differences. In this section the analysis of these symmetrical systems will be considered by the use of matrix algebra.

To fix the ideas, let us consider the oscillations of the system of Fig. 9. This is a system of n

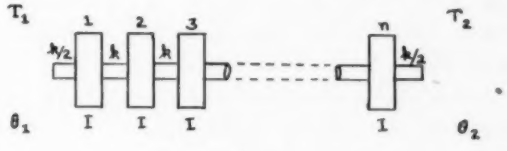

FIG. 9.

identical disks of moments of inertia I about the axis of rotation fastened together by sections of shafting of torsional flexibility k and free at both ends. The system of Fig. 9 may be regarded as made up by the interconnection of n fundamental units of the type shown in Fig. 10.

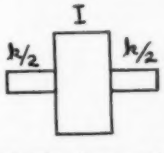

FIG. 10. Fundamental unit.

This fundamental unit consists of a disk of moment of inertia I to which are fastened two sections of shafting of torsional flexibility $k/2$ as shown. The associated matrix of this fundamental unit is given by:

$$\begin{bmatrix} 1 & 0 \\ k/2 & 1 \end{bmatrix} \begin{bmatrix} 1-\omega^2 I & \\ 0 & 1 \end{bmatrix} \begin{bmatrix} 1 & 0 \\ k/2 & 1 \end{bmatrix} = \begin{bmatrix} \left(1-\frac{\omega^2 Ik}{2}\right) - & \omega^2 I \\ \left(k-\frac{k^2\omega^2 I}{4}\right) & \left(1-\frac{\omega^2 Ik}{2}\right) \end{bmatrix}. \quad (32)$$

Now since the system of Fig. 9 is a chain of n units of the fundamental type of Fig. 10, we may write:

$$\begin{Bmatrix} T_1 \\ \theta_1 \end{Bmatrix} = \begin{bmatrix} A & B \\ C & D \end{bmatrix}^n \begin{Bmatrix} T_2 \\ \theta_2 \end{Bmatrix}, \tag{33}$$

where A, B, C, and D are the elements of the associated matrix of the fundamental unit given by (32). We note that

$$A = D = (1 - \omega^2 Ik/2). \tag{34}$$

This is a consequence of the symmetry of the fundamental unit.

To obtain the frequency equation of the system of Fig. 9, we could, of course, raise the associated matrix of the fundamental unit to a high power and then follow the procedure of Section III. This would be a very tedious procedure. Instead we take advantage of a theorem in matrix algebra which enables us to write down the power of a matrix directly.

This theorem is established in the Appendix. The theorem states that

$$\begin{bmatrix} A & B \\ C & D \end{bmatrix}^n = \begin{bmatrix} \cosh(an) & Z_0 \sinh(an) \\ \dfrac{\sinh(an)}{Z_0} & \cosh(an) \end{bmatrix}, \tag{35}$$

where

$$\cosh(a) = \frac{A+D}{2} = \left(1 - \frac{\omega^2 Ik}{2}\right), \tag{36}$$

$$Z_0 = \frac{((A+D)^2-4)^{\frac{1}{2}}}{2c} = \frac{\sinh(a)}{k\cosh^2(a/2)} = \frac{\sinh(a)}{c}, \tag{37}$$

provided that

$$A = D \tag{38}$$

and

$$(A+D) \neq \pm 2. \tag{39}$$

To simplify the writing let us use the notation

$$\begin{bmatrix} \cosh(an) & Z_0 \sinh(an) \\ \dfrac{\sinh(an)}{Z_0} & \cosh(an) \end{bmatrix} = \begin{bmatrix} A_n & B_n \\ C_n & D_n \end{bmatrix} = \begin{bmatrix} A & B \\ C & D \end{bmatrix}^n. \tag{40}$$

a. Natural Frequency of Free Shaft

We are now in a position to compute the natural frequencies of the free shaft of Fig. 9. Since the right end of the system is free, $T_2 = 0$ and we may write:

$$\begin{Bmatrix} T_1 \\ \theta_1 \end{Bmatrix} = \begin{bmatrix} A_n & B_n \\ C_n & D_n \end{bmatrix} \begin{Bmatrix} 0 \\ \theta_2 \end{Bmatrix}. \tag{41}$$

Carrying out the matrix multiplication, we obtain:

$$T_1 = B_n \theta_2. \tag{42}$$

Since the left end of the system is free, $T_1 = 0$ and it follows that:

$$B_n = Z_0 \sinh(an) = [\sinh(a) \sinh(an)/k\cosh^2(a/2)] = 0. \tag{43}$$

This is the frequency equation of the system of Fig. 9. From this we obtain

$$\sinh(an) = 0, \tag{44}$$

and

$$an = r\pi j, \quad r = 0, 1, 2, \cdots. \tag{45}$$

Hence

$$a_r = r\pi j/n, \quad r = 0, 1, 2, \cdots, \quad j = \sqrt{-1}. \tag{46}$$

Now the condition (39) excludes the value 0, and n that may be taken by r. The value $r = 0$ corresponds to the system rotating as a whole without any relative motion with the system. To obtain the natural frequencies we have

$$\cosh(a_r) = \left(1 - \omega^2{}_r \frac{Ik}{2}\right) = \cosh\left(\frac{r\pi j}{n}\right) = \cos\left(\frac{r\pi}{n}\right). \tag{47}$$

Hence

$$\omega^2{}_r = \frac{2}{Ik}\left[1 - \cos\left(\frac{r\pi}{n}\right)\right] = \frac{4}{Ik}\sin^2\left(\frac{r\pi}{2n}\right), \tag{48}$$

or

$$\omega_r = \frac{2}{(Ik)^{\frac{1}{2}}}\sin\left(\frac{r\pi}{2n}\right) \quad r = 1, 2, \cdots (n-1). \tag{49}$$

The possible natural angular frequencies of the system are given by (49).

b. Natural Frequency of Shaft Fixed at Both Ends

Let us now consider the system of Fig. 11. In this case the two ends of the system are fastened

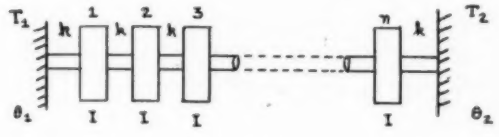

FIG. 11.

to rigid supports as shown. We can write $\theta_2=0$, and hence

$$\begin{Bmatrix} T_1 \\ \theta_1 \end{Bmatrix} = \begin{bmatrix} 1 & 0 \\ k/2 & 1 \end{bmatrix} \begin{bmatrix} A_n & B_n \\ C_n & D_n \end{bmatrix} \begin{bmatrix} 1 & 0 \\ k/2 & 1 \end{bmatrix} \begin{Bmatrix} T_2 \\ 0 \end{Bmatrix}. \quad (50)$$

Carrying out the matrix multiplication, we obtain:

$$\theta_1/T_2=(A_n+D_n)k/2+C_n+B_nk^2/4. \quad (51)$$

Since the left end of the system is fixed, $\theta_1=0$ and hence the right member of (51) must vanish. Substituting the values of A_n, B_n, C_n, and D_n from (35) into the resulting expression, we obtain:

$$\frac{\cosh(an)+\sinh(a)\sinh(an)}{4\cosh^2(a/2)} + \frac{\sinh(an)\cosh^2(a/2)}{\sinh(a)} = 0, \quad (52)$$

or

$$[\sinh(n+1)a/\sinh(a)]=0. \quad (53)$$

The solution of the transcendental equation (53) is

$$a_r=r\pi j/(n+1), \quad r=1, 2, 3, \cdots n. \quad (54)$$

Substituting these values of a into (36), we obtain

$$\omega_r=\frac{2}{(Ik)^{\frac{1}{2}}}\sin\left[\frac{r\pi}{2(n+1)}\right], \quad r=1, 2, \cdots n \quad (55)$$

for the natural frequencies of the system of Fig. 11.

c. Natural Frequencies of Shaft Fixed at One End

The system of Fig. 12 represents a uniform shaft carrying n identical disks equidistantly

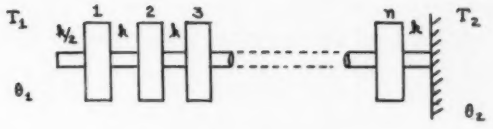

FIG. 12.

spaced, free at the left end and fixed at the right as shown. In this case we have $\theta_2=0$ and we can write:

$$\begin{Bmatrix} T_1 \\ \theta_1 \end{Bmatrix} = \begin{bmatrix} A_n & B_n \\ C_n & D_n \end{bmatrix} \begin{bmatrix} 1 & 0 \\ k/2 & 1 \end{bmatrix} \begin{Bmatrix} T_2 \\ 0 \end{Bmatrix}. \quad (56)$$

Carrying out the matrix multiplication, we have:

$$T_1=\left(A_n+\frac{k}{2}B_n\right)T_2. \quad (57)$$

Since $T_1=0$, we must have

$$\left(A_n+\frac{k}{2}B_n\right)=\cosh(an)$$

$$+\frac{\sinh(a)\sinh(an)}{2\cosh^2(a/2)}=0. \quad (58)$$

This may be written in the form

$$\frac{\cosh\frac{(2n+1)a}{2}\cosh\left(\frac{a}{2}\right)}{\cosh^2(a/2)}=0. \quad (59)$$

Hence

$$\cosh[(2n+1)a/2]=0. \quad (60)$$

This leads to

$$a_r=\frac{(2r-1)\pi j}{(2n+1)}, \quad r=1, 2, \cdots n. \quad (61)$$

Then from (36) we obtain

$$\omega_r=\frac{2}{(Ik)^{\frac{1}{2}}}\sin\left[\frac{(2r-1)\pi}{2(2n+1)}\right], \quad r=1, 2, \cdots n. \quad (62)$$

d. Natural Frequencies of General Terminal Conditions

In the simple cases that we have considered, the frequency equations have been particularly simple transcendental equations whose solution was easily written down. Let us now consider the case of Fig. 13. This arrangement may be

considered formed from the system of Fig. 9 by the addition of shafting of torsional flexibility.

$$k_1 = K_1 - k/2, \tag{63}$$

$$k_2 = K_2 - k/2, \tag{64}$$

at the left and right ends, respectively, and two disks of moments of inertia I_1 and I_2 as shown.

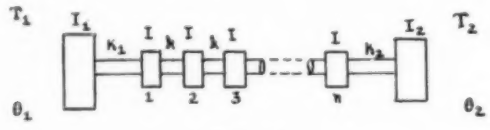

FIG. 13.

By the methods of Section III we can obtain the associated matrices of the terminal portions of the system by direct matrix multiplication. We may then write:

$$\begin{Bmatrix} T_1 \\ \theta_1 \end{Bmatrix} = \begin{bmatrix} (1-\omega^2 I_1 k_1) & -\omega^2 I_1 \\ k_1 & 1 \end{bmatrix} \times \begin{bmatrix} A_n & B_n \\ C_n & D_n \end{bmatrix} \begin{bmatrix} 1 - & \omega^2 I_2 \\ k_2 & (1-\omega^2 I_2 k_2) \end{bmatrix} \begin{Bmatrix} T_2 \\ \theta_2 \end{Bmatrix}. \tag{65}$$

For free oscillations of the system we must have $T_1 = 0$, $T_2 = 0$. Carrying out the matrix multiplication, we obtain after some reductions

$$\tan(bn) = [M_1 M/(M_2 M^2 - M_3)], \tag{66}$$

where

$$a = (jb), \quad j = \sqrt{-1} \tag{67}$$

and

$$M = \frac{\sin(b)}{k \cos^2(b/2)}, \tag{68}$$

$$M_1 = \omega^4 I_1 I_2 (k_1 + k_2) - \omega^2 (I_1 + I_2), \tag{69}$$

$$M_2 = \omega^4 I_1 I_2 k_1 k_2 - \omega^2 (I_1 k_1 + I_2 k_2) + 1, \tag{70}$$

$$M_3 = \omega^4 I_1 I_2, \tag{71}$$

$$\omega = \frac{2}{(Ik)^{\frac{1}{2}}} \sin\left(\frac{b}{2}\right). \tag{72}$$

By means of (72), the right member of (66) is transformed to a function of b. The transcendental Eq. (66) may be solved graphically for b. From these values of b and Eq. (72) we obtain the natural frequencies of the system. A form of Eq. (66) more suitable for graphical solution has been obtained by Biot.[3]

e. Connection with Holzer's Method

H. Holzer[6] has given a method for the calculation of the natural frequencies of torsional oscillations of shafts. In the interest of unity it is well to show the relation of the matrix method to Holzer's method. To fix the ideas, a system discussed in reference 1, page 227, will be considered. This system is shown in Fig. 14.

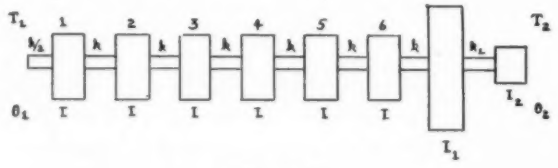

FIG. 14.

This system represents the equivalent of a six-cylinder Diesel engine with a flywheel directly coupled to a ship propeller through a long propeller shaft as regards torsional oscillations. It is evident that this system may be regarded as formed by the interconnection of six identical fundamental units, as shown in Fig. 10, a section of shaft of torsional flexibility $k/2$, a disk of moment of inertia I_1, and a system consisting of a shaft of torsional flexibility k_1, and a disk of moment of inertia I_2. Accordingly, we may write:

$$\begin{Bmatrix} T_1 \\ \theta_1 \end{Bmatrix} = \begin{bmatrix} A_6 & B_6 \\ C_6 & D_6 \end{bmatrix} \begin{bmatrix} 1 & 0 \\ k/2 & 1 \end{bmatrix} \begin{bmatrix} 1-\omega^2 I_1 & \\ 0 & 1 \end{bmatrix} \times \begin{bmatrix} 1 & 0 \\ k_1 & 1 \end{bmatrix} \begin{bmatrix} 1-\omega^2 I_2 & \\ 0 & 1 \end{bmatrix} \begin{Bmatrix} T_2 \\ \theta_2 \end{Bmatrix}. \tag{73}$$

Carrying out the matrix multiplication, we have:

$$\begin{Bmatrix} T_1 \\ \theta_1 \end{Bmatrix} = \begin{bmatrix} A_6 & B_6 \\ C_6 & D_6 \end{bmatrix} \begin{bmatrix} 1- & \omega^2 I_1 \\ \frac{k}{2} & \left(1-\frac{\omega^2 I_1 k}{2}\right) \end{bmatrix} \times \begin{bmatrix} 1 - & \omega^2 I_2 \\ k_1 & (1-\omega^2 I_1 k_1) \end{bmatrix} \begin{Bmatrix} T_2 \\ \theta_2 \end{Bmatrix}. \tag{74}$$

By introducing the transformation (67) into Eq. (40) we obtain:

$$A_n = \cos(bn) = D_n, \tag{75}$$

[6] H. Holzer, *Die Berechnung der Drehschwingungen* (J. Springer, Berlin).

$$B_n=\frac{-\sin(bn)\sin(b)}{k\cos^2(b/2)}, \tag{76}$$

$$C_n=\frac{\sin(bn)}{\sin(b)}k\cos^2\left(\frac{b}{2}\right). \tag{77}$$

From (72) we have the relation

$$\sin\left(\frac{b}{2}\right)=\frac{\omega(Ik)^{\frac{1}{2}}}{2}. \tag{78}$$

The essential feature of the Holzer procedure is to realize that in the case of free oscillations $T_1=T_2=0$. If then, one assumes an *arbitrary* displacement θ_2 having placed $T_2=0$, then if ω in (74) has the value of one of the natural frequencies, T_1 will come out equal to zero. The method of Holzer consists in trying various values of ω in Eq. (74) until one is found that gives $T_1=0$ for an arbitrary choice of θ_2, rather than in solving the transcendental equation which results when (74) is expanded and T_1 set equal to zero.

The advantage of formulating the Holzer process in matrix form is that if the system possesses component parts of identical sections, then the associated matrices of these parts may be written down and the numerical work greatly reduced. For example, in the system of Fig. 14 it is evident that if the system is vibrating in the fundamental mode, the system may be replaced by a system of two disks connected through a shaft for an approximate calculation of ω_1 the fundamental angular frequency. Starting with this first value of ω we use (78) to calculate b and (75), (76), and (77) to compute A_6, B_6, C_6, D_6. Then we see whether we obtain $T_1=0$ when $T_2=0$ and θ_2 is arbitrary. By successive trials we adjust ω until we do obtain the required relation; this gives w_1, etc. In (3) the natural frequencies of the system of Fig. 14 are obtained by using the methods of finite differences.

V. GEARED SYSTEMS

The matrix method is very well suited to the analysis of torsional oscillations of systems whose component parts contain gears and pinions. All that is necessary is to obtain the associated matrix of a system composed of two massless gears, as shown in Fig. 15. Let the gear ratio of the upper gear to the lower gear be $n:1$. We then have the relations:

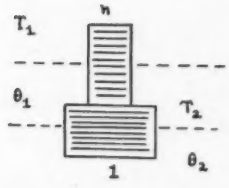

FIG. 15.

$$\theta_2=-n\theta_1, \quad T_2=-(T_1/n), \tag{79}$$

or in matrix form

$$\begin{Bmatrix} T_1 \\ \theta_1 \end{Bmatrix}=\begin{bmatrix} -n & 0 \\ 0 & -(1/n) \end{bmatrix}\begin{Bmatrix} T_2 \\ \theta_2 \end{Bmatrix}. \tag{80}$$

The square matrix of Eq. (80) is the associated matrix of the gear system of Fig. 15. As an

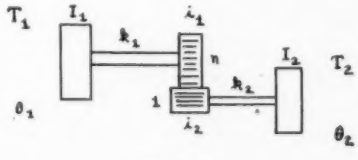

FIG. 16.

example of the use of this associated matrix, let us obtain the frequency equation of the system of Fig. 16. Let the gear ratio of the upper gear to the lower gear be n and let the moments of inertia of the two gears be i_1 and i_2 as shown. The two gears are connected to disks of moments of inertia I_1 and I_2 by shafts of torsional flexibility k_1 and k_2 as shown. We then have:

$$\begin{Bmatrix} T_1 \\ \theta_1 \end{Bmatrix}=\begin{bmatrix} (1-\omega^2I_1k_1) & -\omega^2I_1 \\ k_1 & 1 \end{bmatrix} \times\begin{bmatrix} 1-\omega^2i_1 & 0 \\ 0 & 1 \end{bmatrix}\begin{bmatrix} -n & 0 \\ 0 & -(1/n) \end{bmatrix}\begin{bmatrix} 1-\omega^2i_2 & 0 \\ 0 & 1 \end{bmatrix} \times\begin{bmatrix} 1- & \omega^2I_2 \\ k_2 & (1-\omega^2I_2k_2) \end{bmatrix}\begin{Bmatrix} T_2 \\ \theta_2 \end{Bmatrix}. \tag{81}$$

Setting $T_2=0$ and performing the indicated matrix multiplication, we obtain from the equation $T_1/\theta_2=0$, the following frequency equation:

$$\omega^4I_0I_1I_2k_1k_2-\omega^2I_0(I_1k_1+I_2k_2) -\omega^2(I_1I_2n^2k_1-I_1I_2k_2)+I_0+(n^2I_2+I_1)=0, \tag{82}$$

where

$$I_0=(n^2i_2+i_1). \tag{83}$$

More complicated systems may be discussed in a similar manner.

VI. CONTINUOUS SHAFTS

In the discussion of the previous sections, the mass of the shafts of the systems considered was neglected. Let us now consider the case where the mass of the shaft, and hence its moment of inertia, may not be neglected. In such a case, we may regard the shaft as being made up of an infinite number of infinitesimal sections of the type of Fig. 17.

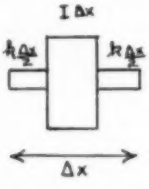

FIG. 17.

The associated matrix of this fundamental unit is given by (32) and may be written in the form:

$$\begin{bmatrix} \left(1-\frac{\omega^2Ik\overline{\Delta x}^2}{2}\right) & \omega^2I\Delta x \\ \left(k\Delta\cdot x-\frac{k^2\omega^2I\overline{\Delta x}^3}{4}\right) & \left(1-\frac{\omega^2Ik\overline{\Delta x}^2}{2}\right) \end{bmatrix} =\begin{bmatrix} A & B \\ C & D \end{bmatrix}, \tag{84}$$

where I is the moment of inertia per unit length, and k the torsional flexibility per unit length of the shaft.

The procedure is to pass to the limit $\Delta x\to 0$ and consider the continuous shaft as composed of an infinite number of sections of the type of Fig. 17. From (36) we have

$$\cosh(a)=\frac{A+D}{2}=1-\frac{\omega^2Ik\overline{\Delta x}^2}{2} =1+\frac{a^2}{2}+\frac{a^4}{4!}+\cdots. \tag{85}$$

From this we obtain the relation

$$\lim_{\Delta x\to 0} a=j\omega(Ik)^{\frac{1}{2}}\overline{\Delta x}, \quad \text{where} \quad j=\sqrt{-1}. \tag{86}$$

Now if n is the number of sections of the type of Fig. 17, we have:

$$\lim_{\substack{n\to\infty\\ \Delta x\to 0}} n\cdot\Delta x=l, \tag{87}$$

where l is the length of the shaft. Now from (37) we have

$$\lim_{\Delta x\to 0} Z=\frac{\left[4\left(1-\frac{\omega^2Ik\overline{\Delta x}^2}{2}\right)^2-4\right]^{\frac{1}{2}}}{2k\Delta x} =j\omega\left(\frac{I}{k}\right)^{\frac{1}{2}} \quad j=\sqrt{-1}. \tag{88}$$

If we now introduce the notation:

$$\phi=\omega l(Ik)^{\frac{1}{2}}, \tag{89}$$

then by making use of (86), (87), and (88) and substituting into (35), we obtain the associated matrix of a shaft of length l, moment of inertia per unit length I, and torsional flexibility per unit length k to be:

$$\begin{bmatrix} \cos\phi & -y\sin\phi \\ \sin\phi/y & \cos\phi \end{bmatrix}=\begin{bmatrix} A & B \\ C & D \end{bmatrix}, \tag{90}$$

where

$$y=\left(\frac{I}{k}\right)^{\frac{1}{2}}. \tag{91}$$

As an example of the use of the associated matrix of a uniform shaft, let us calculate the natural frequencies of the system of Fig. 18. The

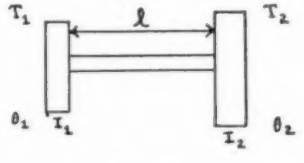

FIG. 18.

system of Fig. 18 consists of a uniform shaft with two disks attached to its end. We are interested in the free vibrations of the system. In this case,

we may write:

$$\begin{Bmatrix} T_1 \\ \theta_1 \end{Bmatrix} = \begin{bmatrix} 1-\omega^2 I_1 & \\ 0 & 1 \end{bmatrix} \begin{bmatrix} \cos\phi & -y\sin\phi \\ \sin\phi/y & \cos\phi \end{bmatrix} \times \begin{bmatrix} 1-\omega^2 I_2 & \\ 0 & 1 \end{bmatrix} \begin{Bmatrix} 0 \\ \theta_2 \end{Bmatrix}. \quad (92)$$

Carrying out the matrix multiplication, we obtain:

$$\frac{T_1}{\theta_2} = -\omega^2 I_2 \cos\phi - y\sin\phi + \frac{\omega^3 I_1 I_2 \sin\phi}{y} - \omega^2 I_1 \cos\phi = 0. \quad (93)$$

This reduces after some reductions to

$$\tan\phi = \frac{\omega y(I_1+I_2)}{\omega^2 I_1 I_2 - y^2}. \quad (94)$$

If we now let $I_0 = lI$ be the total moment of inertia of the shaft, and introduce the notation:

$$m = I_1/I_0, \quad n = I_2/I_0, \quad (95)$$

Eq. (94) may be written in the form:

$$\tan\phi = \frac{(m+n)\phi}{(mn\phi^2-1)}. \quad (96)$$

From (89) we obtain the relation:

$$\omega = \phi/l(Ik)^{\frac{1}{2}}. \quad (97)$$

Equation (96) is a transcendental equation for ϕ and the various angular frequencies are obtained from the roots of this equation by (97). The solution of this equation may be easily carried out graphically for any special case. If the left end of the system is fixed, then $I_1 \to \infty$ and (96) reduces to

$$\tan\phi = 1/n\phi. \quad (98)$$

If the moments of inertia of the disks I_1 and I_2 are much larger than I_0, then (96) reduces to

$$\phi\tan\phi = (1/m+1/n). \quad (99)$$

Many other special cases may be considered.

VII. CONCLUSION

The simple and natural manner in which matrix algebra enters into the analysis of torsional oscillations is evident from this discussion. The conciseness of the results and the unity of approach should prove helpful to workers in this field. The simple operation of matrix multiplication replaces the more complex methods of differential equations, Holzer tables, and difference equations in the conventional treatment of the subject. The only advanced result used is Eq. (35). This is derived in the Appendix.

APPENDIX

Consider the matrix

$$[u] = \begin{bmatrix} \left(1-\frac{\omega^2 Ik}{2}\right) & -\omega^2 I \\ \left(k-\frac{k^2\omega^2 I}{4}\right) & \left(1-\frac{\omega^2 Ik}{2}\right) \end{bmatrix} = \begin{bmatrix} A & B \\ C & D \end{bmatrix}. \quad (1)$$

The determinant of the matrix $[u]$ has the important property that

$$|u| = \begin{vmatrix} A & B \\ C & D \end{vmatrix} = AD - BC = 1. \quad (2)$$

The characteristic matrix of $[u]$ is given by

$$[f(q)] = \begin{bmatrix} (q-A) & -B \\ -C & (q-D) \end{bmatrix}, \quad (3)$$

and the characteristic equation of $[u]$ is

$$\Delta(q) = |f(q)| = q^2 - q(A+D) + 1 = 0. \quad (4)$$

The latent roots of $[u]$ are, therefore,

$$q_{1,2} = \left(\frac{A+D}{2}\right) \pm \left[\frac{(A+D)^2}{4} - 1\right]^{\frac{1}{2}}, \quad (5)$$

provided that

$$(A+D) \neq \pm 2. \quad (6)$$

The latent roots have the property that

$$q_1 \cdot q_2 = 1, \quad (7)$$

$$q_1 + q_2 = (A+D). \quad (8)$$

In the special case we are considering, the matrix $[u]$ has the property that $A = D$. Now let

$$q_1 = \epsilon^a, \quad q_2 = \epsilon^{-a}. \quad (9)$$

Then in view of (8) we obtain

$$\cosh(a) = (A+D)/2 = A. \quad (10)$$

The adjoint matrix of $[u]$ is given by

$$[F(q)] = \begin{bmatrix} (q-D) & B \\ C & (q-A) \end{bmatrix}. \quad (11)$$

Now by Sylvester's theorem[7] we have that provided q_1 and q_2 are distinct

$$[u]^n=\frac{q_1^n}{2q_1-(A+D)}\begin{bmatrix}(q_1-D) & B\\ C & (q_1-A)\end{bmatrix}+\frac{q_2^n}{2q_2-(A+D)}\begin{bmatrix}(q_2-D) & B\\ C & (q_2-A)\end{bmatrix}. \quad (12)$$

Now on making use of (2), (10), and the fact that $(A=D)$ we obtain after some reductions, the relation

$$[u]^n=\begin{bmatrix}\cosh(an) & Z_0\sinh(an)\\ \dfrac{\sinh(an)}{Z_0} & \cosh(an)\end{bmatrix}, \quad (13)$$

where n is a positive or negative integer, and

$$Z_0=\sinh(a)/C. \quad (14)$$

This is Eq. (35) of Section IV. Applications of this theorem to electrical circuit theory are found in reference 8.

[7] R. A. Frazer, W. J. Duncan, and A. R. Collar, *Elementary Matrices* (Cambridge, 1938), pp. 78–79.

[8] L. A. Pipes, "The matrix theory of four-terminal networks," Phil. Mag. **30**, 370 (1940).

The Mechanism of the Electric Spark

JOHN ZELENY
Sloane Physics Laboratory, Yale University, New Haven, Connecticut
(Received May 18, 1942)

Meek's criterion for the formation of a spark discharge in a gas is criticized. An error in the derivation of his formula for the radial field about an electron avalanche channel is noted, and the value adopted for this field is shown to be too small to draw the postulated number of electrons into the channel from the space outside. The importance attached to the radial field is found to be misplaced because of the above and because a criterion based solely on the total number of ions produced in an avalanche gives results for sparking potentials for different spark lengths and for a gas at different pressures in agreement with those obtained by Meek's method. Both methods give results which, using the values assigned to the constants, fall more and more below the experimental values of the sparking potentials as the length of the spark gap, δ, is increased until at 20 cm the deviation is over 7 percent. To bring the computed value for $\delta=20$ cm into agreement with the experimental value the constants in the equations would have to be increased by a factor 2×10^{16} over the values which give agreement between formulas and experiment for $\delta=1$ cm. The dominant exponential term in each formula is based on the incorrect assumption that the field is not affected by the space charges in the avalanche. That a large amount of ionization, postulated by Loeb and Meek, is produced by a high potential wave which travels through the channel as soon as the positive streamer reaches the cathode is questioned because the fields found in such waves are too small to produce ionization by electron collision in air at atmospheric pressure.

INTRODUCTION

THE application of the Wilson cloud chamber to the study of the distribution of ions along the paths of disruptive discharges at different, very short time intervals after the discharge voltage is applied to the gap revealed some interesting facts about the early stages of such discharges. In discharges from pointed conductors to which such study was first applied,[1] the ion tracks for negative discharges always show the ions distributed throughout a single conical-shaped volume rounded at its forward end, whereas with positively charged points the tracks, which are more difficult to obtain, often show a number of branches.

In uniform fields the tracks for the shortest times after the voltage is applied show a rapid development from the cathode of Townsend electron avalanches, and these tracks have in general the same appearance as those observed with negative point discharges. Contrary to what would result from electron diffusion alone, some of these avalanches cease to increase in diameter as they proceed, and indeed appear to contract during the last half of their length.[2]

The tracks formed in uniform fields after the electron avalanche has reached the anode indicate that a form of discharge is now moving from the anode to the cathode, and these tracks possess branches similar to those found on tracks with positive discharges from points.

[1] L. B. Snoddy and C. D. Bradley, Phys. Rev. **45**, 432, 751 (1934); **47**, 541 (1935); H. Raether, Zeits. f. Physik **94**, 567 (1935).

[2] H. Raether, Zeits. f. Physik **37**, 560 (1936); **107**, 91 (1937).

When several electron avalanches are developed at the same time the evidence shows that the final spark path is evolved from but one of these avalanches.[2]

Several hypotheses have in recent years been advanced to account for the transformation of an electron avalanche into a continuous conducting path between the electrodes. In one of these, thermal ionization arising from heat generated in the avalanche was invoked. In another, the applied field was supposed to be augmented so greatly near the cathode owing to space charges as to make ionization by positive ions possible even in gases at atmospheric pressure. Such space charge fields have been called upon, too, to produce the essential new supply of electrons by detaching these from ions which were formed in the gas before the avalanche started, or by having high speed positive ions eject them from the surface of the cathode.

At the present time the prime agent for supplying the necessary electrons to the space behind the head of the avalanche is generally considered to be photo-ionization.

The radiation responsible for this ionization is believed to have its origin in the avalanche itself where some of the molecules have been raised to excited states by the high speed electrons. That a high frequency radiation capable of ionizing a gas is emitted along a part of the path of a disruptive discharge has long been known,[3] but only recently has further study directed attention to this radiation,[4] and while at first it was hesitatingly looked upon as only a possible source of the electrons in question it is now considered the main source of such electrons.

The space charge arising from the comparatively immobile positive ions in the avalanche channel which previously was invoked for activating other processes is now called upon to increase the ionizing power of the electrons released there by photo-ionization; and it is postulated that when this production of ions is sufficiently great a retrograde streamer may form which, moving toward the cathode, creates a conducting path between the two electrodes along which the main discharge eventually passes.

The detailed action of such a positive streamer was described by Simpson[5] in connection with the discharge of positively charged clouds to earth. However, Simpson assumed that the ionization at the head of the positive streamer arose from electrons which are normally liberated in air by various agencies, and Cravath and Loeb[6] also at first assumed these agencies to be the sources of the electrons, when they applied the positive streamer theory to ordinary sparks. The number of electrons liberated by these omnipresent agencies is now considered inadequate for the purpose and their function is assigned to the ionizing radiation developed in the avalanche itself.

MEEK'S CRITERION FOR SPARK FORMATION

Meek[7] has postulated a criterion for determining quantitatively the condition under which a retrograde streamer will form from an electron avalanche and develop into a spark. This criterion states that such a streamer will form when the *radial* field X_1 about the positive space charge in an electron avalanche attains a value of the order of the applied field X_a. The supposed function of this radial field is to draw into the main avalanche channel some of the electrons which are liberated outside of it by photo-ionization and thus make of the channel a conducting plasma.

Meek evaluated, roughly, the radial field near the head of the avalanche in terms of the total number of positive ions in the whole avalanche, and by reason of the postulated criterion set this equal to KX_a. Then assuming arbitrarily a value unity for the constant K, the field X_a necessary for the production of a spark was found by a trial and error method by means of the experimentally obtained relation between Townsend's ionization coefficient α and X/p, p being the gas pressure. Later the value 0.1 was adopted for K because the use of this number gave an exact agreement between the computed and experimental values of X_a for a

[3] E. Wiedemann, Zeits. f. Elektrochemie **2**, 159 (1895); J. J. Thomson, Proc. Camb. Phil. Soc. **10**, 74 (1899).
[4] A. M. Cravath, Phys. Rev. **47**, 254 (1935); L. B. Loeb, Rev. Mod. Phys. **8**, 267 (1936); H. Raether, Physik. Zeits. **37**, 560 (1936).
[5] G. C. Simpson, Proc. Roy. Soc. **111**, 56 (1926).
[6] A. M. Cravath and L. B. Loeb, Physics **6**, 125 (1935).
[7] J. M. Meek, Phys. Rev. **57**, 722 (1940).

spark gap $\delta = 1$ cm, although the computed result was not altered much by this large change in K.

I propose to show that the derivation of the formula for the radial field as given by Meek is erroneous; that when K is given the adopted value 0.1 the radial field cannot be expected to draw any large number of electrons into the avalanche from the outside, as is postulated; and that it is highly illusory to find support for the role played by radial fields in spark phenomena in the fair agreement that exists between sparking potentials computed by Meek's method for sparks of different lengths and the corresponding values found by experiment.

Some general features of an electron avalanche will first be considered. After an electron has traversed a distance x in a uniform field the number of electrons in the avalanche produced by it will be $n = e^{\alpha x}$, where α is the ionization coefficient. As actually determined experimentally n must include not only the electrons that owe their liberation by collision directly to the initial electron but also those produced anywhere in the inter-electrode space by radiation, as well as the progeny of such electrons. At the present time these additional electrons are thought to comprise but a small part of the total number.

So long as the field remains essentially unchanged while an avalanche is advancing, all of the electrons in it are confined to a more or less spherical volume at its forward end, the diameter of which increases with time owing to diffusion and the action of electrical forces. The density of the electrons in this volume is largest at the center of the sphere and diminishes outward toward its indefinite periphery. In the forward part of the sphere electrons predominate greatly over positive ions while at its rear end the positive ions are largely in excess.

Raether[8] found the radius of the head of an avalanche in air at atmospheric pressure, 1 cm from its origin, to be 0.013 cm when the applied field was 30 kv/cm. A calculation shows that at that distance, in the volume occupied by them, the electrons predominate over positive ions in the ratio of about 5 to 1. The remainder of the positive ions are in the trail of the avalanche extending back to the cathode.

[8] H. Raether, Zeits. f. Physik **107**, 91 (1937).

The preponderance of electrons in the forward portion of the avalanche not only tends to spread out the electrons fanwise but also enhances the applied field in this region. Since the electrons in the avalanche increase rapidly in number as it approaches the anode, this space charge effect may cause a substantial increase in the field near the anode; and as the coefficient α increases more rapidly than does the field the rate of production of new electrons must here be much greater than it is in the unmodified field. Such a large increase in the axial field at the head of an avalanche may well be the cause of what Flegler and Raether[9] call an instability in the avalanches they observed in overvolted gaps where a narrower and faster moving streamer suddenly shot out from the forward end of the avalanche as it approached the anode. This was followed by another fast streamer that went rearward to the cathode, and which must have resulted from an increase in the field in this region also, as is generally postulated for all positive streamers. That an increase in the field owing to the positive charge can occur here is conditioned by the fact that the charge is limited to a narrow channel and that in this channel the charge decreases rapidly toward the cathode.

Since the fields in front of the avalanche head and back of it are both greater than normal there must be a region in between the two opposite charges where the field is smaller than the normal applied field. As the avalanche moves toward the anode, these modifications in the field should rapidly distort the shape of the volume occupied by the electrons from the simple spherical form it would have in a uniform field.

Eventually all the electrons in the avalanche proper reach the anode, and it is at this final stage, when the comparatively immobile positive ions alone remain in the channel, that Meek proceeds to find the radial field near the anode arising from all of the ions in the whole avalanche. For ease of calculation these ions are all assumed to be contained in a spherical volume whose radius, r, is the average distance that electrons in the avalanche had diffused from its axis in the time taken by the avalanche to cross

[9] E. Flegler and H. Raether, Zeits. f. Physik **112**, 464 (1939).

the spark gap; and the field X_1 is computed for this radial distance r. Naturally, many of the positive ions were formed at a greater distance from the axis than r and these contribute nothing to the field at r. Assuming the ions in the spherical volume to be distributed in shells of uniform density, the field at a distance r from the center is,

$$X_1=\frac{\epsilon e^{\alpha\delta}}{r^2}, \tag{1}$$

where ϵ is the charge on each ion and δ is the length of the spark gap.

Meek now introduces the ion density N into the formula, obtaining

$$X_1=(4/3)\pi\epsilon rN, \tag{2}$$

and then eliminates N by a faulty procedure. Assuming that the avalanche contains $n=e^{\alpha x}$ electrons, which presupposes that it has not yet reached the anode, he lets each electron advance a distance dx so that $dn=\alpha e^{\alpha x}dx$ new electrons are liberated and an equal number of positive ions formed. These oppositely charged particles are both distributed over the whole volume of the sphere and therefore add nothing to the radial field. However, Meek divides this dn, the *increase* in the number of positive ions, by an imaginary volume πr^2dx, which these ions do not occupy, and obtains for the positive ion density, $N=\alpha e^{\alpha x}/\pi r^2$, which substituted in Eq. (2) gives,

$$X_1=4\alpha\epsilon e^{\alpha x}/3r. \tag{3}$$

This value of X_1 only differs from the one given by Eq. (1) by a factor $4\alpha r/3$, since the errors in the derivation happen in large part to cancel one another. Using values of α and r given by Loeb and Meek[10] for the sparking distances 0.5 cm and 20 cm, the values of the above factor are, respectively, 0.4 and 0.09, and these have only a small effect upon the sparking potentials computed by Meek's method.

Meek attaches great importance to the radial field because as already stated he assigns to it the function of drawing some of the electrons, that are liberated outside of the avalanche by photo-ionization, into the avalanche channel and making of it a conducting plasma. However, when K is given the adopted value 0.1, the inward deviation of the electron paths produced by the radial field is only 0.1 radian at the distance r from the axis of the avalanche for which X_1 was derived above, a point which is well within the avalanche. For a place somewhat farther from the axis, say at a distance $3r$, the radial field is so weak that electron paths would be deviated by it only about a half degree of arc. This is certainly without significance for drawing enough electrons into the avalanche to make of it a conducting plasma, especially as the radial field was computed for the part of the avalanche near the anode where the electrons have but a very short distance to travel before they reach the anode.

It thus appears that radial fields arising from positive space charges in the avalanche can play only a very minor role, if any, in the initiation of a spark. More evidence on this point, quite different in character, will be presented later.

The contention that the radial field is dependent upon the ion density in the avalanche rather than upon their total number n is not altogether justified because the appearance of r as well as of N in Eq. (2) shows that n is also involved in X_1.

CRITERION BASED ON $n=e^{\alpha\delta}$

Now it is the *axial* fields due to the space charges in the avalanche rather than the radial fields which must play an important role in spark formation since, as already shown, they enhance the applied field both in front of and in back of the electron cloud in the avalanche. In the high applied fields here prevailing the ionization coefficient α increases rapidly with field intensity and hence even a moderate increase in the field will increase enormously the number of new ions produced by electron collisions.

The only electrons present to the rear of the main electron cloud in the avalanche upon which the enhanced axial field can act are those liberated there by photo-ionization. The intensity of the radiation which produces this ionization is doubtless proportional, at least roughly, to the number of ionizing collisions

[10] L. B. Loeb and J. M. Meek, *The mechanism of the electric spark* (Stanford University Press, 1941).

that electrons make in the whole avalanche. Since the positive space charge in the avalanche is also dependent upon the total number of ions in the avalanche, a meaning may thus be attached to the fair degree of correspondence that is obtained between computed and experimental values of sparking potentials when it is assumed, simply, that a positive streamer can establish a conducting path between the electrodes as soon as the applied field reaches a value such as to produce some given large number of ions in a single electron avalanche while this is traversing the spark gap.

The simple relation to be now used as a criterion for sparking is $n=e^{\alpha\delta}$, which assumes, as was done for Eq. (1), that the applied field remains unchanged by space charges. In evaluating some sparking potentials by aid of this relation the constant value adopted for n was 10^9 since this number gives a value of α for $\delta=1$ cm from which a sparking field in close agreement with experiment is obtained, by making use of the experimental relation between α/p and X/p. The values of α for spark gaps of different length are then found from the constancy of the product $\alpha\delta$.

Calculations of the spark distances obtainable in given uniform fields were made by Schumann[11] by empirical equations also based on the constancy of the product $\alpha\delta$, and Loeb and Meek,[12] too, were aware that a formula of this form gives results in fair agreement with experiment, but they considered the formula as purely empirical and so without special significance.

PASCHEN'S LAW

Paschen's law regarding sparking potentials, which states that for a given gas the sparking potential for a uniform field remains constant when the product of the gas pressure p by the spark gap length δ is constant, follows at once from the assumption that the liberation of a given number of electrons in an avalanche is a sufficient criterion for the initiation of a spark. Since $n=e^{\alpha\delta}=e^{\alpha\cdot p\delta/p}$, it follows if n and $p\delta$ remain constant that α/p is also constant and hence also X/p and $V=(X/p)\cdot p\delta$.

[11] W. O. Schumann, *Electrische Durchbruchstärke von Gasen* (Julius Springer, 1923).
[12] Reference 10, p. 118.

TABLE I. Variation of sparking potential with air pressure p, for $\delta=1$ cm.

p mm	V_1 kv	V_M kv
7600	248.5	248
3800	131.5	131
760	32.5	32.2
380	18.9	18.6
200	11.35	11.1
100	6.83	6.55

V_1—computed for $n=10^9$. V_M—computed by Meek's formula.

Some sparking potentials obtained in the manner indicated for different values of $p\delta$ are given in Table I under V_1, n being taken as 10^9, δ as 1 cm, and p having the values tabulated. Except for $p=100$ mm, these potentials are in very close agreement with those obtained by aid of Meek's formula,[13] which are shown under V_M. No experimental data covering this range of pressures are available for comparison.

VARIATION OF SPARKING POTENTIAL WITH SPARK LENGTH

Sparking potentials computed by the two methods for air under a constant pressure of 760 mm when the distance δ between the electrodes is varied from 0.5 cm to 20 cm are given in Table II and these are again seen to be in good agreement.

The values under V_1 are those found when n is assumed to be 10^9 throughout, while under V_M are those given by Meek's formula.[14]

These computed values are to be compared with the experimental potentials, V_{exp}, found by Edwards and Smee[15] for sparks between spheres whose diameters were large relative to the sparking distances used.

It is to be noted that, while the computed values are in close agreement with the experimental values for δ around 1 cm, none the less they are farther and farther below the latter values as δ increases, until at $\delta=20$ cm the deviation is over 7 percent. The value of δ for which the theoretical and experimental results would agree is evidently dependent upon the values of K and n assumed in the two formulas used.

[13] Reference 10, p. 116.
[14] Reference 10, p. 114.
[15] F. S. Edwards and J. F. Smee, J. A. I. E. E. **82**, 655 (1938).

TABLE II. Variation of sparking potential with spark length δ, for $p=760$ mm.

δ cm	V_1 kv	V_M kv	V_{exp} kv
0.5	18.9	18.25	17.3
1.0	32.8	32.2	31.6
2.5	71.3	70.5	73.0
5.0	132	132	138
10	249	249	265
15	361	363	386
20	473	474	510

V_1 by $n=10^9$. V_M by Meek's formula. V_{exp}, experimental values.

DISCUSSION

Thus as regards dependence of sparking potential in a uniform field both on spark length and on gas pressure there is little to choose between the values obtained by Meek's formula and by the one based solely on the total number of ions produced in an electron avalanche during its passage across the spark gap.

Considering the number of factors involved in spark formation it cannot be expected that any simple formula will accurately represent them all, even though the final solution is made to rest empirically upon the complicated experimental relation between α and X. Hence the discrepancies shown between the computed and the experimental results that have been discussed may not at first appear excessive.

However, sparking potentials, owing to the rapid way in which α increases with X, are so extremely insensitive to very large changes in the exponential term $e^{\alpha\delta}$, which is the dominant quantity in each of the two formulas involved, that it is not justifiable to attach great significance to a hypothesis underlying any formula simply because this gives sparking potentials that are in fair agreement only with experimental values. This fact was recognized by Meek himself.[7]

The high degree of the insensitivity involved in the present problem is easily shown by using Meek's formula backwards to find K for spark lengths other than 1 cm. Thus, assuming the correctness of the experimental results given in Table II for sparking potentials at different electrode distances, the corresponding values of X/p are first computed and from these α is obtained in each case from the experimental curve showing the relation between α and X/p. These two quantities are now substituted into Meek's formula to find the value of K for each gap.

The values of K thus obtained for the sparking distances, 0.5, 1, 5, and 20 cm, for example, are 0.01, 0.09, 2×10^5, and 2×10^{15}, respectively. Instead of being alike, as is postulated by Meek's criterion, the two extreme numbers differ by a factor 2×10^{17}. In other words, when K is chosen so that the computed sparking potential agrees with its experimental value at $\delta=1$ cm, as was done by Meek, then the use of the same K for $\delta=20$ cm gives a sparking potential only about 7 percent below that found by experiment, yet in order to bring this computed value into actual agreement with experiment it is necessary to increase K by a factor 2×10^{16}. Had Meek chosen the experimental value of the sparking potential for $\delta=5$ cm, for example, for determining the constant K in his formula he would have obtained for it a value 2×10^5, indicating an absurdly high radial field. It is thus by mere chance that K was found to be of the order of 1.

From what has been said it appears that the results which have been presented lend no support whatever to the basic idea about radial fields on which Meek's formula rests.

When the relation $n=e^{\alpha\delta}$ is tested in a similar way by finding the values of n which will make the computed potentials for different sparking distances agree exactly with those found by experiment, the disagreement among the values of n is equally as large as that found above for the K's in Meek's formula.

Since the exponential term $e^{\alpha\delta}$ is the all important quantity in both of the equations under consideration, it evidently does not represent properly the processes going on in the spark gap. This exponential term gives the total number of ions produced in an electron avalanche while it is traversing the whole gap on the supposition that the field remains unchanged. Actually, the space charges developed in the avalanche alter the applied field so markedly as to make calculations based on a uniform field altogether invalid. As has already been shown, these changes in the field are far from simple and it is not possible as yet to subject their effect to computation.

It may well be that for voltages near the

sparking threshold, especially in case of long sparks, the initial avalanche does not continue to grow in intensity after it has built itself up to some limiting value, but owing to changes in the field is able subsequently to produce only a constant number of ions per centimeter of its path as it proceeds to the anode. After the electrons from the head of the avalanche have all entered the anode, the increase in the positive charge which results may then give rise to a positive streamer which in like manner makes its way to the cathode establishing a conducting path between the electrodes, as has been postulated.

Once the positive streamer reaches the cathode it may not be necessary to look for processes other than the ones usually active at this electrode in continuous discharges through gases, for supplying the channel with electrons whose number will be limited only by resistance and other factors in the circuit.

When the current in a spark has attained a very high value and a near equality between the electrons and positive ions in the channel has established itself, it is possible that the cross-sectional area of the channel, now at a high temperature, is prevented from expanding owing to the so-called pinch effect due to the magnetic field.

Loeb and Meek[16] have recently added a new process to the theory of the mechanism of a spark. They state that after a positive streamer has reached the cathode there is a rush of electrons from the metal into the avalanche which gives rise to a high potential wave that passes up the channel to the anode and multiplies the electrons there present by a large factor, thus making the channel highly conducting. I can find no evidence that the fields in waves of that character are sufficiently high to give electrons speeds adequate for the ionization of air at atmospherio pressure.

Snoddy, Dietrich, and Beams[17] measured the fields in such impulse waves started by a sudden flow of charge from a condenser charged to 125 kv and found as the pressure of the gas was raised from 0.04 mm to 1.3 mm that the field changed from 2300 volts/cm to 420 volts/cm. Presumably at higher pressures the field would be still weaker. Such fields are far too small to produce ionization in air at atmospheric pressure.

[16] Reference 10, p. 40.
[17] L. B. Snoddy, J. R. Dietrich, and J. W. Beams, Phys. Rev. **52**, 739 (1937).

The Photographic Action of Electrons in the Range Between 40 and 212 Kilovolts

R. F. Baker, E. G. Ramberg, and J. Hillier
Research Laboratories, RCA Manufacturing Company, Camden, New Jersey

(Received April 7, 1942)

The Hurter and Driffield curves and the absolute sensitivities of Eastman medium lantern slide plates are determined for electrons accelerated through differences of potential from 40 to 212 kilovolts. Within experimental error the H and D curves are identical in shape for the different voltages. The sensitivity reaches a peak near 100 kv and then drops off rapidly. This phenomenon may be utilized to increase the effective sensitivity of plates at high voltages by applying a thin, high density intensifying screen to the surface of the emulsion.

INTRODUCTION

THE advent of the electron microscope has increased the need for information regarding the action of electrons on photographic materials. Thus, any translation of density variations in an electron microscope picture into mass thickness variations of the object[1] must begin with a knowledge of the change in the photographic density of the sensitive emulsion with the amount of charge per unit area which has reached the emulsion during exposure. Again, an acquaintance with the variation of the sensitivity and contrast properties of the emulsion used with the accelerating voltage employed is of importance in determining the most suitable operating voltage

[1] L. Marton and L. I. Schiff, J. App. Phys. **12**, 759 (1941).

and may lead to methods for enhancing the effective sensitivity of the recording materials.

Earlier measurements of the electron sensitivity and of the density-exposure curves of photographic materials have been carried out with electrons having velocities up to 100 ekv on the one hand,[2–4] and with beta-rays from radium *B* and *C*, with velocities in excess of 200 ekv, on the other.[5] In the first range a consistent increase of sensitivity with voltage was found, at least for low photographic densities. The converse was found to hold for the beta-rays. These results—and those of a number of other authors as well—have been discussed in detail by Charlesby,[6] who derived a general formula for the slope variation of the density-*vs*.-log (exposure) curves (H and D curves) in terms of the grain size and the absorption and excitation properties of the grains as well as the absorption of the emulsion as a whole.

The reciprocity law, stating that the photographic density depends only on the total charge per unit area falling on the emulsion (for a given voltage) and not on the length of exposure, is generally accepted for fast electrons (see, e.g., Becker and Kipphan[2] and Bothe[7]). Deviations from this law, in the direction of lower densities for shorter exposures, have been noted by Borries and Knoll,[4] working with exposures of the order of 10^{-8} second. It appears safe, however, to regard the reciprocity law as valid at least within the range of exposure times used in the electron microscope.

The contrasting results of Schäffer,[3] Becker and Kipphan,[2] and Borries and Knoll[4] for voltages less than 100 kilovolts, and of Aston and Ellis[5] for voltages above 200 kilovolts make the existence of a maximum of photographic sensitivity in the region from 100 to 200 kilovolts a practical certainty. The presence of this maximum also follows from the commonly accepted laws which determine the energy loss of electrons in matter if the photographic density is assumed to be proportional to the energy per unit area absorbed by the emulsion. These laws are: (1) the Lenard law of absorption that

$$I = I_0 e^{-\alpha x}, \tag{1}$$

where I_0 is the incident electron current and I that which remains at a depth x. α is a constant which, in the region up to about 50 kilovolts, according to Terrill's measurements,[8] is proportional to the inverse fourth power of the mean electron velocity and to the density of the material; and (2) the Thomson-Whiddington law[9,10] governing the mean loss of kinetic energy eV of the electrons in passing through a layer of matter of thickness x. This law is stated as

$$V_0^2 - V^2 = bx, \tag{2}$$

where the constant b is approximately proportional to the density of the material.

The Thomson-Whiddington law by itself predicts an almost linear increase of the energy loss in the emulsion (for constant incident current) up to a voltage $V_0 = (bx)^{\frac{1}{2}}$, since up to this point practically all of the electron energy is dissipated in the emulsion. Beyond this point an increasing proportion of the electrons (according to Eq. (1)) with an increasing amount of kinetic energy (Eq. (2)) pass through the emulsion into the backing. The maximum of energy loss within the emulsion occurs at the voltage for which the rate of increase in the total energy of the electrons leaving the emulsion is just equal to the rate of increase with voltage of the energy of the incident electrons. This maximum must exist if the absorption coefficient α decreases with increasing voltage in proportion to the reciprocal of the latter or more rapidly than this. This is true since, for very large values of V_0, by Eqs. (1) and (2), the rate of change of the energy loss in the emulsion is given by

$$\frac{d}{dV_0}(I_0 V_0 - IV) = -I_0 x\left(\frac{b}{2V_0^2} - \frac{d(\alpha V_0)}{dV_0}\right), \tag{3}$$

which becomes negative under the conditions stated.

[2] A. Becker and E. Kipphan, Ann. d. Physik [5], **10**, 15 (1931).
[3] H. Schäffer, Arch. f. Elektrotechnik **26**, 313 (1932).
[4] B. v. Borries and M. Knoll, Physik. Zeits. **35**, 279 (1934).
[5] C. D. Ellis and G. H. Aston, Proc. Roy. Soc. **A119**, 645 (1928).
[6] A. Charlesby, Proc. Phys. Soc. **52**, 657 (1940).
[7] W. Bothe, Zeits. f. Physik **8**, 243 (1922).
[8] H. M. Terrill, Phys. Rev. **24**, 616 (1924).
[9] For the constant b, H. M. Terrill, Phys. Rev. **22**, 101 (1922), finds the value $4 \cdot 10^{11}\rho$ volt²/cm, ρ denoting the density, for the constant α, $12\rho/\beta^4$, β being the ratio of mean velocity of the electrons to the velocity of light (reference 8).
[10] For a different formulation of the energy-loss relation, see E. J. Williams, Proc. Roy. Soc. **A130**, 310 (1932).

Equations (1) and (2), however, are not adequate for deriving the variation in photographic density with voltage, for the following reasons: (1) the variation of α with voltage is not known beyond about 50 kilovolts; (2) the Lenard law fails at low electron velocities;[8] (3) it is necessary to take account both of the velocity distribution[11] and of the angular scattering of the electrons in the emulsion, the latter determining the effective values of x in the Thomson-Whiddington law; and (4) there is some evidence that radiation emitted by the glass backing of photographic plates under the influence of electron bombardment may contribute to their blackening.[4] Even so, it is evident from the above considerations that the variation of photographic density with voltage must vary with emulsion thickness, the voltage corresponding to maximum photographic density for a given charge density increasing with the latter.

MEASUREMENTS

All of the measurements reported in this paper were made with the RCA high voltage electron microscope[12] with the object holder removed. Eastman lantern slide plates (medium) with the same emulsion number were used throughout, as these exhibit favorable characteristics with regard to grain size, sensitivity, and contrast properties for electron microscope work. Development was standardized at 3 minutes at 19°C in Eastman D-72 developer diluted in a ratio 1 : 2 with water.

The measurements may conveniently be divided into two parts: the determination of the H and D curves for the different voltages, using relative values for the exposure; and the determination of the plate sensitivities in terms of the number of coulombs/cm², required to produce a given blackening. In order to obtain data for the H and D curves, the projector lens current of the electron microscope was adjusted so as to give a large magnification and the mask above the plate was adjusted to expose a single $\frac{1}{4}''$ strip of the $2''\times10''$ plate at a time. With the microscope voltage placed successively at 40, 78, 127, 170, and 212 kilovolts, strips were exposed for 5, 10, 20, 40, and 80 seconds, leaving clear spaces between adjacent steps. Nine such plates, with 25 photometer strips apiece, were taken. The densities of the strips, as compared with those of the intervening clear spaces, were measured with an

[11] E. J. Williams, Proc. Roy. Soc. **A125**, 420 (1929).
[12] V. K. Zworykin, J. Hillier, and A. W. Vance, J. App. Phys. **12**, 738 (1941).

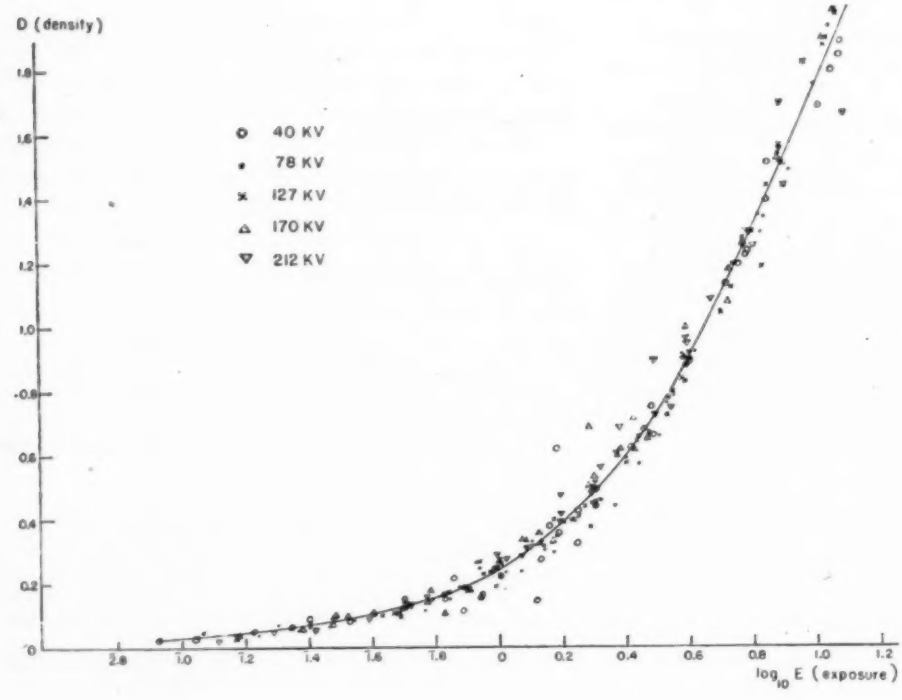

FIG. 1. Variation of the photographic density with the logarithm of the exposures for Eastman medium lantern slide plates.

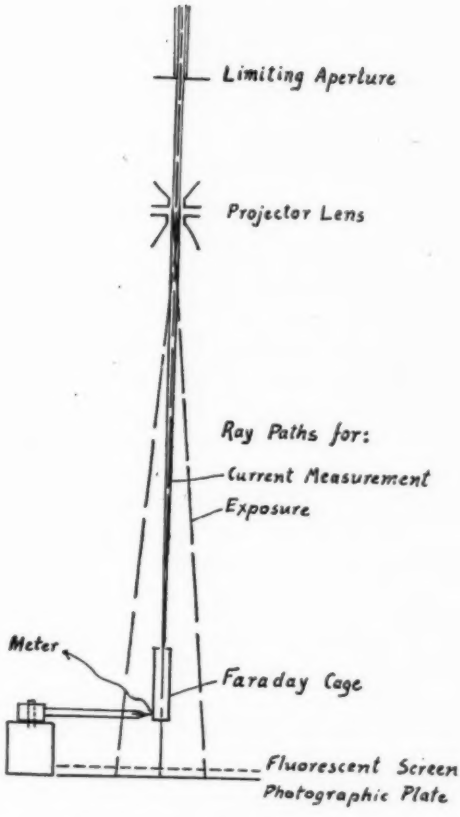

FIG. 2. Measurement of absolute plate sensitivity.

improvised microphotometer consisting of an RCA 931 electron multiplier tube[13] operated with a regulated power source and mounted on a plate with an aperture and inserted in place of a plate holder in the camera of a Leitz panphot microscope. The magnification used was between 60 and 100. The output currents, ranging from 0.5 to 400 microamperes, were measured with an ultrasensitive d.c. vacuum-tube microammeter.[14]

After conversion of the current readings into densities, the latter values plotted against the logarithm of the exposure yielded nine sets of five points for each voltage. Shifting the sets of points along the exposure axis so as to cause them to fall, as nearly as possible, on the same curve in order to account for differences in the beam intensity used for the different plates, it was possible to obtain an average H and D curve characteristic for each voltage. The curves so obtained were found to be identical within experimental error. Bringing the five curves for different voltages, again, as nearly as possible to coincidence by shifts along the exposure axis resulted in obtaining the mean H and D curve shown, together with all the individual measured points, in Fig. 1.

The measurement of the absolute plate sensitivities requires a measurement of the current producing the blackening on the plate. For this purpose a Faraday cage in the form of a nickel cylinder $\frac{5}{16}$ inches in diameter and $1\frac{1}{2}$ inches in length provided with an aperture 0.150 inch in diameter was placed above the shutter (Fig. 2), and centered so as to receive all the current passed by the limiting aperture A above the projector lens when the lens current was reduced to a very small value. Quartz insulation was provided for the lead from the cage, which was carried out through a seal in a Pyrex window of the viewing chamber and connected through a shielded cable to the ultrasensitive d.c. vacuum microammeter. The currents measured were of the order of $5 \cdot 10^{-10}$ ampere; a bias of ± 90 volts did not affect the reading.

After the meter was read, the Faraday cage was swung out of the way with the aid of a hook mounted on a sylphon bellows, the projector lens current was increased until there was a luminous disk approximately 4 cm in diameter on the fluorescent screen, and a 10-second exposure was made. After development of the negative, carried out as before, each "disk" was marked with equally separated rings along two diameters, as shown in Fig. 3a. Density measurements were made in each ring and the results for rings lying on a circle about the center averaged, yielding a curve for the variation of the density outward, $D(\rho)$ (Fig. 3b). This was found necessary, as even a small amount of distortion of the projector lens

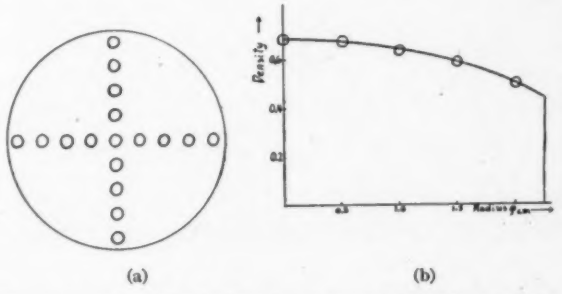

(a) (b)

FIG. 3. Density distribution on plate: (a) Marking of plate; (b) example of density distribution.

[13] J. A. Rajchman and R. L. Snyder, Electronics (December 1940), p. 20.
[14] A. W. Vance, Rev. Sci. Inst. 7, 489 (1936).

results in a considerable dropping off of intensity in the marginal regions of the exposed area.

Since it had been found that the H and D curves for different voltages were the same except for a shift along the log (exposure) axis, the true exposures in coulombs/cm² at the voltage V required to produce the densities D are given by

$$E_V(D) = E(D) \backslash C_V, \tag{4}$$

where $E(D)$ is given by the curve in Fig. 1. The constant C_V, on the other hand, is a direct measure of the relative sensitivity of the plate at different voltages. Now the total amount of charge reaching the plate during exposure is

$$2\pi \int_0^{\rho_1} E_V(\rho) \rho d\rho = i \cdot t,$$

where ρ_1 is the radius of the blackened circle, i the measured current, and t the exposure time. Since

$$E_V(\rho) = E(D[\rho]) / C_V = E(\rho) / C_V,$$

where $E(\rho)$ can be obtained from $D(\rho)$ with the aid of the curve in Fig. 1, C_V can be determined by a graphical integration:

$$C_V = \frac{2\pi \int_0^{\rho_1} E(\rho) \rho d\rho}{i \cdot t}. \tag{5}$$

Figure 4 shows the results of four measurements of C_V for each of the voltages 40, 79, 127, 170, and 212 kilovolts and of two measurements for the intermediate voltages 67, 96, and 105 kilovolts, together with their probable errors, the latter being indicated by the length of the line segments.

DISCUSSION AND APPLICATION

Figure 5 shows the H and D curves for Eastman lantern slide plates (medium) in absolute units, as determined from the above data, and compares them with the results of Becker and Kipphan[2] on Agfa Extrarapid plates and of Borries and Knoll[4] on Agfa Isochromfilm, the exposure times in the latter case being of the order of 10^{-8} second. As was to be expected, the lantern slide plates are somewhat slower than the Extrarapid plate. Apart from this the principal difference between the present results and those of Becker and Kipphan is the absence of intersections between the curves in the present measurements.

The fact that for voltages in excess of 100 kilovolts the plate sensitivity rises rapidly with decreasing voltage may be utilized to enhance the effective sensitivity of the plate at high voltages by means of an "intensifying screen." If this is in the form of a thin film of high density (e.g., gold or silver), the velocity reduction as well as the angular scattering within the film will enhance the action of the electrons on the emulsion without appreciably affecting the sharpness of the image.

Figure 6 shows the effect of an evaporated silver film with a mass thickness of 3.4 mg/cm²

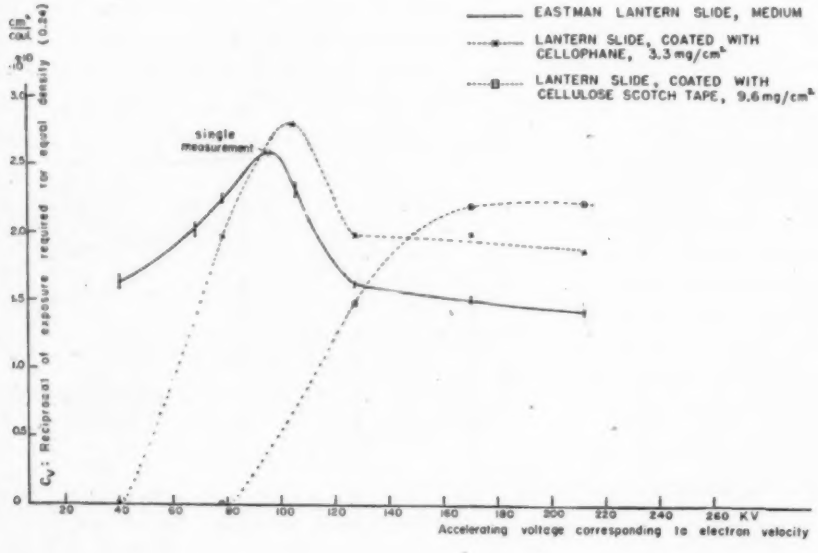

FIG. 4. Variation of plate sensitivity with accelerating voltage.

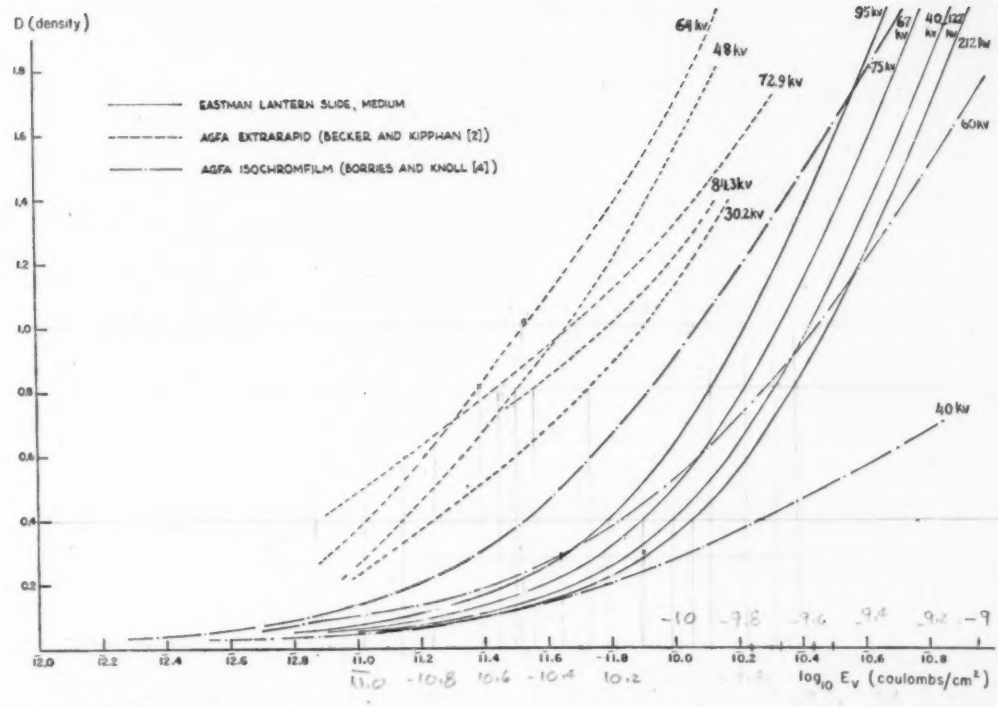

FIG. 5. H and D curves for different accelerating voltages and different negative materials.

placed directly on the emulsion at a beam voltage of 127 kv. The film covered the area with the lighter background in the photograph. It is seen that the sharpness of the image (zinc oxide smoke) does not suffer due to the presence of the film where the latter adheres closely, even though the reproduction represents a sixfold optical enlargement of the original negative. At the edge of the film there results a brightening of the background and a darker appearance of the film itself from the lateral scattering at the (slightly raised) film.

In order to obtain a quantitative estimate of the effect of such "intensifying screens" on the sensitivity of the plate at different voltages, Cellophane foil and cellulose Scotch tape were used to coat a portion of a lantern slide plate exposed to the unobstructed electron beam in the electron microscope, the voltage being varied from 40 to 212 kilovolts. The use of cellulose in place of the more suitable heavy metal screens for intensity measurements is justified since the degree of scattering and absorption of high speed electrons depends primarily only on the mass thickness of the scattering and absorbing layer.

After standard development of the negative the densities of the portion exposed under the screen and of that exposed directly were measured. If the same shape is assumed for the H and D curve for the plate with the intensity screen as without, the difference in log E corresponding to the two densities, according to the general H and D curve in Fig. 1, yields the ratio of the exposures required to produce the same density on the

FIG. 6. Electron micrograph of zinc oxide smoke taken on plate partly covered by silver film (3.4 mg/cm²). Magnification optical enlargement 6×.

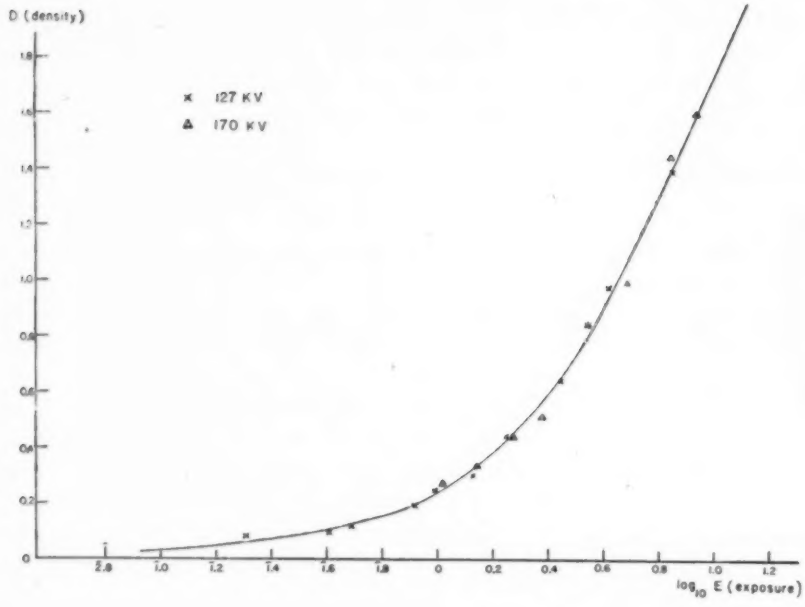

FIG. 7. Variation of the density with the logarithm of the exposure (or lantern slide plates coated with cellulose Scotch tape (9.6 mg/cm²) for two different voltages. Drawn-out curve for uncoated plates (from Fig. 1). Origin of exposure scale shifted to approximate coincidence of the different curves.

coated and the uncoated plate. The validity of assuming the same shape of the H and D curve for the coated as for the uncoated plates was established by making separate measurements of the curve for a plate coated with cellulose Scotch tape at 127 and 170 kilovolts, i.e., at voltages for which the screen definitely reduces and increases, respectively, the sensitivity of the plate. As shown in Fig. 7, the shape of the H and D curve for the coated material does not deviate from the general curve for the uncoated plate by more than experimental error. Multiplying the sensitivity curve (Fig. 4) for the uncoated plate by the exposure ratios corresponding to the differences in density of the coated and the uncoated plate leads to the sensitivity curves for the coated plates, as shown by the dotted lines in Fig. 4. It is seen that

1. At low voltages the sensitivity is reduced due to the absorption and energy losses of the electrons in the screen.
2. The maximum of sensitivity is shifted toward higher voltages in proportion as the screen is made thicker.
3. For thin screens the sensitivity maximum is higher than for the uncoated plate, due to the lateral scattering within the screen, causing more oblique incidence of the electrons on the emulsion.
4. For thicker screens the maximum is lower and broader, due to appreciable absorption in the screen and to the large velocity spread of the transmitted electrons.

An apparently simpler solution for utilizing the intensity maximum near 100 kilovolts in recording high voltage electrons consists in introducing decelerating electrodes which bring the kinetic energy of the electrons down to about 100 kv before they reach the plate—just as, in cathode-ray oscillographs, electrons are at times given a final acceleration in order to increase the light output of the fluorescent screen. More often than not, however, the introduction of the necessary additional high voltage electrodes will constitute a serious drawback for construction and operation.

Again, an even somewhat greater increase of the plate sensitivity at high voltages than with the passive intensifying screen could be attained by increasing the emulsion thickness by a corresponding number of mg/cm². However, the added thickness would, due to the smaller density of the emulsion, have to be larger than for a heavy metal screen, the spreading of the electrons in the emulsion would be greater, and correspondingly the resolving power of the plate would be reduced by a larger amount.

We wish to express our appreciation of the many valuable suggestions given by Dr. V. K. Zworykin, under whose direction this work was carried out.

The Torsion of a Prism with Cross Section the Inverse of an Ellipse

THOMAS JAMES HIGGINS
Tulane University of Louisiana, New Orleans, Louisiana
(Received May 1, 1942)

Saint-Venant's torsion problem is solved for the linear prism with right cross section bounded by the curve, an inverse of an ellipse with respect to its center. By a method developed recently by R. M. Morris, explicit formulas are obtained for the torsion, conjugate torsion, and complex torsion functions; for the twisting moment; for the stress function and the components of shearing stress. This work is of interest as complementing recent work by A. C. Stevenson and by D. L. Holl and D. H. Rock; further, as an addition to the very few exact solutions that have been effected for cross sections bounded by single, closed, continuous, partially concave curves.

A. C. STEVENSON[1] and D. L. Holl and D. H. Rock[2] published, independently and nearly simultaneously, solutions of Saint-Venant's torsion problem for the linear prism with right cross section bounded by an elliptic limacon. This curve is the inverse of an ellipse with respect to a focus. As complementing the work of these three it is of interest to possess the solution for a kindred curve, the inverse of an ellipse with respect to its center—i.e., the curve $v=0$ in the net defined by

$$z=c\sec(w+ik),\quad z=x+iy,\quad w=u+iv, \tag{1}$$

c and k constants defining the semi-major and semi-minor axes of the ellipse of inversion, respectively directed along the x and the y axes and of length $c^{-1}\cosh k$ and $c^{-1}\sinh k$. Additional interest attaches to this contour in that a recent exhaustive survey of the known *analytical* solutions of Saint-Venant's torsion problem (by the writer; to appear elsewhere shortly) revealed that *exact* solutions have been effected for but very few cross sections bounded by curves of this type; that is, by single, closed, continuous curves possessing concavity.

We utilize the powerful method of treating two-dimensional physical problems recently developed by R. M. Morris.[3-5] With respect to the torsion problem for singly-connected cross sections, Morris has proved that if the boundary curve is $v=0$ in the net defined by

$$z=\sum_{m=0}^{\infty}a_m\epsilon^{imw},\quad z=x+iy,\quad w=u+iv, \tag{2}$$

and if $v=\infty$ is the sole singularity within the cross section, the complex torsion function is

$$\Omega=ib_0/2+i\sum_{m=1}^{\infty}b_m\epsilon^{imw}, \tag{3}$$

and the twisting moment is the real part of

$$M=(\tau\mu\pi/2)[c_0b_0+\sum_{m=1}^{\infty}(c_m\bar{b}_m+c_{-m}b_m)-2\sum_{m=1}^{\infty}mb_m\bar{b}_m], \tag{4}$$

where

$$b_m=\sum_{s=0}^{\infty}\bar{a}_sa_{m+s};\qquad \bar{b}_m=\sum_{s=0}^{\infty}a_s\bar{a}_{m+s}, \tag{5}$$

$$c_m=\sum_{s=0}^{\infty}(m+s)\bar{a}_sa_{m+s};\quad c_{-m}=\sum_{s=0}^{\infty}sa_s\bar{a}_{m+s}, \tag{6}$$

the bar indicating the complex conjugate.

[1] A. C. Stevenson, Proc. Math. Soc. London [2] **45**, 126 (1939).
[2] D. L. Holl and D. H. Rock, Zeits. f. angew. Math. u. Mechanik **19**, 141 (1939).
[3] R. M. Morris, Math. Ann. **116**, 374 (1939).
[4] R. M. Morris, Math. Ann. **117**, 31 (1939).
[5] R. M. Morris, Proc. Math. Soc. London [2] **46**, 81 (1940).

It is convenient to note here the following identities:

$$\sec(w+ik)=2\sum_{r=1}^{\infty}(-1)^{(r-1)/2}\epsilon^{-rk}\epsilon^{irw} \qquad (r=1,3,5\cdots), \quad (7)$$

$$\operatorname{csch} 2k=2\sum_{r=1}^{\infty}\epsilon^{-2rk} \qquad (r=1,3,5\cdots), \quad (8)$$

$$\operatorname{csch}(2k)\coth(2k)=2\sum_{r=1}^{\infty}r\epsilon^{-2rk} \qquad (r=1,3,5\cdots), \quad (9)$$

$$\operatorname{csch}^2 2k=2\sum_{n=2}^{\infty}n\epsilon^{-2nk} \qquad (n=2,4,6\cdots), \quad (10)$$

$$1-\coth 2k=-2\sum_{n=2}^{\infty}\epsilon^{-2nk} \qquad (n=2,4,6\cdots). \quad (11)$$

In light of these identities we understand hereafter that r designates only an *odd* integer, and that n designates only *zero* or an *even* integer.

Use of (7) enables us to write (1) in the form of (2)

$$z=2c\sum_{r=1}^{\infty}(-1)^{(r-1)/2}\epsilon^{-rk}\epsilon^{irw}; \quad (12)$$

whence comparison of (12) with (2) reveals that

$$a_m=0,\ m \text{ even or zero}; \quad a_m=a_r=2c(-1)^{(r-1)/2}\epsilon^{-rk},\ m \text{ odd}. \quad (13)$$

By (13) $a_s a_{m+s}$ vanishes except if s is odd and m is even. Accordingly, by (5) and (13)

$$b_m=\bar{b}_m=b_n=\sum_{r=1}^{\infty}a_r a_{n+r}=4c^2(-1)^{n/2}\epsilon^{-nk}\sum_{r=1}^{\infty}\epsilon^{-2rk}; \quad (14)$$

whence by (8)

$$b_n=2c^2\operatorname{csch}(2k)(-1)^{n/2}\epsilon^{-nk}. \quad (15)$$

Substituting (15) in (3) and utilizing (7) yields

$$\begin{aligned}\Omega&=ic^2\operatorname{csch}(2k)[1-\epsilon^{i(w+ik)}\sec(w+ik)]\\&=c^2\operatorname{csch}(2k)\tan(w+ik).\end{aligned} \quad (16)$$

The real and imaginary parts of Ω are, respectively, the torsion function ϕ and i times the conjugate torsion function ψ. Utilizing the relationships $\phi=(\Omega+\bar{\Omega})/2$ and $\psi=(\Omega-\bar{\Omega})/2i$, simple trigonometric analysis yields

$$\Omega=\phi+i\psi=c^2\operatorname{csch}(2k)[\sin 2u+i\sinh 2(v+k)][\cos 2u+\cosh 2(v+k)]^{-1}. \quad (17)$$

The stress function Ψ is defined by

$$\Psi=\psi-(x^2+y^2)/2. \quad (18)$$

As by (1)

$$x^2+y^2=z\bar{z}=c^2\sec(w+ik)\sec(\bar{w}-ik)=2c^2[\cos 2u+\cosh 2(v+k)]^{-1}, \quad (19)$$

we have from (17) and (18)

$$\Psi=-c^2[1-\operatorname{csch}(2k)\sinh 2(v+k)][\cos 2u+\cosh 2(v+k)]^{-1}. \quad (20)$$

The shearing stresses are given by

$$X_z=\tau\mu\partial\Psi/\partial y; \quad Y_z=-\tau\mu\partial\Psi/\partial x. \quad (21)$$

From

$$\frac{\partial \Psi}{\partial x}=\left[\frac{\partial \Psi}{\partial u}\frac{\partial x}{\partial u}+\frac{\partial \Psi}{\partial v}\frac{\partial x}{\partial v}\right]\left[\left(\frac{\partial x}{\partial u}\right)^2+\left(\frac{\partial x}{\partial v}\right)^2\right]^{-1}, \tag{22}$$

$$\frac{\partial \Psi}{\partial y}=-\left[\frac{\partial \Psi}{\partial u}\frac{\partial x}{\partial v}+\frac{\partial \Psi}{\partial v}\frac{\partial x}{\partial u}\right]\left[\left(\frac{\partial x}{\partial u}\right)^2+\left(\frac{\partial x}{\partial v}\right)^2\right]^{-1}, \tag{23}$$

we obtain by carrying out the simple but lengthy analysis indicated

$$X_z=-2\tau\mu c\sin u\left[\frac{\operatorname{csch}(2k)\cosh(v+k)}{\cos 2u-\cosh 2(v+k)}+\frac{\sinh(v+k)}{\cos 2u+\cosh 2(v+k)}\right], \tag{24}$$

$$Y_z=-2\tau\mu c\cos u\left[\frac{\operatorname{csch}(2k)\sinh(v+k)}{\cos 2u-\cosh 2(v+k)}-\frac{\cosh(v+k)}{\cos 2u+\cosh 2(v+k)}\right]. \tag{25}$$

Calculation of the twisting moment requires evaluation of the c coefficients. Noting the remark preceding (14), we have from (6) and (13)

$$c_{-m}=c_{-n}=\sum_{r=1}^{\infty} r a_r a_{n+r}=4c^2(-1)^{n/2}\epsilon^{-nk}\sum_{r=1}^{\infty} r\epsilon^{-2rk}, \tag{26}$$

whence by (9)

$$c_{-n}=2c^2\operatorname{csch}(2k)\coth(2k)(-1)^{n/2}\epsilon^{-nk}. \tag{27}$$

The a coefficients being real, we have by (5) and (6)

$$c_m=c_n=\sum_{r=1}^{\infty}(n+r)a_r a_{n+r}=nb_n+c_{-n}. \tag{28}$$

Accordingly, in view of (28) we have for (4)

$$M=(\tau\mu\pi/2)[c_0 b_0+\sum_{n=2}^{\infty}(2c_{-n}b_n-nb_n^2)]. \tag{29}$$

Evaluating (29) by use of (15) and (28) yields

$$M=(\tau\mu\pi/2)[4c^4\operatorname{csch}^2(2k)\coth 2k+8c^4\operatorname{csch}^2(2k)\coth 2k\sum_{n=2}^{\infty}\epsilon^{-2nk}-4c^4\operatorname{csch}^2 2k\sum_{n=2}^{\infty}n\epsilon^{-2nk}], \tag{30}$$

whence by (10) and (11)

$$M=\tau\mu\pi c^4(2\operatorname{csch}^2 2k+\operatorname{csch}^4 2k). \tag{31}$$

As the semi-minor and semi-major axes of the cross section are, respectively, $a=c\operatorname{sech} k$ and $b=c\operatorname{csch} k$, (31) can be transformed easily into

$$M=\tau\mu\pi(a^4+b^4+6a^2b^2)/16. \tag{32}$$

Corroboratively, if $a=b$, the original ellipse is a circle, the inverse with respect to its center is a circle, and (32) yields the known expression for the twisting moment of a torsed circular cylinder: $M=\tau\mu\pi a^4/2$.

From (24) and (25) the shearing stresses on the contour at the ends of the semi-major and semi-minor axes are

$$X_z=-\tau\mu(a^2+b^2)/2b;\quad Y_z=\tau\mu(a^2+b^2)/2a. \tag{33}$$

Corroboratively, if $a=b$, (33) yields the known expression $\tau\mu a$ for the shearing stress on the surface of a torsed circular cylinder.

Human Trajectories

RUFUS OLDENBURGER
Illinois Institute of Technology, Chicago, Illinois
(Received May 21, 1942)

It is proved that a human being M falling from a ledge A through the air to the ground below will attain the greatest range if M falls forward while standing upright. If M was found on the ground at a position B beyond this range of fall, M furnished energy himself to attain B. An analysis of trajectories from A to the ground due to an effort on the part of M is made. If the kinetic energy which M must produce to reach B is much greater than that which M can furnish after loss of balance, M made the trip from A to B by a premeditated jump. Such analyses are important for determining suicides.

INTRODUCTION

A STUDY of the possible motions of a human being M from an initial position A to a final position B will be made here by the use of the fundamental laws of motion only.

We let M stand upright on a horizontal rod R. We let h designate the distance from the center C of mass of M to R and let r represent the radius of gyration of M with respect to R. For a particular body M, the numbers h and r can be obtained by the usual balancing and pendulum methods.

We suppose that air resistance can be neglected,* as is true, for example, if B is no more than 100 feet below A. Since once the body M is in the air the center of mass C moves approximately along a parabola, we may restrict our study to plane motions. Because on contact with the ground the center of mass C no longer continues to move in a parabola, we shall analyze our motions as if C continued to follow the parabola traversed by C before contact with the ground. In this case C would strike the ground at a point D. We let b designate the distance A is above D. We set up a Cartesian coordinate (x, y)-system with origin at A, the x-axis horizontal, and D to the right of A. We let $D^*=(a, -b)$ be the coordinates of the given point which corresponds to the actual motion taken by the body M from A to the horizontal line $y=-b$, which motion is to be determined from A and D^*, as well as other properties of the motion. (See Fig. 1.)

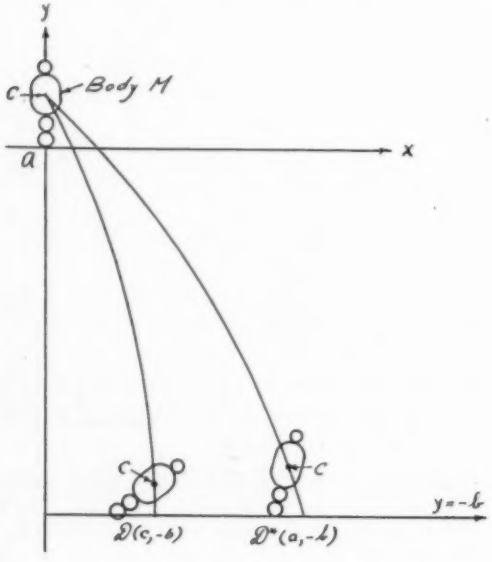

FIG. 1.

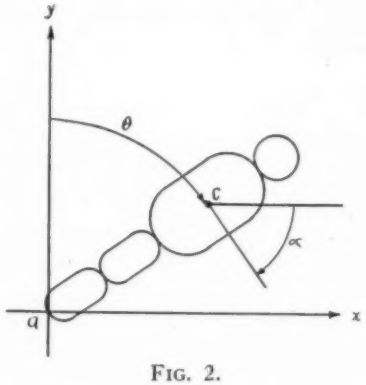

FIG. 2.

ANALYSIS OF THEORY

1. Falls

We shall consider a fall from A to the line $y=-b$. We let $(c, -b)$ denote the coordinate of

* Computation shows that a 10 m.p.h. wind would deviate M by less than an inch in a drop of 30 feet.

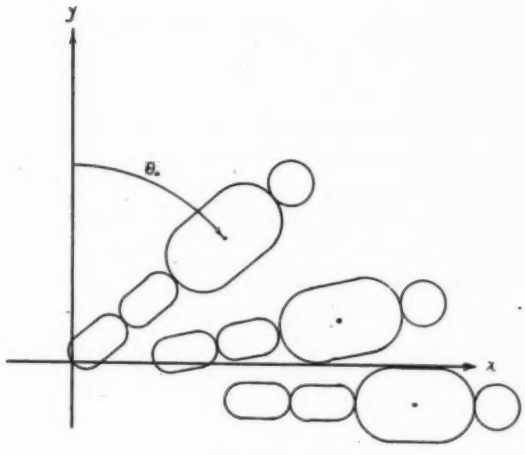

FIG. 3.

the point D in this case. We shall determine the maximum value of c for all possible falls from A to the line $y=-b$.

We suppose that M stands erect at A and falls forward. Until M departs from the point A the distance $AC=h$ remains practically unchanged. We let θ be the angle measured from the positive half of the y-axis to the line AC at any time before departure of M from A (Fig. 2). We let m and g designate the mass and acceleration of gravity of M in the usual units. The torque L on M with respect to A is $mgh \sin\theta$. We let I denote the moment of inertia of M with respect to A, whence $I=mr^2$. From the fundamental relation $L=I\theta''$, where θ'' is the angular acceleration of C, we have

$$\theta''=\frac{gh}{r^2}\sin\theta.$$

Integrating, using the initial condition that $\theta'=0$ when $\theta=0$, we obtain

$$\theta'=\frac{2(gh)^{\frac{1}{2}}\sin\theta/2}{r}. \tag{1}$$

The centrifugal force F_c acting on M is

$$F_c=m(\theta')^2h.$$

When this force equals the component g_{ac} of gravity along the line AC, the body M flies out into space, the constraint being zero. Equating F_c and g_{ac} we obtain

$$mg\cos\theta=\frac{2mgh^2}{r^2}(1-\cos\theta),$$

whence

$$\cos\theta=\frac{2}{2+\tau^2}, \tag{2}$$

where $\tau=r/h$. The solution θ of (2) will be called the "angle of departure." Experiment shows that for a body M, the number τ^2 is about $\frac{3}{2}$, whence $\theta=55°$. If we let θ_0 designate the solution of (2) (see Figs. 3 and 4), by (1) and $|v|=h\theta'$ the linear velocity v of the point C at the instant t_0 of departure has the magnitude

$$|v|=\frac{2(gh)^{\frac{1}{2}}}{\tau}\sin\frac{\theta_0}{2}, \tag{3}$$

and is directed downward along the tangent to $x^2+y^2=h^2$ at the point $C_0=(h\sin\theta_0,\ h\cos\theta_0)$ occupied by C at the instant t_0. The components v_x and v_y of v in the x and y directions have the magnitudes $|v|\cos\theta_0$, $|v|\sin\theta_0$, respectively. Upon departure the point C travels along the well-known parabola

$$y-k=(x-j)\tan\alpha-\frac{16(x-j)^2}{|v|^2\cos^2\alpha}, \tag{4}$$

where $(j,\ k)=C_0$, $\alpha=-\theta_0$ (see Fig. 2). Setting

FIG. 4. Falling rod which was released from the vertical position. Exposure frequency—15 per second. In 4th position, the rod makes an angle of 60° with the vertical, and has already left the ledge.

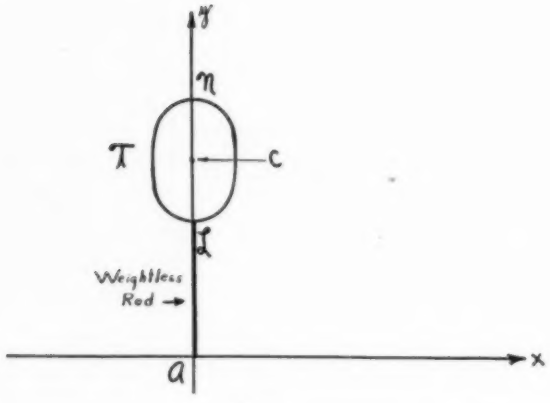

FIG. 5.

$y=-b$ in (4), and solving for x we obtain the abscissa c of D. For $\theta_0=55°$ this abscissa c is given by

$$c=.0025[5.74(56h-|v|^2)+|v|(33|v|^2+448(7b+4h))^{\frac{1}{2}}]. \quad (5)$$

In the above paragraph we supposed that M fell forward while erect. It remains to show that the range c thus obtained is a maximum for all falls from A to the line $y=-b$. We shall accomplish this proof by showing that as the center of gravity of M is lowered, as when M crouches, the *range* on $y=-b$ is shortened, i.e., the abscissa of the point where C meets $y=-b$ is decreased. We shall actually carry through the converse argument by treating the trajectories as M straightens up.

Experiment shows that when AC makes an angle of about 10° with the vertical, a body M loses balance and falls over. We shall term this angle the *angle of loss of balance*. It follows that M cannot lean over very far from the vertical without starting to fall over. In view of the continuity of the functions involved, mathematical computations show that the substitution of a position of M where AC makes an angle $\theta(0\leqq\theta\leqq10°)$ with the vertical for the position where AC is vertical will affect the range on the line $y=-b$ by a relatively small amount. It will therefore be no restriction on the generality of the method to compare trajectories where AC is initially vertical.

The trajectory of M is influenced most by the trunk and head of the body, and only in a small way by the legs. We shall, for the moment, neglect the legs, and compare trajectories which arise when the trunk T of M is raised in such a manner that one vertical chord LN of M is kept vertical. We understand the *trunk* T to refer to the part of M above the legs. (See Fig. 5.) The center of gravity C is near the y axis, for which reason we shall suppose that C is on the y axis. We shall suppose that T is raised through a distance ϵ. It follows that the distance h from A to the center of gravity C increases from h to $\bar{h}=h+\epsilon$. We shall determine how the radius of gyration r of T with respect to A varies under this elevation of T. The point (x, y) in T goes into $(x, y+\epsilon)$ under this change. Thus the moment I_x of inertia of T with respect to the x axis goes into

$$I_x'=I_x+2\epsilon m_x+\epsilon^2 m,$$

where m_x is the first moment of T with respect to the x axis before T is raised, and m is the mass of T. Under the elevation of T the moment of inertia of T with respect to the y axis remains invariant. Thus the moment of inertia I' of T with respect to A after elevation is related to the corresponding initial moment of inertia I by the formula

$$I'=I_x'+I_y'=I+2\epsilon m_x+\epsilon^2 m. \quad (6)$$

We let $\bar{r}$ designate the radius of gyration of T after elevation. By (6) we have

$$\bar{r}^2=r^2+k,$$

where

$$k=2\epsilon h+\epsilon^2.$$

We also have $\bar{h}^2=h^2+k$, whence

$$\bar{\tau}^2=\frac{\bar{r}^2}{\bar{h}^2}=\frac{\tau^2+\rho}{1+\rho}, \quad (7)$$

where $\rho h^2=k$. Since $\tau>1$ for M, we have $\bar{\tau}<\tau$, from which (2) implies that the angle $\bar{\theta}_0$ of departure for the elevated trunk is smaller than the initial departure angle θ_0. We can write (3) as

$$|v|=\left(\frac{2gh}{2+\tau^2}\right)^{\frac{1}{2}}.$$

It follows that the magnitude of the new velocity vector $\bar{v}$ of T is greater than $|v|$ for the initial

departure velocity v of T. The abscissa j of the point C of departure of T for $\epsilon=0$ is $h\sin\theta_0$, whence

$$j=\frac{h(\sigma^2+4\sigma)^{\frac{1}{2}}}{2+\sigma},\quad \sigma=\tau^2. \tag{8}$$

For small values of ϵ, we have $\rho<1$, whence we can write $\bar{\sigma}=\bar{\tau}^2$, given in (7), as

$$\sigma+\rho(1-\sigma)(1-\rho+\rho^2-\cdots).$$

Writing $\Delta\sigma=\bar{\sigma}-\sigma$, $\Delta h=\epsilon$, expressing ρ in terms of Δh, and observing that $\rho\to 0$ as $\epsilon\to 0$, we have

$$\frac{d\sigma}{dh}=\frac{2}{h}(1-\sigma).$$

Now (8) implies

$$\frac{dj}{dh}=\frac{\sigma^2(\sigma+6)+8}{(\sigma^2+4\sigma)^{\frac{1}{2}}(2+\sigma)^2}. \tag{9}$$

Certainly

$$dj/dh>0, \tag{10}$$

whence j increases with an increase in h. Thus the abscissa $\bar{j}$ of the point $(\bar{j},\bar{k})$ of departure of C, where $AC=h+\epsilon=\bar{h}$ is greater than j. It follows that we have the situation illustrated in

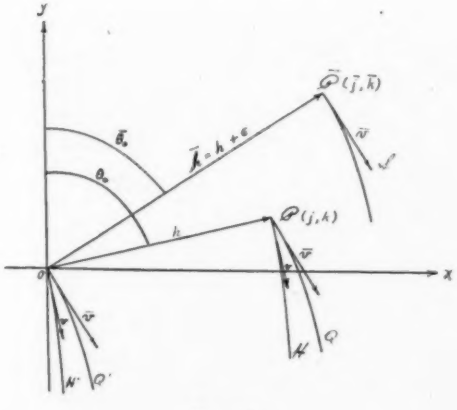

FIG. 6.

Fig. 6. We have proved the validity of the set of inequalities $|\bar{v}|>|v|$, $\bar{j}>j$, $\bar{h}>h$, $\bar{\theta}_0<\theta_0$. If we replace the trajectory S determined by $\bar{v}$ at $\bar{P}$ by a trajectory Q determined by $\bar{v}$ acting at P, the range on $y=-b$ is decreased. Thus, if the range of Q on $y=-b$ exceeds the range of the trajectory H, determined by v at P, on

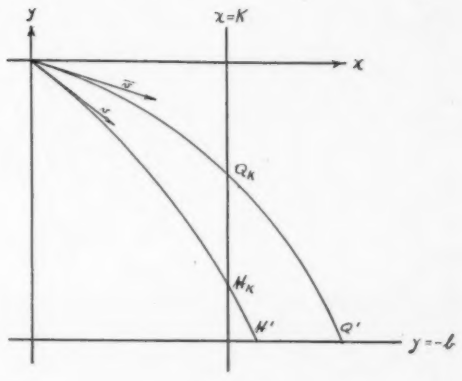

FIG. 7.

$y=-b$, this is certainly true if Q is replaced by S. Since we have reduced the comparison of S and H to that of trajectories Q and H emanating from the same point P, we shall compare corresponding trajectories Q' and H' passing through O with the velocities $\bar{v}$ and v, respectively. Our equation of motion is (4) with $(j,k)=(0,0)$. The slope dy/dx of the trajectory (4) through A is given by

$$y'=\tan\alpha-\frac{32x}{|v|^2\cos^2\alpha}.$$

We assign to x a positive value K. We are interested in negative values of α. Now the absolute value $|y'|$ of y' is

$$-\tan\alpha+32K/|v|^2\cos^2\alpha.$$

As $|v|$ is increased, $|y'|$ is decreased, whereas as $|\alpha|$ is decreased, $|y'|$ is also decreased. We let Q_K and H_K designate the points on Q' and H', respectively, obtained by setting $x=K$ (Fig. 7). The slope of Q' at Q_K is numerically less than that of H' at H_K. Since v makes a larger angle with the x axis than $\bar{v}$, the point Q_K is above H_K for small values of K. On the other hand, for Q' to cross H' at some point $Q_K\equiv H_K$, the slope of Q' must be greater numerically than that of H' at this point. It follows that the trajectory Q' lies above H' for each K. Thus the range of Q' on each line $y=-b$ is greater than that of H'. It follows that the range of S on $y=-b$ is greater than that of Q on this same line, whence elevating T increases the range on $y=-b$.

In the above treatment of T, we used the property that the motion of M is dominated

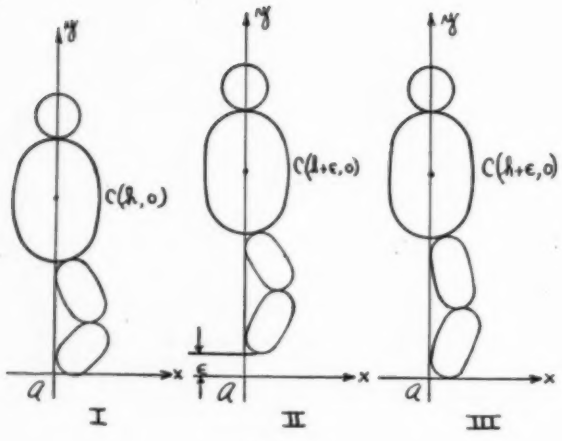

FIG. 8.

by T. We shall now show that the effect of the legs on the trajectory leaves invariant the property that the range on $y=-b$ is increased as T is raised. When M is raised so that T is elevated through a distance ϵ while the feet of M are kept in contact with A, this change of the position of M may be thought of as being accomplished in two steps, namely, the elevation of M as a rigid body though a distance ϵ, and the subsequent dropping of the bottoms of the feet through a distance ϵ as illustrated in Fig. 8. We imagine that a rigid weightless rod R is affixed to M and joins A in II along the y axis with the body M. We let Π_{II} be the trajectory traversed by C as M affixed to R falls forward. We let Π_I and Π_{III} be the corresponding trajectories for I and III, respectively. In view of the development above the range of Π_{II} on $y=-b$ is greater than that of Π_I. We shall show that as we go from II to III we do not decrease the range of Π_{II} on $y=-b$ in such a way that this range for Π_{III} is less than that of Π_I. We let $\bar{h}$ and $\bar{r}$ be the distance from A in III to the center of gravity of M, and the radius of gyration of M with respect to A, respectively. We let h and r be the corresponding numbers for I. We let (x, y) be the coordinates of a point P in the legs of M in the position I, and $(\bar{x}, y+\epsilon-\epsilon')$ the coordinates of P in the position III. We write

$$m\bar{\epsilon}=\int_l \epsilon' dm,$$

where m is the mass of M, and the integral is taken over the legs l of M. Since the trunk T of M is kept fixed in the transition from II to III, the first moment M_T of T with respect to the x axis AX is invariant. The first moment M'_{AX} of M in III with respect to AX is related to

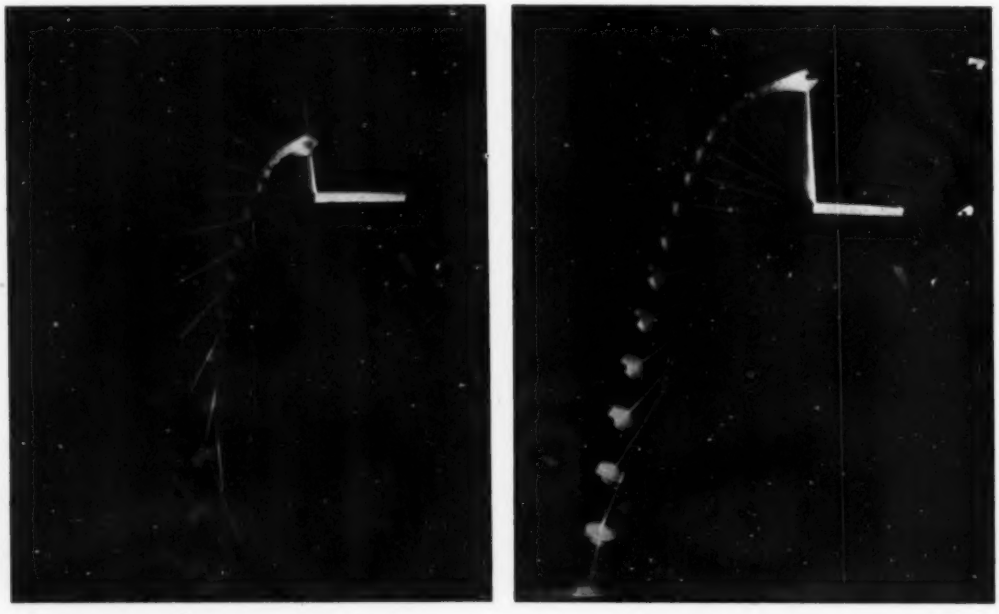

FIG. 9. These figures (20 exposures per second) show that the range of the center of gravity (knob) is increased as a weight is moved out on a rod.

this moment M_{AX} for the position I by the formula

$$M'_{AX}=M_{AX}-m\bar{\epsilon}+m\epsilon.$$

Hence we have

$$\bar{h}=h+(\epsilon-\bar{\epsilon}) \tag{11}$$

approximately, since the abscissa of the center of gravity $\bar{C}$ of M in III is very small relative to $\epsilon-\bar{\epsilon}$. The moment of inertia I'_{AX} of M in III with respect to AX is related to this moment of M in I by the formula

$$I'_{AX}=I_{AX}+[2(\epsilon h-\mu)+(\epsilon^2+v^2)]m, \tag{12}$$

where

$$\mu m=\int_l (y+\epsilon)\epsilon' dm, \quad v^2 m=\int_l (\epsilon')^2 dm.$$

Thus approximately (neglecting infinitesimals of higher order than 1) by (11) and (12)

$$\bar{\tau}^2=\frac{r^2+2\epsilon h-2\mu}{h^2+2\epsilon h-2\bar{\epsilon}h}. \tag{13}$$

For $\bar{\epsilon}$ small relative to ϵ, we have

$$(1-\bar{\epsilon}/\epsilon)r>h.$$

For a body M this last inequality is satisfied, whence $\bar{\tau}<\tau$. Thus the angle θ_0' of departure for III is less than the corresponding angle θ_0 for I. Now the velocity of departure v' for III has a magnitude greater than that for I, since $\bar{\tau}<\tau$, and $\bar{h}>h$. We let τ_1 be the number for II corresponding to τ for I. The ratio τ_1^2 is approximately

$$\tau_1^2=\frac{r^2+2\epsilon h}{h^2+2\epsilon h}. \tag{14}$$

When $h>y+\epsilon$ for each point (x, y) in l, we have $\bar{\epsilon}h>\mu$. Now τ_1^2 is obtained from $\bar{\tau}^2$ in (13) by adding $2\bar{\epsilon}h$, and 2μ to the denominator and numerator, respectively. Thus

$$\tau>\bar{\tau}>\tau_1. \tag{15}$$

In view of (15), the derivative $d\sigma/dh[\sigma=\tau^2]$ for changes of the type from I to III is numerically less than $d\sigma/dh$ for changes of the type from I to II. It follows that the derivative of j as given in (8) with respect to h is at least as great for changes from I to III as for changes from I to II. Thus dj/dh satisfies (10). It follows from the theory developed above for transitions from I to II that the range of M for III on $y=-b$ is at least as great as the corresponding range for I. We have proved that the effect of the legs is not enough to prevent the range from increasing as the trunk of M is elevated vertically. (See Figs. 9 and 10.)

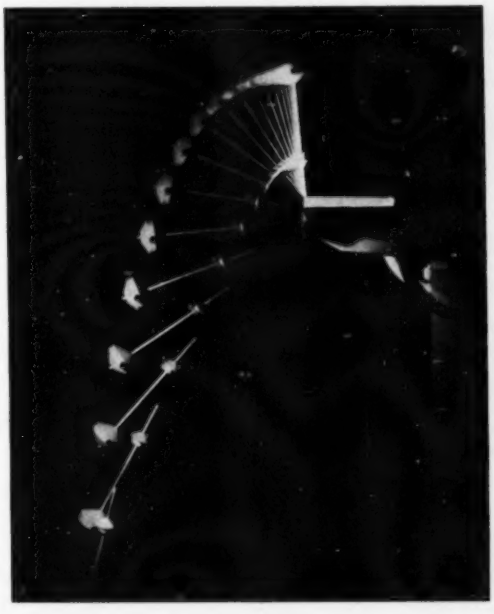

FIG. 10. Comparing Figs. 9 and 10 shows that the effect of an additional weight on the rod near the ledge affects the trajectory of the center of gravity only negligibly. Exposure frequency for Fig. 10—15 per second.

We have omitted above the treatment of the case where the axis of the trunk T of M is inclined from the vertical. We consider a trunk T which is symmetrical with respect to two mutually perpendicular lines CJ and CK through the center of gravity C of T. We shall compare the trajectories of T for an angle of 0° between CJ and the positive half of the y axis, where C is on the y axis, and the trajectory obtained by inclining CJ through an angle α about C as illustrated in Fig. 11. A point P with polar coordinates (ρ, ψ) in Fig. 11, I, relative to CK as axis, goes into a point with coordinates $(\rho, \psi-\alpha)$ in Fig. 11, II. The center of gravity of T remains invariant under transition from I to II. This is also true of the moment of inertia with respect to A, since the moment I_A of inertia of T in the

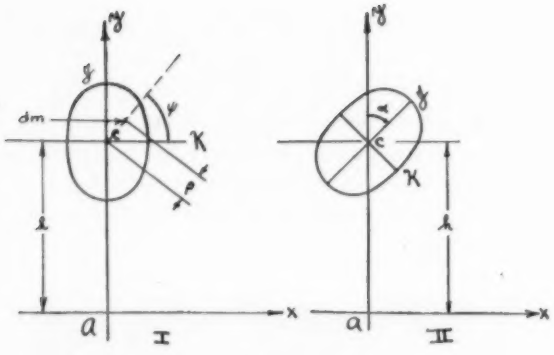

FIG. 11.

position I with respect to A is given by

$$I_A = \int_T (h^2+\rho^2+2\rho l \sin\psi)dm,$$

(dm is the usual element of mass) whereas this moment I_A' for II is

$$I_A' = I_A + 2h\int_T \rho[\sin(\psi-\alpha)-\sin\psi]dm,$$

whence using the symmetry properties in splitting the integral over T into integrals over the four regions obtained from T by using CK and CJ as cutting lines, we obtain $I_A' = I_A$. Since the radius of gyration r of T with respect to A, and h are invariant, the trajectories obtained by letting M fall forward, with T in the initial positions I and II are identical. (See Fig. 12.) As in the treatment of the elevation of T, introducing the effect of the legs will cause only a small deviation in the range on $y=-b$. Also a small deviation of C from AY in the initial position of M, and a reasonable departure of T from symmetry with respect to CJ and CK will have only small effect on the range $y=-b$ as some simple trials of deviations show.

If the body M falls forward while M is not resting on his feet, the center of mass of M is much closer to A than when M is standing erect on his feet, whence, by simple mathematical considerations, the range of M on $y=-b$ will be considerably less than when M falls forward from the erect standing position. It follows from all of these considerations that the most efficient fall of M from A is attained when the initial state of M is the erect standing position. (See Fig. 13.)

That a body M should fall in such a manner that the maximum range C in (5) is attained is exceedingly unlikely. If in a given physical case the range exceeds the C of (5) we may conclude that the body M furnished energy himself to attain the given range.

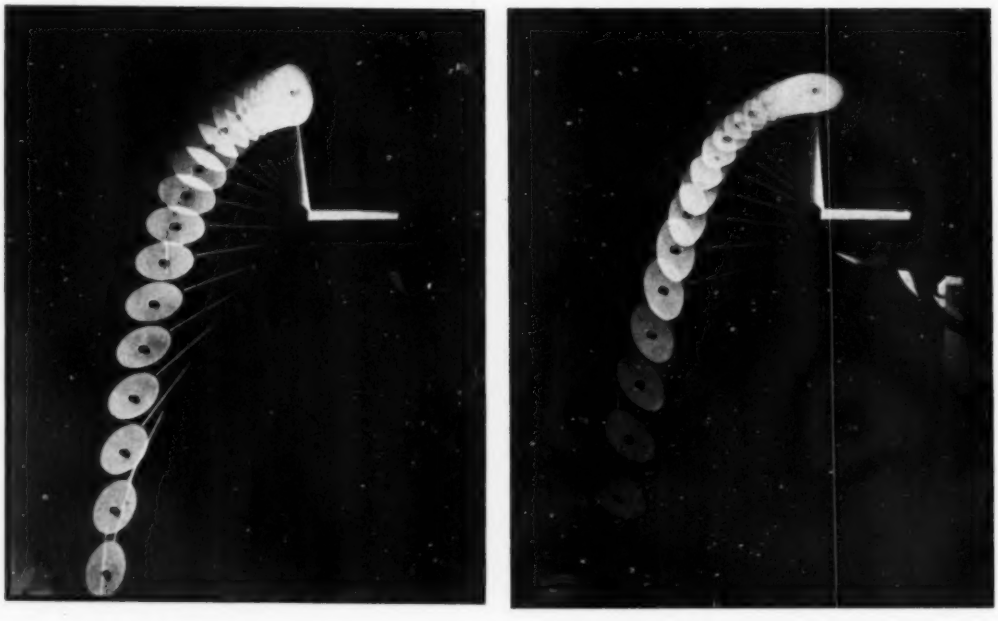

FIG. 12. The trajectories of the center of mass for these figures are identical. Exposure frequency—20 per second.

FIG. 13. Experimental set-up for photographing falling rod. The author is shown on the left and Mr. Howard T. Betz of the Armour Research Foundation on the right. The above photographs were taken by Mr. Betz.

From the well-known formula $s=16t^2$, we find that the angle the "axis" of M makes with the positive horizontal direction, measured clockwise, is by (1) given as

$$\theta_0+\frac{\sin\theta_0/2}{2r}[gh(b+h\cos\theta_0)]^{\frac{1}{2}} \qquad (16)$$

at the instant C strikes $y=-b$, provided the angular velocity of M has been constant during flight, a state which may be considered normal. From (16) one can determine whether or not a most efficient fall of M would land M on his head, or on his feet, or flat on the ground.

2. Jumps

In making a jump from the point A the center of gravity C of M must be within a distance h of A at the instant t_0 of departure, whence C is within or on the circle Γ with equation $x^2+y^2=h^2$ at this instant. We shall now determine the point which must be occupied by C if M is to leave A with the minimum speed, and thus minimum kinetic energy, and still reach $D^*=(a,-b)$, and we shall derive this minimum velocity and energy.

The argument here was worked out by D. B. Dekker.† Solving (4) for $|v|$ after setting $(x, y)=(a,-b)$ we obtain

$$|v|^2=\frac{16(a-j)^2\sec\alpha}{[(a-j)\tan\alpha+(k+b)]}.$$

We shall minimize $|v|$ by varying α. Now $|v|$ is a minimum when $|v|^2$ is a minimum. Setting $d|v|^2/d\alpha$ equal to zero, and solving we obtain

$$\tan\alpha=\frac{-(b+k)+[(b+k)^2+(a-j)^2]^{\frac{1}{2}}}{(a-j)}. \qquad (17)$$

We have used the + sign in (17), because M cannot jump downward, and the − sign would by $j<a$ yield a negative $\tan\alpha$ and negative α. For α as given in (17) we have

$$|v|^2=32\{[(b+k)^2+(a-j)^2]^{\frac{1}{2}}-(b+k)\}. \qquad (18)$$

At the point (j, k), the speed $|v|$ of C as given in (18) is the least speed with which C can depart from (j, k) and reach D^*. At a particular point (j, k), the speed $|v|$ of (18) takes on a fixed value, which we shall denote by $\sqrt{\eta}$. Replacing (j, k) by (x, y) in (18) we get the parabola

$$(x-a)^2=\frac{\eta}{16}(y+b)+\left(\frac{\eta}{32}\right)^2, \qquad (19)$$

which is the locus of all points (x, y) for which the minimum speed is the same. The curve (19) is concave up with negative slope to the left of $x=a$. As we vary η we obtain a one-parameter

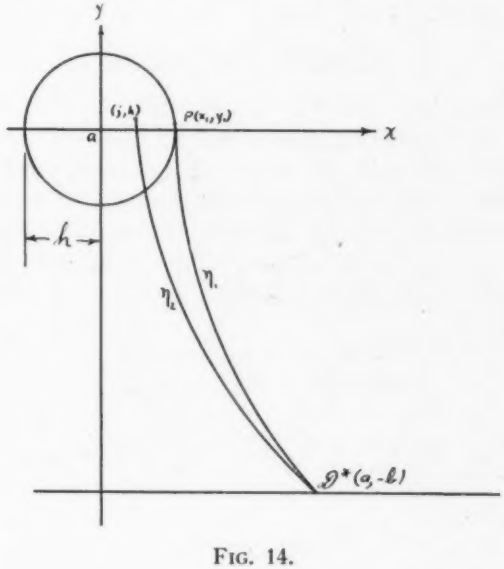

FIG. 14.

† Assistant in the Department of Mathematics, Illinois Institute of Technology.

family F of parabolas. In particular, if $\eta=0$, we have the vertical line $x=a$ through D^*. As η is increased the corresponding parabola is lowered, in the sense that the parabola $(x\leqq a)$ for $\eta=\eta_1$ lies above the parabola for $\eta=\eta_2$ when $\eta_2>\eta_1$. (See Fig. 14.) It follows that the point P which must be occupied by C, at the starting instant t, where the speed is a minimum is the point on the circle Γ where a member of the family F is tangent to Γ. We let (x_1, y_1) designate the coordinates of P. The normal to the curve of F through P is given by

$$y=\eta x/32(a-x_1). \tag{20}$$

Setting $(x, y)=(x_1, y_1)$ in (19) and (20), solving for η, and substituting for η in (19), we obtain

$$x_1^2(x_1-a)=-2x_1y_1(y_1-b)+y_1^2(x_1-a). \tag{21}$$

The point P is determined by (21) and

$$x_1^2+y_1^2=h^2. \tag{22}$$

The solution of (21) and (22) for (x_1, y_1) can be reduced to that of a sextic in x_1. Setting (j, k) in (18) equal to (x_1, y_1) we obtain the minimum speed. The minimum kinetic energy which must be generated in jumping from A to D^* is thus

$$E=16m[((b+y_1)^2+(c-x_1)^2)^{\frac{1}{2}}-(b+y_1)]. \tag{23}$$

The angle α of departure for the most efficient jump is given by (17) with $(j, k)=(x_1, y_1)$. If a is large enough, e.g., when $(a, b)=(15, 30)$, the energy E of (23) is near the minimum kinetic energy E_M which must be furnished by M to reach D^*.

3. Combination Fall and Jump

By falling forward while jumping the body M can decrease the kinetic energy which he must furnish to reach D^*. We shall find a number E_f which is numerically greater than this decrease.

From (3) with $g=32$ we find that the x-component v_x of the velocity v_f of M after falling forward through an angle θ while standing on A is

$$v_x=\frac{8\sqrt{h}}{\tau}\cos\theta(1-\cos\theta)^{\frac{1}{2}}.$$

Setting $dv_x/d\theta=0$, we find that $\cos\theta=\frac{2}{3}$, when v_x is a maximum, whence this maximum component is

$$v_x=16(3h)^{\frac{1}{2}}/9\tau.$$

Since, in jumping, the angle α which the velocity v of departure makes with the x axis is positive, the contribution which v_f makes to v, is less than v_x, inasmuch as the component of v_f on v is less than v_x in magnitude. Thus the kinetic energy furnished by a fall does not exceed

$$E_f=128mh/27\tau^2. \tag{24}$$

It follows from (23) and (24) that the kinetic energy which must be furnished by M is at least $E-E_f$.

In experiments track athletes, aged 20, were not able to develop 100 foot pounds of kinetic energy after loss of balance. This was determined from the maximum range that could be attained by athletes jumping after loss of balance. If M is a normal individual and the trajectory of M is such that $E-E_f>100$, one may conclude that this trajectory was made by a premeditated jump.

4. Steps

In making a step forward the velocity is practically horizontal. Using $(j, k)=(0, 0)$, $\alpha=0$, in (4) we obtain a trajectory with the range

$$x=\frac{|v|}{4}\sqrt{b} \tag{25}$$

on the line $y=-b$. For 3 and 4 m.p.h. (4.4 and 5.9 ft. per sec.) (25) yields $1.1\sqrt{b}$ and $1.5\sqrt{b}$, respectively. Since the center of gravity C of M for a normal body M is at $(j, k)=(1.5, 3)$ instead of $(0, 0)$ at the instant of departure the range on $y=-b$ is actually

$$x=1.5+\frac{|v|}{4}(b+3)^{\frac{1}{2}}. \tag{26}$$

By comparing x of (26) with the actual range a one can determine whether or not the actual trajectory to D^* could have been attained by a step with velocity v. We remark that the first step of a walk at v ft. per sec. is much more difficult to make than succeeding steps.

A SPECIAL CASE

In a New York Life Insurance case, a man M weighing 150 lb., 5 ft. 8 in. tall, left a ledge A, was found on the concrete pavement 30 ft.

below A, and with all points of M in the final state over 14 ft. from the vertical AY through A. On contact with the pavement the center of gravity C of M was traveling nearly along a vertical line and the point was at least 14 feet from the line AY on contact of M with the ground, for otherwise either M would have fallen flat on the ground, or would have struck on the head or legs, and due to lever action part of M would have been found nearer to AY than 14 ft. Actually from the crushing state of the head it was established that M struck the pavement on his head. In analyzing the motion we compare ranges on a line $y=-27$, supposing that the range on this line was 14 ft., so that $D^*=(14, -27)$. For M, we have $h=10/3$, $r=4$. By (3) the velocity of departure for the most efficient fall had the magnitude 7.9 ft. per sec., and by (5) the center of mass for such a fall would have been 7.8 feet out on $y=-27$. This means that M would have been found no more than 7 ft. out (allowing for end corrections). Thus M produced energy of motion himself. From (26), with allowances for the ends, M would have been found about 7 or 9 ft. out if M had stepped forward at 3 or 4 m.p.h., respectively. Thus M could not have made such a step. From (21) and (22), the point (x_1, y_1) from which C could have departed with the least kinetic energy and reach $(14, -27)$ was $(3.25, 0.55)$. The minimum possible energy E was over 150 ft. lb., whereas the possible energy E_f due to falling forward was less than 50 ft. lb. Actually, M furnished at least 150 ft. lb. himself. Because of M's age and condition, M could have furnished only an energy much less than 100 ft. lb. after loss of balance. Thus M made a premeditated jump of considerable magnitude.

New Instrument Booklets

Research Progress for June, 1942, symmarizes in an article entitled "Inside Stories Told by Atoms" investigations in various fields by means of radioactive tracers, emphasizing work on metals now being carried out at Westinghouse. This is a bi-monthly publication of the Westinghouse Research Laboratories, East Pittsburgh, Pennsylvania.

General Radio Experimenter, May, 1942 issue, presents the following articles: "The Type 727-A Vacuum Tube Voltmeter" and "Dielectric Strength Tests with the Variac." Issued by the General Radio Company, 30 State Street, Cambridge, Massachusetts.

Cenco News Chats for May, 1942, occasional publication of the Central Scientific Company, 1700 Irving Park Road, Chicago, Illinois, contains the usual descriptions of apparatus and a number of interesting photos of the new Northwestern Technological Institute at Northwestern University. Lord Kelvin is the subject of the cover picture. The leading article is entitled "This is a War of Science."

Bakelite Review, April, 1942 issue, presents in a 24-page booklet the latest developments in plastics and their applications, including Part 2 of a series of three articles on "Designing Molded Plastic Parts." "A Useful Table of Plywood Adhesives—Their Characteristics and Methods of Handling" lists 24 properties of the ten principal types of wood adhesives used commercially at present. Quarterly publication of the Bakelite Corporation, Unit of Union Carbide and Carbon Corporation, 30 East 42 Street, New York, New York.

Science and Appliance for May, 1942, publication of the Ohio State University Research Foundation, Columbus, Ohio, features a discussion of the sources of the important war metal, magnesium, and its production from dolomite and ferrosilicon.

The 32-page Spring Edition of *Inco*, issued by the International Nickel Company, 67 Wall Street, New York, New York, discusses the salvage of scrap; the part which nickel and nickel alloys play in the production of essential wartime material, including tungsten and plastics used in the construction of military and naval airplanes; and describes the development of a new type of rivet which eliminates blind fastening.

The Spring, 1942, edition of *Modern Precision* has just been issued by Leeds & Northrup Company, 4934 Stenton Avenue, Philadelphia, Pennsylvania. This is a 16-page paper containing brief news items about L & N instruments, controls, and heat-treating methods. It supplements the regular catalogs, bulletins, and circulars which will continue to be issued as before.

In the Tin Research Institute's *Report for 1941* it is stated that since Japan began the Far Eastern campaign the main problem has become one of how to make the best use of the supplies available by curtailing the use of tin in commodities not essential to the war effort; by improving the processes in essential uses; and by recovering tin. The Institute has been appointed by the Ministry of Supply to advise on all technical questions affecting the use of tin.

Collaboration with manufacturers and with government departments in the application of electro-tinning for parts of armaments was continued during the year, and there has also been considerable interest in electro-tinning for small soldering tags, terminals, and clips. Other sections of the *Report* review the progress made in research on tin-rich bearing alloys, foil, and bronzes. Copies may be obtained free of charge from the Tin Research Institute, Fraser Road, Greenford, Middlesex, England.

Low-voltage air circuit breakers designed for use on alternating current circuits up to 600 volts and direct current circuits of 250 or 750 volts are described and illustrated in a new 12-page publication, Catalog 2150, just released by the Roller-Smith Company, Bethelehem, Pennsylvania. The catalog lists closing and tripping currents, shows typical methods of making connections to large breakers, gives dimensions of both manual and electrical designs, and indicates the number and size of terminals for various capacity breakers.

Innovations in Instruments

Microfilm Reader

The Spencer Microfilm Reader, developed as a result of studies by the Committee on Scientific Aids to Learning, is the first inexpensive instrument designed to reproduce the almost microscopic characters of microfilm with brilliant fidelity. The instrument consists of a projection head, a glass film book, and a shadow box and screen. The projection head incorporates an inexpensive spotlight type of longlife bulb, the proper condensing system, and a specially designed projection lens. This head is held by spring clips to the shadow box, which also serves as a support, and may be rotated to project the film in either a vertical or horizontal meridian as desired. Operation of the instrument is simple. The microfilm is placed in a convenient glass film book which consists of two pieces of glass, hinged and bound at the edges with transparent Cellophane tape. This tape serves to space the film properly to protect it from scratching and to orient the film in relation to the focal plane of the objective. The image is projected onto the screen and is so protected by the shadow box that a darkened room is unnecessary. The image is flat and undistorted and should not cause optical fatigue or discomfort.

The instrument is regularly supplied with one bulb and one glass film book, at a list price of $37.50. A roll film attachment designed to accommodate rolls of film up to 100 feet in length is listed at $15.00. Further details may be obtained from the Spencer Lens Company, Buffalo, New York.

New Cellulose Product

A new cellulose product, Onco "V", has been developed by Brown Company, 500 Fifth Avenue, New York, New York. The cellulose base for Onco "V" was originally discovered during research experiments on filter materials for gas masks. First commercial use of Onco "V" was as an insole fabric to replace latex-impregnated materials commonly used before the rubber restrictions. It is announced that this product can be used as a substitute for leather and cork in the manufacture of luggage and linoleum, gaskets, and leather goods.

Improved Blackout Bulb Unit

Changes in blackout bulb specifications are announced by the Wabash Appliance Corporation, Brooklyn, New York, whose silver-lined blackout bulb, placed on the market in early January, has been tested in actual city-wide blackouts in practically every state.

The most important specification change is in color of light from blue and red to the deep orange recommended by the Office of Civilian Defense. The new bulb is smaller in size, with a reduced current consumption of 15 watts. The built-in reflector has been eliminated, and an improved type of heavy black silicate coating is used to prevent light leakage. The bulb will fit any household socket and will list at 45¢.

New Wood Table Radios

Substantial savings of formaldehyde, resins, and other chemicals and materials used to make plastics needed for national defense have been made possible in the production of two new RCA Victor wood table radios to replace several plastic-housed instruments of similar type. The instruments, designated as Models 35X and 36X, operate on a.c.-d.c. current, and both have Underwriters' approval. Standard broadcasts and police calls are received.

Model 35X is housed in a solid walnut cabinet and has a new Spread-Vision dial which, with extra large tuning knobs and 12 : 1 ratio vernier tuning, provides precision tuning. The 36X is similar to the famed RCA Victor Super Six instrument in a wood cabinet. It also employs the new Spread-Vision dial. A 6-tube instrument, the 36X has a 2-point high frequency tone control and an extra large built-in Magic Loop antenna. Both new models employ Magnetite core transformers for greater selectivity.